ALMA MATER STUDIORUM – UNIVERSITA' DI BOLOGNA

Dipartimento di Ingegneria dell'Energia Elettrica e dell'Informazione

"Guglielmo Marconi"- DEI

DOTTORATO DI RICERCA IN INGEGNERIA BIOMEDICA, ELETTRICA E DEI SISTEMI

XXXII Ciclo

Settore Concorsuale: 09/G2

Settore scientifico disciplinare di afferenza: ING/IND-34

Methods for objective and interpretative evaluation of function and motor control: gait in perturbed condition and in the aquatic therapy

Presentata da:

Giulia Pacini Panebianco

Coordinatore di Dottorato

Prof. Daniele Vigo, Ph. D.

Supervisore:

Prof. Silvia Fantozzi, Ph. D.

Co-Supervisore:

Prof. Rita Stagni, Ph.D.

Esame finale anno 2020

A mia madre

“Somewhere, something incredible is waiting to be known.”

Carl Sagan

ABSTRACT

Gait analysis allows to characterize motor function, highlighting deviations from normal motor behavior related to an underlying pathology. The assessment of abnormal gait contributes to differentiate between specific pathologies and to evaluate disease progression and therapeutic effects over time. Laboratory gait analysis, exploiting stereophotogrammetry and force platforms, has become, in the last decades, the *de facto* standard for motor quantitative assessment, although the evaluation of ecological gait, out of the laboratory would allow a better insight in the actual motor function in daily living conditions, and in how it is related to environmental conditions and, potentially, pathology.

The relatively recent availability of wearable inertial sensors, suitable to quantify motion out of the laboratory, has opened the way to the evaluation of ecological gait, although a standard approach is not available yet. A variety of methodological approaches and algorithms have been proposed for the characterization of gait from inertial measures (e.g. for temporal parameters, motor stability and variability, specific pathological alterations such as freezing). However, no comparative analysis of their performance (i.e. accuracy, repeatability) was available yet, in particular, analysing how this performance is affected by extrinsic (i.e. sensor location, computational approach, analysed variable, testing environmental constraints) and intrinsic (i.e. functional alterations resulting from pathology) factors. This lack of information does not allow to define evidence-based criteria for the selection of the most appropriate protocol/algorithm to respond to specific clinical questions, preventing the definition of a standardised approach to support the reliability of the results for clinical application.

The aim of the present project was to fill this gap, comparatively analyzing the influence of intrinsic and extrinsic factors on the performance of the numerous algorithms proposed in the literature for the quantification of specific characteristics (i.e. timing, variability/stability) and alterations (i.e. freezing) of gait.

Considering extrinsic factors, the influence of sensor location, analyzed variable, and computational approach on the performance of a selection of gait segmentation algorithms from a literature review was analysed in different environmental conditions (e.g. solid ground, sand, in water). In general, shank- and foot-based algorithms performed better than trunk-based ones, as well as angular velocity-based compared to acceleration-based ones, while the performance of different computational approaches varied depending on sensor positioning. Differences in algorithm performance were related to the repeatability of the stride pattern of the analyzed variable over trials, subjects and environmental conditions, leading to the proposal of an objective criterion to pre-evaluate the suitability of an algorithm to the specific application. Moreover, the influence of altered environmental conditions (i.e. in water) was analyzed as referred to the minimum number of stride necessary to obtain reliable estimates of gait variability and stability metrics, integrating what already available in the literature for over ground gait in healthy subjects.

Considering intrinsic factors, the influence of specific pathological conditions (i.e. Parkinson's Disease) was analyzed as affecting the performance of segmentation algorithms, with and without freezing, showing results in line with what observed for the perturbed gait of healthy subjects. Based on these results a decision tree was proposed for the evidence-based selection of the most appropriate algorithm for specific operative conditions, and for possible algorithm optimization. Finally, the analysis of the performance of algorithms for the detection of gait freezing showed how results depend on the domain of implementation (frequency-based algorithms perform better than time and time-frequency based ones) and IMU position (shank- and foot-based algorithms perform better than trunk-based one).

Without exhausting all the methodological issues to be addressed to define a standard approach for motion analysis using wearable sensors, the results of the present PhD project provides a significant contribution in the field, providing evidence and objective criteria for the evaluation of 1) the most appropriate algorithm for gait segmentation, 2) the applicability of repeatability and stability metrics, 3) the choice of the most appropriate approach for the detection of gait freezing in perturbed gait conditions, overcoming the general limitation of reference data only from healthy subjects in unperturbed conditions, and addressing specific technical aspects (e.g. sensor positioning, analyzed variable, computational approach and domain) to support the design of more effective algorithms of ecological gait.

TABLE OF CONTENTS

Nomenclature

GE Gait Event

GTP Gait Temporal Parameter

HS Heel Strike

TO Toe Off

FC Foot Contact

FO Foot Off

AP Anterior Posterior

V Vertical

ML Medio Lateral

PSD1 short term Poincarè Plots; PSD2 long term Poincarè Plots

SD Standard Deviation of the stride time

Avg Average Length of Diagonal Line

Max Maximum diagonal line length

Div Divergence

rr Recurrence Rate

Det Determinism

RQA Recurrence Quantification Analysis

MSE Multiscale Entropy

SE Sample Entropy

IMU Inertial Measurement Unit

FIR Finite Impulse Response

IIR Infinite Impulse Response

WT Wavelet Transform

Med Median

Dmed Dispersion around median value

ICC Intraclass correlation coefficient

WDL walking on dry land

WW walking in water

PDP Parkinson's disease patient

FOG Freezing of Gait

TA Tibialis Anterior

GM Gastrocnemius Medialis

GL Gastrocnemius Lateralis

Introduction

Gait is a motor paradigm of human daily living, essential to sustain motor function and guarantee quality of life [1,2]. Gait assessment allows to identify deviations from the reference healthy behavior [1,3,4], providing information regarding the overall health status [5,6]. Assessing abnormal gait supports the evaluation of disease progression and therapeutic effects over time [7].

Clinical motion analysis in laboratory conditions, using stereophotogrammetry, force platform, and other integrate tools [8], has become a *de facto* standard for the functional assessment of gait. On the other hand, its analysis in ecological conditions has raised increasing interest, especially in recent years; the analysis of ecological gait has the potential to actually assess how the analyzed subject walks during daily living, how different environmental constraints affect motor performance and control, how pathology alters gait in real life. The development and wide spread availability of inertial measurement units has given the chance to investigate gait in the afore mentioned ecological conditions [9], providing the potential to characterize motor performance in both healthy and pathological subjects out of laboratory constraints [10,11].

Although the suitability of the technology, the extensive use, and the numerous algorithms proposed for the assessment of different characteristics of gait (e.g. temporal parameters, motor stability and variability, specific pathological alterations of gait such as freezing), no standards have been defined yet for the use of inertial measurement units in gait analysis, not for laboratory testing conditions, even less for the assessment of gait in ecological conditions, and very little information is available regarding the performance of the different proposed algorithms and how testing conditions, environmental constraints, and pathological alterations affect their performance.

The aim of the PhD project described in the present thesis was to fill this gap. The research was addressed to comparatively analyse the performance of different algorithms proposed for the assessment of gait characteristics, such as timing, variability, stability, and freezing, from inertial measurements. In particular, the influence of different implementation characteristics (e.g. sensor

location, analysed variable, computational approach, number of analysed strides) and of alterations resulting from extrinsic (e.g. different types of walking surface and environment) and/or intrinsic (e.g. gait alteration related to pathological conditions) factors.

The present thesis includes one general background chapter and 2 sections describing the research activity and results: Section 1 focuses on the influence of extrinsic factors on the performance of the different algorithms for the characterization of gait timing, variability, and stability in healthy adults; Section 2 focuses on the influence of intrinsic factor, addressing how performance is affected by alterations associated to pathologic gait. Among several pathologies, Parkinson's disease was chosen considering the effectiveness of the aquatic therapy in the rehabilitation and recovery, in order to assess the influence of intrinsic and extrinsic factors in gait alterations and to provide a starting point for future investigations of clinical implications.

In particular:

- The background chapter includes a description of: i) the methods for gait temporal segmentation available in the literature, ii) the non-linear metrics for the characterization of motor control during gait in healthy subjects, and iii) the existing methods for automatic detection of freezing of gait in people with Parkinson's Disease.
- Section 1: the first chapter, 'Segmentation of gait on solid ground', assesses the performance of the algorithms for gait timing estimation during walking of healthy people in controlled laboratory conditions. The second and third chapters, 'Segmentation of gait in water' and 'Segmentation of gait on a damping surface (sand)', respectively, aim to quantify how the alteration of the gait pattern associated to walking in different environmental constraints affect the performance of the segmentation algorithms, designed for gait timing estimation on solid surface. The fourth chapter, 'Non-linear metrics of gait in water', aims to evaluate the minimum number of strides required for a reliable application of non-linear metrics during walking in water at different level of immersion.
- Section 2 assessed methodological aspects of gait in Parkinson's disease patients. The first chapter, 'Segmentation of gait on solid ground', aims to analyse the performance of gait segmentation algorithms during walking on solid ground. The second chapter, 'Detection of freezing events during gait on solid ground', assesses the performance of existing algorithms for automatic identification of freezing episodes.
- Conclusions.

Finally, a complementary chapter proposes a statistical approach for the analysis of muscle activation patterns in the gait of Parkinson's disease patients.

- Appendix: a statistical method is proposed to effectively assess the variability of muscle activation patterns during walking on solid ground in people with Parkinson’s disease.

1.

BACKGROUND

Overview

In recent years, the need to analyse data outside the laboratory constraints and capture information about the human gait during everyday activities has led to the wide diffusion of wearable inertial sensors (IMU). Since they gained a widespread use, numerous methods for providing quantitative information about gait in healthy and pathological people using IMU have been promoted. In fact, numerous algorithms were proposed in clinical applications to assess different characteristics of gait, considering specific environmental constraints and pathological populations [10]. In particular, the assessment of specific characteristics of gait, i.e. temporal parameters, motor stability/variability, and pathological alterations of gait such as freezing are worth to be considered for assisting diagnosis and evaluating changes caused by treatments [2,12–14]. In this dissertation, the influence of extrinsic factors on the performance of algorithms for gait timing segmentation, and stability/variability of motor performance in healthy subjects was investigated considering gait in different environment constraints (i.e. dry land, water and sand). Then, among the various neurological disorders, the analysis of Parkinson's disease was considered as an intrinsic factor for the algorithms characterization for a pathological population, investigating methodological aspects that are specifically related to this pathology, i.e. assessment of algorithms for gait timing estimation and automatic identification of freezing of gait. Given the dataset acquired for PDPs, the evaluation of muscle activation during gait was performed. This aspect assumes an important role for the characterization of motor disorder in PDPs [15] and was assessed from a clinical point of view. Considering the main aim of the thesis and that no methodological characterization for the algorithms applied was performed, this part was inserted as additional material in the Appendix.

In the following, an overview of the available methods for the quantification of gait in terms of segmentation timing and variability/stability in healthy people is proposed. Then, considering Parkinson’s disease, a general overview of the existing methods for the automatic identification of freezing of gait was reported.

1.1 Methods for gait timing estimation in healthy people

As mentioned before, high relevance in the clinical context was represented by the assessment of gait timing, which requires appropriate gait segmentation methods [16]. In order to clarify the definition of gait events (GEs) and gait temporal parameters (GTPs), their description is proposed and reported here below.

A complete gait cycle (Stride Time) begins at the heel strike (HS) of one foot and continues until the heel strike of the same foot [17]. Differently, Step Time is defined as the distance between initial contacts of the alternating feet [18]. The gait cycle consists of the stance phase and the swing phase. The stance phase, which comprises approximately 62% of the gait cycle, begins with heel strike of one foot and ends with toe off (TO) of the same foot. During this phase, the foot is weight bearing [19]. The remaining 38% of the gait cycle is represented by the swing phase, during which the foot is non-weight bearing as it moves from one step to another [19]. The stance phase of the gait cycle is further divided into different periods [18]: i) Initial contact occurs when foot contacts the ground, representing the first phase of double limb support. The aim of this phase is to stabilize the limb in preparation of the forward translation of body weight. ii) Loading response marks the beginning of the initial double limb stance and occurs after initial contact until elevation of opposite limb. The aim of Loading response is shock absorption, weight bearing stability and preservation of progression. iii) Mid-stance starts from elevation of opposite limb and lasts until both ankles are aligned in coronal plane. The body weight is fully supported on one leg. iv) Terminal stance begins when the supporting heel rises from the ground and continues until the opposite heel touches the ground; v) Pre-swing is the final phase of stance. The other limb has now begun a new stance phase and is in the initial contact phase. The limb is rapidly off loaded with a forward push to transfer the weight onto the opposite limb. Similarly, the swing phase is constituted by different periods [18]: i) Initial Swing starts when foot is lifted off the floor during the midstance phase of the other leg, and is completed when the off-loading limb is level with the leg in stance phase. ii) Mid-swing represents the moment when the limb swings forward of the body, the foot is clear of the floor. iii) Terminal swing starts from point when tibia is vertical and ends just prior the initial contact. Gait cycle phases are illustrated in Figure 1.

Figure 1. Functional divisions of the gait cycle according to Perry et al. [18].

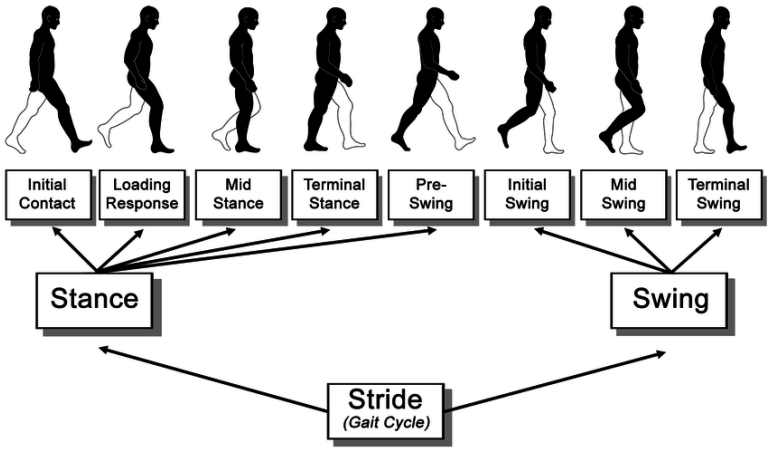

In recent years, many algorithms were proposed for the estimation of GE and GTP using IMUs. These sensors measure linear acceleration (accelerometers), angular velocity (gyroscopes) and orientation (magnetometers) of the body segment in which they are placed.

Gait events can be estimated by the recognition of specific features (e.g. peak identification and zero crossing) in the acceleration and angular velocity signals [20,20–22]. Alternatively, advanced methods for gait segmentation involving machine learning techniques, e.g. neural networks [23], hidden Markov models [24], Gaussian mixture models [25], were proposed in the literature. However, these methods are not usually implemented in commercially available packages and their implementation rely on self-determinant models, without considering the heuristic identification of specific signal features. Thus, they were not considered in the current dissertation.

Most published works proposed and tested [9,14,20,26,27] the performance of one specific algorithm in the estimation of GEs and GTPs, rarely addressing a direct comparison with others. Most of all, each study validated the single algorithm on walking tasks of healthy subjects, without characterizing the influence of different implementation features and/or without considering different environmental constraints. In this dissertation, a systematic review of the current methods implemented and applied for GE and GTP estimation using IMUs was performed. Then, the selected algorithms were classified based on the implementation characteristics, i.e. IMU position, Target variable and Computational approach.

Articles were searched in PubMed, Scopus and ISI Web of Knowledge until 20 November 2017. Searches consisted of a combination of the following keywords: (1) assessment or estimation

or measurement; (2) wearable or inertial sensor or accelerometer or gyroscope or inertial measurement unit; (3) temporal or parameters; (4) gait or walking. Keyword search was performed to match words in the title, abstract, or keyword fields. Studies published in English as full papers, involving original methods for the estimation of GEs using accelerometer and gyroscope attached to the lower trunk, shanks and feet were included based on criteria summarized in Table 1.

Table 1. Inclusion criteria considered for the systematic review.

Criteria	Definition
Measurement instruments	Wearable inertial sensors
Body positioning of IMUs	Trunk, both shanks and both feet
Motor tasks	Walking
Areas of interest	Gait events definition: Heel Strike and Toe Off Temporal parameters estimation
Publication type	Journal articles and papers in English
Participants under investigation	Healthy adults and able-bodied humans

These positionings were identified based on the higher number of citation (>500) in comparison with others (i.e. heel, pelvis on the right side, thigh, lateral tibial condyle). Only healthy and able-bodied adult humans were considered. Articles were excluded for movement activities other than gait. Articles that did not involve living human subjects, such as animal studies and articles that did not involve primary research were excluded.

The search yielded 271 (PubMed), 191 (Scopus), and 350 (ISI Web of Knowledge) results. All titles and abstracts of articles retrieved from the databases search were reviewed to exclude unrelated and duplicated articles. The full text was then retrieved and further reviewed for all articles that could not be excluded based on the title and abstract alone. After the application of inclusion and exclusion criteria a set of 36 articles were identified. Articles purposing the same implementation rules for GE estimation were grouped together and the first published and most cited ones were considered as original references for the algorithms, resulting in a final set of 17 articles [7–23].

The 17 articles resulting from the systematic review and the remaining 19 articles associated to the singular original article were reported here below in Table 2.

Table 2. Original algorithms selected for the study with position, relative number of citations, and the list of studies proposing algorithms that follow the same implementation rules, with relative number of citations.

Original algorithms	Position	Number of citations	Algorithms following the same implementation rules and relative number of citations	
Bugané et al., 2012 [26]	Trunk	59	M. Pau et al., «Clinical assessment of gait in individuals with multiple sclerosis using wearable inertial sensors: Comparison with patient-based measure», Mult. Scler. Relat. Disord., vol. 10, pagg. 187–191, nov. 2016.	7
Lee et al., 2009 [28]		7	-	
McCamley et al., 2012 [29]		51	F. A. Storm, C. J. Buckley, e C. Mazzà, «Gait event detection in laboratory and real life settings: Accuracy of ankle and waist sensor based methods», Gait Posture, vol. 50, pagg. 42–46, 2016	11
			A. Godfrey, S. Del Din, G. Barry, J. C. Mathers, e L. Rochester, «Instrumenting gait with an accelerometer: a system and algorithm examination», Med. Eng. Phys., vol. 37, n. 4, pagg. 400–407, apr. 2015.	36
Gonzaléz et al., 2010 [21]		85	-	
Shin et al., 2011 [30]		26	-	
Zijlstra et al., 2003 [31]		384	E. Grimpampi, S. Oesen, B. Halper, M. Hofmann, B. Wessner, e C. Mazzà, «Reliability of gait variability assessment in older individuals during a six-minute walk test», J. Biomech., vol. 48, n. 15, pagg. 4185–4189, nov. 2015.	10
			C. Little, J. B. Lee, D. A. James, e K. Davison, «An evaluation of inertial sensor technology in the discrimination of human gait», J. Sports Sci., vol. 31, n. 12, pagg. 1312–1318, 2013.	9
			W. Zijlstra, «Assessment of spatio-temporal parameters during unconstrained walking», Eur. J. Appl. Physiol., vol. 92, n. 1–2, pagg. 39–44, giu. 2004.	155
			R. Senden, H. H. C. M. Savelberg, B. Grimm, I. C. Heyligers, e K. Meijer, «Accelerometry-based gait analysis, an additional objective approach to screen subjects at risk for falling», Gait Posture, vol. 36, n. 2, pagg. 296–300, giu. 2012.	43
			W. Johnston, M. Patterson, N. O'Mahony, e B. Caulfield, «Validation and comparison of shank and lumbar-worn IMUs for step time estimation», Biomed. Tech. (Berl), vol. 62, n. 5, pagg. 537–545, ott. 2017.	0
			A. Hartmann, K. Murer, R. A. de Bie, e E. D. de Bruin, «Reproducibility of spatio-temporal gait parameters under different conditions in older adults using a trunk tri-axial accelerometer system», Gait Posture, vol. 30, n. 3, pagg. 351–355, ott. 2009.	52
			X. Chen, S. Liao, S. Cao, D. Wu, e X. Zhang, «An Acceleration-Based Gait Assessment Method for Children with Cerebral Palsy», Sensors, vol. 17, n. 5, pag. 1002, mag. 2017.	1
			I. González, J. Fontecha, R. Hervás, e J. Bravo, «Estimation of Temporal Gait Events from a Single Accelerometer Through the Scale-Space Filtering Idea», J. Med. Syst., vol. 40, n. 12, pag. 251, dic. 2016.	4
Lee et al., 2010 [32]	Shank	41	-	
Trojaniello et al., 2014 [27]		42	F. A. Storm, C. J. Buckley, e C. Mazzà, «Gait event detection in laboratory and real life settings: Accuracy of ankle and waist sensor based methods», Gait Posture, vol. 50, pagg. 42–46, 2016	11
Khandelwal et al., 2014 [33]		8	-	
Catalfamo et al., 2010 [34]		60	P. C. Formento, R. Acevedo, S. Ghoussayni, e D. Ewins, «Gait Event Detection during Stair Walking Using a Rate Gyroscope», Sensors, vol. 14, n. 3, pagg. 5470–5485, mar. 2014.	16
			D. Gouwanda e A. A. Gopalai, «A robust real-time gait event detection using wireless gyroscope and its application on normal and altered gaits», Med. Eng. Phys., vol. 37, n. 2, pagg. 219–225, feb. 2015.	24
Greene et al., 2010 [35]		77	B. R. Greene, D. McGrath, K. J. O'Donovan, R. O'Neill, A. Burns, e B. Caulfield, «Adaptive estimation of temporal gait parameters using body-worn gyroscopes», Conf. Proc. Annu. Int. Conf. IEEE Eng. Med. Biol. Soc. IEEE Eng. Med. Biol. Soc. Annu. Conf., vol. 2010, pagg. 1296–1299, 2010.	15

			W. Johnston, M. Patterson, N. O'Mahony, e B. Caulfield, «Validation and comparison of shank and lumbar-worn IMUs for step time estimation», Biomed. Tech. (Berl), vol. 62, n. 5, pagg. 537–545, ott. 2017.	0
Salarian et al., 2004 [20]		276	S. Wüest, F. Massé, K. Aminian, R. Gonzenbach, e E. D. de Bruin, «Reliability and validity of the inertial sensor-based Timed "Up and Go" test in individuals affected by stroke», J. Rehabil. Res. Dev., vol. 53, n. 5, pagg. 599–610, 2016.	3
Aminian et al., 2002 [36]		396	-	
Jasiewicz et al., 2006 [37]	Foot	165	S. Sessa, M. Zecca, L. Bartolomeo, T. Takashima, H. Fujimoto, e A. Takanishi, «Reliability of the step phase detection using inertial measurement units: pilot study», Healthc. Technol. Lett., vol. 2, n. 2, pagg. 58–63, mar. 2015.	5
Sabatini et al., 2005 [38]		326	D. Hamacher, D. Hamacher, W. R. Taylor, N. B. Singh, e L. Schega, «Towards clinical application: repetitive sensor position re-calibration for improved reliability of gait parameters», Gait Posture, vol. 39, n. 4, pagg. 1146–1148, apr. 2014.	23
Ferrari et al, 2016 [39]		14	-	
Mariani et al., 2013 [40]		76	-	

The 17 algorithms were revised and classified based on:

i) IMU position (i.e. lower trunk shanks, feet)

ii) Target variable (i.e. acceleration, angular velocity)

iii) Computational approach: 'peak identification' and 'zero crossing', on raw or filtered target variable (i.e. finite impulse response, FIR, infinite impulse response IIR, wavelet transform, WT filtering). 'Peak identification' aims to identify specific peaks on the target variable, corresponding to specific temporal events: local maxima or minima of the vertical or antero-posterior component for acceleration-based algorithms; local minima of the sagittal component for angular velocity-based algorithms. 'Zero crossing' aims to identify the instants of sign change in the target variable, corresponding to specific temporal events: in the antero-posterior component for acceleration-based algorithms; in the sagittal component for angular velocity-based algorithms

Of the 17 algorithms, as summarized in Table 3:

- 6 were trunk-based (of which only 2 provided both HS and TO [21,29], while 4 defined only HS [26,28,30,31]), all analysing acceleration, 3 using 'peak identification', of which 1 with IIR [26], 1 with FIR [28] and 1 with WT filtering (detecting HS and TO) [29], and 3 using 'zero crossing' approach, of which one with raw signal [30], 1 with FIR filtering (detecting HS and TO) [21] and 1 with IIR filtering [31];
- 7 were shank-based, of which 3 analysing acceleration with 'peak identification', 1 with raw signal [27], 1 with IIR [32] and 1 with WT filtering [33], and 4 analysing angular velocity

with ‘peak identification’, 2 with raw signal [20,35], 1 with IIR [34] and 1 with WT filtering [36];

- 4 were foot-based, of which 1 analysing acceleration with ‘peak identification’ of raw signal [37], and 3 analysing angular velocity, 2 with ‘peak identification’, 1 adopting raw signal [39] and 1 with IIR filtering [40] and 1 with ‘zero crossing’ of IIR filtered signal [38].

Table 3. Details of algorithms identified from the literature review classified according to the three criteria.

Algorithms	***Sensor position***	***Target Variable***	***Computational Approach***	***Analysed subjects***
Bugané et al., 2012 [26]	Trunk	Acceleration	‘peak identification’ (IIR)	Healthy
Lee et al., 2009 [28]	Trunk	Acceleration	‘peak identification’ (FIR)	Healthy Hemiplegic after stroke
McCamley et al., 2012 [29]	Trunk	Acceleration	‘peak identification’ (WT)	Healthy
Gonzaléz et al., 2010 [21]	Trunk	Acceleration	‘zero crossing’ (FIR)	Healthy
Shin et al., 2011 [30]	Trunk	Acceleration	‘zero crossing’ (Raw)	Healthy
Zijlstra et al., 2003 [31]	Trunk	Acceleration	‘zero crossing’ (IIR)	Healthy
Lee et al., 2010 [32]	Shank	Acceleration	‘peak identification’ (IIR)	Healthy
Trojaniello et al., 2014 [27]	Shank	Acceleration	‘peak identification’ (Raw)	Healthy Hemiparetic Choreic Parkinson’s disease
Khandelwal et al., 2014 [33]	Shank	Acceleration	‘peak identification’ (WT)	Healthy
Catalfamo et al., 2010 [34]	Shank	Angular velocity	‘peak identification’ (IIR)	Healthy
Greene et al., 2010 [35]	Shank	Angular velocity	‘peak identification’ (Raw)	Healthy
Salarian et al., 2004 [20]	Shank	Angular velocity	‘peak identification’ (Raw)	Healthy Parkinson’s disease
Aminian et al., 2002 [36]	Shank	Angular velocity	‘peak identification’ (WT)	Healthy
Jasiewicz et al., 2006 [37]	Foot	Acceleration	‘peak identification’ (Raw)	Healthy Spinal-cord injured
Sabatini et al., 2005 [38]	Foot	Angular velocity	‘peak identification’ (IIR)	Healthy
Ferrari et al, 2016 [39]	Foot	Angular velocity	‘peak identification’ (Raw)	Healthy Parkinson’s disease
Mariani et al., 2013 [40]	Foot	Angular velocity	‘zero crossing’ (IIR)	Healthy Parkinson’s disease

1.2 Methods for the assessment of variability and stability of gait in healthy people

In recent years, several methods for quantifying motor control during gait have been proposed in the literature using IMUs [12]. In particular, signals collected from IMUs during walking on the solid ground have been used to calculate non-linear metrics, which demonstrated their effectiveness in the prevention of falls, especially among elderly subjects and pathologic individuals, allowing quantitative evaluations of prevention and rehabilitation procedures [41].

In this context, the systematic review of the literature performed by Riva et al. [42] significantly contributed to the critical evaluation of the adoption of non-linear metrics in the field of biomechanics. Successively, lot of efforts were carried out to address methodological aspects related to the application of these metrics during walking in healthy people, evaluating the potential influence of testing conditions (i.e. environment and test protocol) [43], assessing the minimum number of strides to obtain a reliable application [44] and analysing the potential influence of reduced sampling frequency in the computation [45]. Also, analysis of the relationship between non-linear metrics and i) clinical rating scales in a subacute stroke population [46], and ii) long- short-term fall history [47] were performed. However, a lot of methodological aspects should be assessed concerning the applicability of non-linear metrics in relation to the environmental constraints (e.g. water or sand) and/or considering pathological populations.

From a mathematical point of view, the angular velocity acquired from medio-lateral angular velocity of the shank was exploited to calculate short term and long term variability of the stride time estimated *via* Poincarè Plots (PSD1, PSD2) and standard deviation of the stride time (SD), while acceleration from trunk was used to calculate non-linear metrics (e.g. harmonic ratio, HR [48], recurrence quantification analysis, RQA [49] and multiscale entropy, MSE [50]), aiming to quantify variability, harmonicity, regularity and complexity of the gait pattern [44,46,51]. More specifically, HR involves decomposing the antero-posterior (AP), vertical (V), and medio-lateral (ML) acceleration directions signal into harmonics by means of discrete Fourier transform and then analyse their spectral components [48,52], provide the regularity and harmonicity of the employed signal. RQA [42,49] provides a characterization of the nature (i.e. chaos, stochastic, noisy signal) and the stability of the observed dynamic system, based on the local recurrence of data points in the reconstructed phase space. The first implementation step of RQA is the reconstruction of the phase

space by means of delay embedding [53]. An embedding dimension of 5 and a delay of 10 samples were used, based on previous studies [12,44,54]. A distance matrix based on Euclidean distances between normalized embedded vectors was then constructed; the recurrence points were obtained by selecting a radius of 40% of the max distance [44,55], and all cells with values below this threshold were identified as recurrence points. Several measures were extracted from RQA, namely Recurrence Rate (rr), Determinism (Det), Average Length of Diagonal Line (Avg), Maximum diagonal line length (Max) and Divergence (Div). RR is the number of recurrent points in the recurrence plot expressed as a percentage of the number of possibly recurrent points and gives an indication about how often a trajectory visits a similar location in the state-space. Det is the percentage of recurrent points which fall on upward diagonal line segments and relates to how often the trajectory re-visits similar state space locations; the higher Det the more regular is the dynamic structure of the data [89,96]. Avg is the average upward diagonal line length, where the diagonal lines are defined following determinism definition. Avg is related to the velocity in the execution of the test (i.e. higher Avg is expected for slower gait), but this duration is not independent from the regularity of the pattern (i.e. the gait is slower because each stride on average is slower) [46,49]. MSE provides an assessment of the complexity of the signal at different time-scales [50]. It was implemented constructing consecutively more coarse-grained time series; this procedure implies averaging increasing numbers of data points in non-overlapping windows of length τ. Sample entropy (SE) [57] was then calculated for each coarse-grained time series to obtain entropy measures at different scales; SE quantifies the conditional probability that two sequences of m consecutive data points similar (distance of data points inferior to a fixed radius r) to each other will remain similar when one more consecutive point is included, thus reflecting the regularity of the time series [50]. MSE was calculated for values of τ ranging from 1 to 12, $m = 4$ and $r = 0.2$, as suggested by Pincus [58] and later applied by Richman and Moorman to biological time series [57]. Poincarè Plots address the variability of the analysed signal and have been widely applied for gait assessment [12,43,59]. In particular, they represent stride time data plots between successive gait cycles, displaying the correlation between consecutive stride times data in a graphical manner. Plots are used to extract indices, such as length, PSD2, and width, PSD1, of the long and the short axes describing the elliptical nature of the plots and hence the short-term and long term variability of stride time [60]. To characterize the variability of the stride time during the walking performance, its standard deviation (SD) is also used [61].

1.3 Methods for the automatic detection of freezing of gait

This dissertation focused on the influence of extrinsic and intrinsic factors on gait analysis, and Parkinson's disease was considered as an example for the algorithm characterization of a pathological population, being one the most common gait disorders in the elderly [62,63].

It is a chronic, progressive neurodegenerative disorder results from lesions of the basal ganglia, affecting motor control and function bilaterally [64]. When the disease symptoms become more pronounced, the patient experiences difficulties with hand function and walking, and prone to falls [65]. Gait disturbances affecting PDPs include reduced stride length and walking speed, increased cadence and double support duration, decreased arm oscillation and trunk rotation [62,66]. Moreover, muscle rigidity and altered activation amplitude of lower limb muscles were observed [65,67]. Freezing of gait (FOG) and festination are features of more advanced Parkinson's disease.

In particular, FOG is defined as "an episodic inability (lasting seconds) to generate effective stepping" despite the intention to walk and represent one of the most debilitating motor symptoms in PDPs [62,68,69]. Accurate FOG detection is significant for PD diagnosis and is an important prerequisite to properly treat patients and reduce both disability burden and health care costs [70]. Usually, clinical evaluation of FOG in PDPs rely on clinical observation during a control visit performed by an expert operator or is based on patient's daily reports, where motor symptom recall can be incomplete and inaccurate. These qualitative and subjective methods for FOG assessment do not allow a detailed and precise knowledge of the motor competences and their variation across time, hindering the opportunity to monitor response to therapy and motor complications, improve medical therapies, enhance surgical treatment decisions and improving rehabilitation interventions [70,71]. To achieve these goals, quantitative and objective assessments of FOG in PDPs in ecological conditions are needed. As underlined before, IMUs represent possible solutions based on wearable and non-obtrusive technologies that have been recently approached for automatic and reliable detection of FOG from inertial measures and many algorithms were implemented for the purpose [72]. Nevertheless, published works proposed and tested [72–74] the performance of one specific algorithm, never addressing a direct comparison with others. Algorithms proposed in the literature for FOG detection considered different body locations for IMU positioning and worked in different domains. In this dissertation, a systematic review of the current methods implemented and applied for FOG estimation using IMUs was performed. Then, the selected algorithms were classified based on the implementation characteristics, i.e. domain of implementation and IMU position.

A systematic search in the Web of Science, PubMed and Scopus databases was conducted until May 2019. These databases were chosen to allow both medical and engineering journals to be included in the search process. Searches consisted of a combination of the following keywords: "Freezing of gait", "Parkinson's disease", "Wearable sensors". A keyword search was performed to match words in the title, abstract, or keyword fields. To identify potentially eligible articles absent in the database, a search in the references of review articles and book chapters that appeared during the search was performed. Studies published in English, involving original and clearly explained methods to detect, measure or monitor FOG in PDPs using inertial wearable sensors located on trunk, shank and foot were included. Motor tasks involving straight walking with turning of 180° or 360° and held in a closed environment were considered. Inclusion criteria are summarized in Table 1.

Table 1. Inclusion criteria considered for the systematic review concerning FOG detection using IMUs.

Criteria	Definition
Subject	Parkinsonian able to walk alone
Measurement instruments	Wearable inertial sensors
Body positioning of IMUs	Trunk, shank and foot
Motor tasks	Straight walking with turning of 180° or 360°
Areas of interest	Instrumental analysis of FOG of the lower limbs
Participants under investigation	Parkinson's disease patients
Publication type	Journal articles and papers in English

The search yielded 443 (PubMed), 69 (Scopus), and 52 (Web of Science) results. A critical examination of the titles and abstracts allowed to exclude unrelated and duplicated articles. Then, all studies i) assessing posture, balance, FOG of the upper limbs and the language; ii) focused on patients walking with an aid (e.g. canes) and/or helped by operators or physiotherapists during the motor tasks; iii) involving time up and go tests, going up and down the stairs, concerning double tasks (e.g. the subject walks and carries an object), and tests with auditory and/or visual stimulation were excluded. After the application of inclusion and exclusion criteria a set of 7 original articles were identified.

All studies considered the visual identification of the phenomenon as gold standard for FOG detection.

The 7 algorithms were revised and classified based on:

i) Domain (i.e. frequency, time-frequency, time)

ii) IMU position (i.e. lower trunk, shank, foot)

Of the 7 algorithms:

- 5 were implemented in the frequency domain, exploiting acceleration from trunk ([75]), shank ([73,75–78]) and foot ([75,76]);
- 1 was implemented in the time-frequency domain, exploiting angular velocity of the shank ([79]);
- 1 was implemented in the time domain, exploiting acceleration of the trunk ([80]) and the shank ([80]).

The implementation of algorithms in frequency domain is based on the calculation of the Freezing Index (FI), defined as the quotient of the power spectral density (PSD) from 3 to 8 Hz (Freezing Band) and the PSD from 0.5 to 3 Hz (Walking Band) of the target variable, considering windows of variable length in relation to the implementation characteristics defined from each author. When the FI exceeds an identified threshold, a FOG episode is considered to have occurred. Most of the algorithms showed a different combination of Windows and Thresholds, that were reported together with details of implementation characteristics in Table 2.

Table 2. Details of algorithms identified from the literature review and classified according to the implementation characteristics (i.e. Domain, IMU position, Target variable); Windows and Thresholds adopted for the implementation. To assist the reader, details for Moore et al. 2013 were reported below the table.

Reference	Domain	IMU position	Target variable (component)	Window (in seconds)	Threshold
Moore et al. 2008 [73]	Frequency	Shank	Acceleration (V)	6	2.9
Jovanov et al. 2009 [76]	Frequency	Shank	Acceleration (V)	4	Manual
				6	
		Foot	Acceleration (V)	4	
				6	
Mancini et al. 2012 [77]	Frequency	Shank	Acceleration (AP)	5	2.9
Morris et al. 2012 [78]	Frequency	Shank	Acceleration (V)	4	2
				6	2
				10	2
Moore et al. 2013 [75]	Frequency	Trunk	Acceleration (V)	From 2.5 to 10 with 2.5 increment	From 0.5 to 7 with 0.5 increment
		Shank			
		Foot			
Djiuric et al. 2014 [79]	Time - Frequency	Shank	Angular velocity (ML)	-	-
Rezvanian et al. 2016 [80]	Time	Trunk	Acceleration (AP)	4	58.9
			Acceleration (ML)	4	59.1
			Acceleration (V)	4	66
		Shank	Acceleration (AP)	4	58.9
			Acceleration (ML)	4	59.1
			Acceleration (V)	4	66

Moore et al. 2013 [75]	Frequency	Shank	Acc (V)	2.5	0.5
					from 1 to 7
				5	0.5
					1
					1.5
					2
					2.5
					3
					3.5
					4
					4.5
					5
					5.5
					6
					6.5
					7
				7.5	0.5
					1
					1.5
					2
					2.5
					3
					3.5
					4
					from 4.5 to 7
				10	0.5
					1
					1.5
					2
					2.5
					3
					3.5
					4
					from 4.5 to 7
				2.5	0.5
					from 1 to 7

		Trunk		5	0.5
					1
					1.5
					2
					2.5
					3
					3.5-7
				7.	0.5
					1
					from 1.5 to 7
				10	0.5
					1
					1.5
					2
					2.5
					3
					3.5-7
		Foot		2.5	0.5
					1
					from 1.5 to 7
				5	0.5
					1
					1.5
					2
					2.5
					3
					3.5
					4
					4.5
					5
					from 5.5 to 7
				7.5	0.5
					1
					1.5
					2
					2.5
					3
					3.5
					4
					from 4.5 to 7
				10	0.5
					1
					1.5
					2
					2.5
					3
					3.5
					4
					from 5 to 7

Synthesis of findings

In the background, systematic searches concerning i) algorithms for gait segmentation, ii) metrics for stability/variability measures in healthy people, and iii) algorithms for freezing of gait identification on PDPs were conducted.

Considering gait segmentation, a final set of 17 original algorithms were identified. Algorithms were differentiated considering sensor position (trunk, shanks and feet), analysed variable (acceleration and angular velocity), and computational approach (peak identification or zero crossing).

Different metrics were identified to quantify stability, complexity, regularity and variability exploiting the acceleration and angular velocity measures provided from sensors attached to trunk and shank, namely RQA, MSE, HR and PSD1/2.

Regarding the automatic identification of FOG in PDPs, 7 original algorithms were identified. They were grouped according to domain of implementation (i.e. frequency, time-frequency, time) and sensor position (i.e. lower trunk, shank, foot).

2.

SECTION 1

INFLUENCE OF EXTRINSIC FACTORS ON THE PERFORMANCE OF ALGORITHMS IN ANALYSING THE GAIT OF HEALTHY ADULTS

Overview

The adoption of inertial sensors for the assessment of gait analysis in ecological conditions has gained an important role in sports and clinical applications. In a supervised setting, as in a clinic or in a laboratory, the external environment is controlled, and participants are focused completely on performing a specific motor task. In an unsupervised setting, the presence of extrinsic factors directly related to the environmental constraints (e.g. poor lighting, uneven walking surfaces and different weather conditions) could lead participants to move differently and adopt specific gait strategies that are more typical of every-day life circumstances. The assessment of the influence of extrinsic factors is of primary importance when analysing movements in ecological conditions and can be adopted to support the selection of specific therapies and treatments, and to provide clinically important information on subject's health status.

In this section, the effect of different environmental constraints was analysed on the gait timing estimation and the motor control of healthy people during walking. Firstly, the gait segmentation algorithms identified from the systematic literature search (and previously explained in the Paragraph 1.1 of the Background) were applied to the gait on solid ground performed in controlled laboratory conditions. Then, the same approaches were extended to a dumping surface (i.e. sand) and in the water environment. Finally, considering this latter ambient, an evaluation of the minimum number of strides required for a reliable application of non-linear metrics during walking in the water at a different level of immersion was performed.

2.1

SEGMENTATION OF GAIT ON SOLID GROUND

The content of this chapter has been published:

i) as abstract in Proceedings of the ESB-ita 2017, Rome (Italy), and of the 3D Analysis of Human Movement Symposium 2018, Manchester (United Kindom), and of the WCB 2018, Dublin (Ireland);

ii) in Pacini Panebianco, Giulia; Stagni, Rita; Fantozzi, Silvia, 'Comparative analysis of 12 methods using wearable inertial sensors for gait parameters estimation during walking', Gait & Posture 57s (2017), 21

iii) as original paper in: G. Pacini Panebianco, M.C. Bisi, R. Stagni, S. Fantozzi, 'Analysis of the performance of 17 algorithms from a systematic review: Influence of sensor position, analysed variable and computational approach in gait timing estimation from IMU measurements', Gait & Posture. 66 (2018) 76–82

Introduction

As highlighted in the Paragraph 1.1 of the Background, the quantification of gait temporal parameters (i.e. step time, stance time) is crucial in human motion analysis and requires the accurate identification of gait events. With the widespread use of inertial wearable sensors, many algorithms were proposed and applied for the purpose. Nevertheless, most published works proposed and tested [20,21,26,28–30,32,34,36–40,81,82] the performance of one specific algorithm, rarely addressing a direct comparison with others. Studies approaching the comparisons of different algorithms usually limited the analysis to the positioning of IMUs [28,81–83]. Storm et al. [82] and Ben Mansour et al. [81] assessed the accuracy of two and three algorithms, respectively, based on shank-worn and lower trunk-worn IMUs. Storm et al. [82] demonstrated that lower trunk method performed worse than shank one in GE detection, but GTP estimation resulted satisfactory with both. Ben Mansour et al. [81] showed that shank method, analysing angular velocity, was the most accurate in estimating both GEs and GTPs, followed by lower trunk acceleration for GEs and shank acceleration for GTPs. Trojanello et al. [83] tested the performance of 5 different methods for GE detection using a single IMU attached to the lower trunk, showing an acceptable accuracy, sensitivity and robustness of all the evaluated methods in determining GTPs requiring the identification of HS, while a worse accuracy was found in determining GTPs requiring also TO identification (e.g. stance duration). These findings highlight differences in the performance of the analysed algorithms as related to different parameters, potentially suggesting that the choice of the most appropriate algorithm can also depend on the specific research question. Moreover, the few available comparison studies analysed each algorithm as a whole, not addressing the influence of specific implementation characteristics, except for sensor positioning, and not providing a comprehensive overview of the numerous solutions proposed in the literature. Only few studies [37,81] compared the combined effect of positioning and target variable, considering either linear acceleration or angular velocity at different positions, but still neglecting the analysis of the computational approach adopted. To date, no comprehensive analysis has been published, investigating the performance of the available algorithms for GE detection as resulting from their specific implementation characteristics. The present study was designed to fill in this gap, starting from a systematic review of the available literature to identify the different proposed methods, aiming to provide relevant information for the selection of the most suitable algorithm for specific applications, and/or for the design and implementation of novel methods for GE detection. The performance of the algorithms was analysed in controlled conditions, to identify methodological intrinsic characteristics, without potential interferences of gait alterations.

Materials and Methods

Participants:

Thirty-five young healthy participants (17 females, 18 males; 26.0±3.8 years; 1.72±0.08 m; 69.0±13.1 Kg) were recruited in the study. All participants were physically active and self-reported no musculoskeletal or neurological disorder. The Bioethics Committee of the University of Bologna approved the study on 12/6/2017 with protocol number 60193, and informed consent was signed by all participants.

Data acquisition:

Each participant walked for 2 minutes back and forth along a 10 m straight pathway at self-selected speed (normalized gait speed: 0.41±0.06 [24]) wearing own comfortable footwear.

Five tri-axial IMUs (Cometa, Milano, Italy sf=285 Hz; accelerometer: sensitivity 156,3 mV/g, range ± 8g; gyroscope: sensitivity 1,3 mV/g, range ±1000°/s weighs less than 8 grams) were attached to the trunk (at L5 level), shanks (about five centimetres above lateral malleolus), and feet (on the dorsal surface of each shoe) (Figure 2). 3D acceleration and 3D angular velocity were acquired from each sensor with a sampling frequency of 285Hz, higher than that in all referred works. Ground reaction forces were recorded (sampling frequency 1000Hz) by two force platforms (Kistler, Winterthur, Switzerland) mounted half-way along the path, assumed as gold standard reference for GE detection. A trigger signal was generated by IMU system at the beginning of each trial for synchronization. The online version of this article contains the collected data.

Figure 2. Attachment of IMU on the different body locations and relative axis orientations.

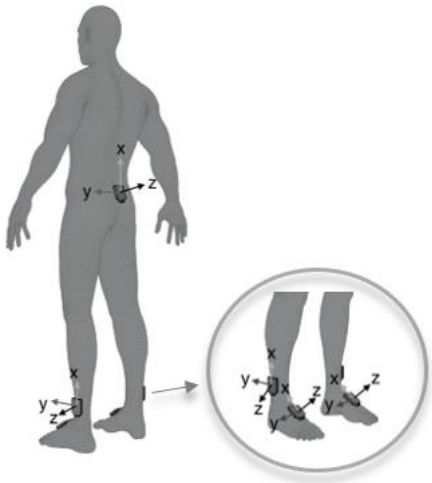

Data analysis:

The 17 algorithms identified from the literature review and reported in detail in the Background Chapter were implemented in MATLAB (MathWorks 2017a, NATHSK, USA), and HS and TO were estimated from IMU data for each participant with each algorithm. A 20N threshold was applied to ground reaction force (GRF) vertical component for the automatic detection of HS and TO [84] for each participant.

For each algorithm, the error (E) was calculated for GEs (E_{GE}) and GTPs (E_{GTP}) as follow:

$$E_{GE} = GE_{IMU} - GE_{GRF} \quad (1)$$

$$E_{GTP} = GTP_{IMU} - GTP_{GRF} \quad (2)$$

Where GE subscripts denote methods of estimation.

If an algorithm allowed identifying only HS, errors were calculated for HS and step time.

Statistical analysis:

12 contacts per participants were included in the statistical analysis. For each parameter (GEs and GTPs), a linear mixed model [85] was applied to test the dependency of error values on each implementation criterion, with a significance level of 0.05. First, the statistical analysis was performed to investigate the influence of IMU position and target variable, alone. Then, the influence of computational approach was investigated separately for each IMU position. Med of the error was calculated to characterize accuracy, and to characterize repeatability Dmed, calculated as 75th percentile minus 25th percentile value of the error. Data processing was performed in MATLAB (MathWorks, Natick, USA), and statistical analysis using R software (R-Core Team., Vienna, Austria, version 3.4.3 2017).

Results

For each subject at least 12 contacts on the force platform were detected, for a total of 420 analysed strides. No false positive or negatives were identified for all the analysed algorithms. Statistical analysis highlighted significant differences for all three implementation characteristics, although the magnitude of errors was comparable.

IMU Position

For HS detection error, no significant difference was found between shank- and trunk-based algorithms ($p=0.978$), while significant differences ($p<0.001$) were found for foot-based algorithms with respect to the others. By analysing error results in detail, shank- and foot-based algorithms resulted more accurate and repeatable in HS detection than trunk-based ones. Foot-based algorithms showed comparable accuracy (Med 63 ms and 62 ms, respectively) and repeatability (Dmed 59 ms and 44 ms, respectively) to shank-based ones, while trunk-based ones resulted less accurate (Med 70 ms) and less repeatable (Dmed 113 ms). For TO detection, statistically significant differences were found for all IMU positions ($p<0.001$). In particular, foot-based algorithms showed the highest accuracy and repeatability, with Med 2 ms and Dmed 57 ms; shank-based algorithms followed with Med -29 ms and Dmed 96 ms; trunk-based ones provided the worst performance with Med -66 ms and Dmed 164 ms. For step time estimation, results showed comparable accuracy and repeatability among all IMU positions (Med/Dmed: 6/41 ms, 6/32 ms, 2/47 ms, for trunk, shank, and foot, respectively). For stance time, foot-based algorithms showed the highest accuracy and repeatability (Med/Dmed -64/120 ms), followed by shanks-based (Med/Dmed -88/151 ms) and trunk-based ones (Med/Dmed -111/159 ms).

Target variable

For HS detection, algorithms exploiting angular velocity showed higher repeatability and comparable accuracy than those exploiting acceleration (Med/Dmed 65/40 ms and 60/111 ms, for angular velocity and acceleration, respectively). For TO detection, angular velocity-based algorithms performed significantly ($p<0.001$) higher than acceleration-based ones in terms of repeatability, with Dmed 68 ms, smaller than the 122 ms of acceleration-based ones, but a lower accuracy, with Med -25 ms versus 6 ms. Acceleration-based algorithms resulted more and equally accurate for stance and step time, respectively, but less repeatable than angular-velocity ones for both parameters (step time Med/Dmed: 7/34 ms and 2/43 ms; stance time Med/Dmed: -84/65 ms, -69/106 ms, for angular velocity and acceleration, respectively).

Error characteristics for HS and TO as related to IMU position and target variable are schematically depicted in Figure 3, and for step and stride time in Figure 4. Numerical values as related to IMU position and target variable are reported in Table 1 and 2, respectively.

Figure 3. Box plot (minimum, 25th percentile, median, 75th percentile, maximum values) for HS (a) and TO (b) estimation errors as related to IMU position and target variable (angular velocity contoured in dots, acceleration no contour) (* p<0.001).

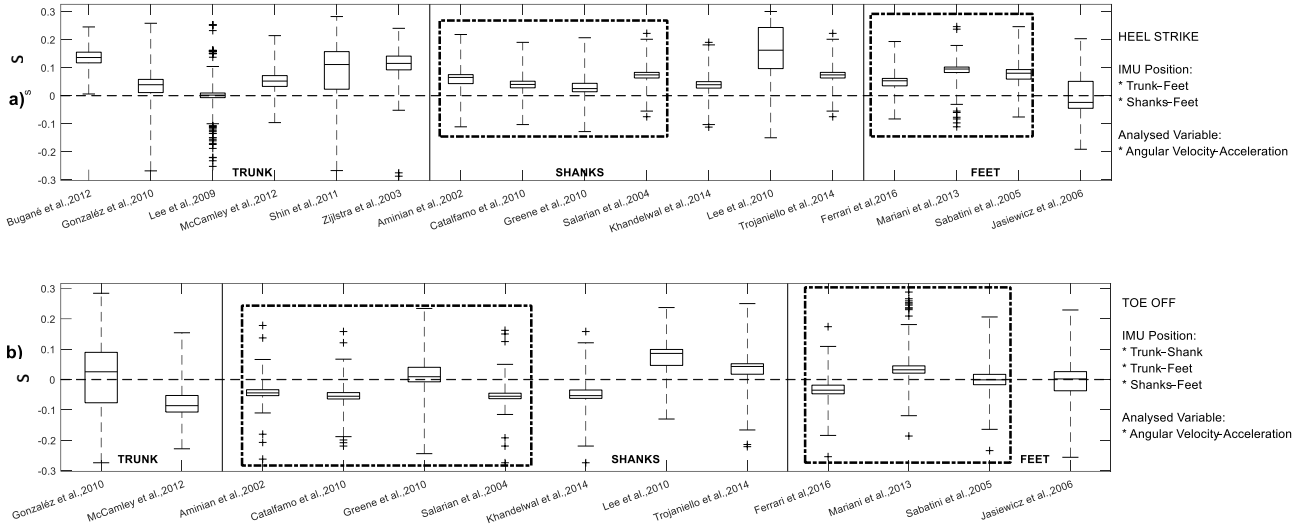

Figure 4. Box plot (minimum, 25th percentile, median, 75th percentile maximum values) for step time (a) and stance time (b) estimation errors as related to IMU position and target variable (angular velocity contoured in dots, acceleration no contour) (* p<0.001).

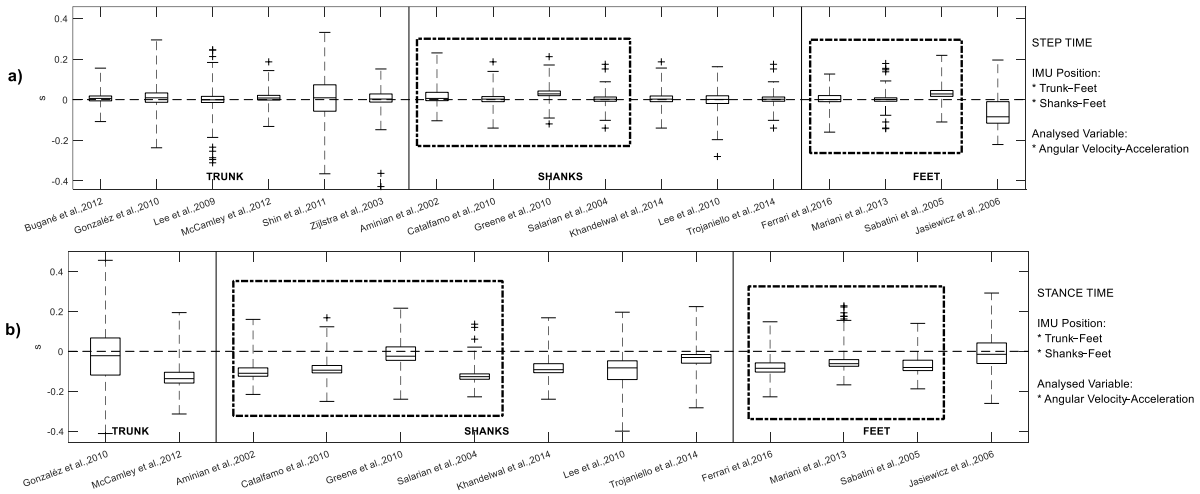

Table 1. Results of statistical analysis for IMU positioning: minimum, 25th quartile, median, 75th quartile, maximum value of estimation error for HS, TO, step time and stance time (* $p<0.001$).

Parameter	*Estimation of errors: IMU position (s)*			*Level of significance*
	Trunk	*Shanks*	*Feet*	
HS	-0.287, 0.015, 0.070, 0.128, 0.282	-0.150, 0.037, 0.062, 0.081, 0.300	-0.191, 0.032, 0.063, 0.091, 0.246	Trunk – Shank Trunk – Feet * Shanks – Feet *
TO	-0.228, -0.097, -0.066, 0.067, 0.284	-0.262, -0.055, -0.029, 0.041, 0.250	-0.256, -0.027, 0.002, 0.030, 0.288	Trunk – Shank * Trunk – Feet * Shanks – Feet *
Step Time	-0.484, -0.013, 0.006, 0.028, 0.484	-0.421, -0.008, 0.006, 0.024, 0.230	-0.221, -0.021, 0.002, 0.026, 0.218	Trunk – Shank Trunk – Feet * Shanks – Feet *
Stance Time	-0.412, -0.145, -0.111, 0.014, 0.456	-0.400, -0.117, -0.088, -0.034, 0.224	-0.261, -0.090, -0.064, -0.030, 0.292	Trunk – Shank Trunk – Feet * Shanks – Feet *

Table 2. Results of statistical analysis for Target variable: minimum, 25th quartile, median, 75th quartile, maximum value of estimation error for HS, TO, step time and stance time (* $p<0.001$).

Parameter	*Estimation of errors: Target variable (s)*		*Level of significance*
	Angular velocity	*Acceleration*	
HS	-0.128, 0.043, 0.065, 0.083, 0.246	-0.287, 0.014, 0.060, 0.125, 0.300	Angular Velocity – Acceleration *
TO	-0.262, -0.051, -0.025, 0.017, 0.288	-0.256, -0.062, 0.006, 0.060, 0.284	Angular Velocity – Acceleration *
Step Time	-0.160, -0.006, 0.007, 0.028, 0.230	-0.484, -0.021, 0.002, 0.022, 0.484	Angular Velocity – Acceleration *
Stance Time	-0.251, -0.111, -0.084, -0.046, 0.228	-0.412, -0.117, -0.069, -0.011, 0.456	Angular Velocity – Acceleration *

Computational approach

Considering the trunk-based algorithms, statistically significant differences were found between the two approaches ($p<0.05$). In particular, 'peak identification' approach with FIR filtering resulted to be the most accurate (Med 2ms) and repeatable (Dmed 16ms) in HS detection. The 'zero crossing' approach with FIR filtering resulted the most accurate (Med 26ms) in TO detection, while 'peak identification' with WT filtering resulted to be the most repeatable (Dmed 54ms). For step time, no significant difference was found among different filtering for each approach ($p>0.597$ for all comparisons among filtering). For stance time, 'zero crossing' with FIR filtering resulted to be the most accurate, while 'peak identification' with WT filtering highlighted the highest repeatability (Med/Dmed: -22/186 ms, -159/32 ms, respectively). Shank-based algorithms exploited only 'peak identification' approach: WT filtering reported the highest accuracy and repeatability in HS detection (Med 47 ms and Dmed 36 ms), while raw data resulted to be the most accurate and repeatable in TO detection (Med -2 ms and Dmed 89 ms). Raw or filtered signals resulted to be equally accurate and repeatable in step time estimation; significant differences were found only between raw signal and IIR filtering, which showed comparable accuracy and repeatability

(Med/Dmed: 8/33 ms and 2/31 ms, respectively). For stance time estimation, raw signal resulted to be the most accurate (Med -46ms), while WT filtering showed the highest repeatability (Dmed 45ms). Considering foot position of IMUs, statistically significant differences ($p<0.05$) were found between the two computational approaches. In particular, 'peak identification' on raw signal resulted to be the most accurate (Med 44 ms) in HS detection, while 'zero crossing' with IIR filtering resulted to be the most repeatable both for HS and TO (Dmed 19 ms and 24 ms, respectively). Referring to the accuracy in TO estimation, 'peak identification' with IIR filtering (Med -1 ms) resulted the most accurate. For GTPs, 'zero crossing' with IIR filtering (Med/Dmed 1/17 ms) resulted the most accurate and repeatable in step detection. No statistically significant difference was found between approaches for stance time ($p=0.676$). Numerical values of error characteristics for GE and GTP as related to computational approach are reported in Table 3. Results are summarized in Figure 5.

Figure 5. Estimated error for HS (a) and TO (b) as related to IMU position, target variable (angular velocity represented by triangles, acceleration represented by circles) and computational approach (zero crossing in grey and peak detection in black).

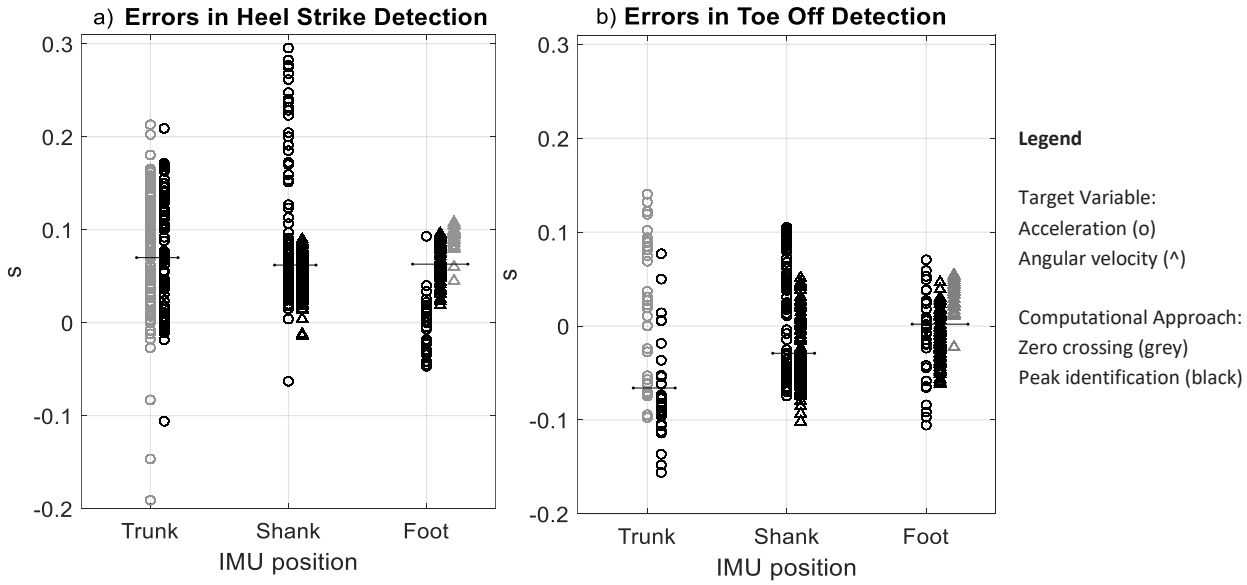

Table 3. Results of statistical analysis for computational approach: minimum, 25th quartile, median, 75th quartile, maximum value of estimation error for HS, TO, step time and stance time (* $p<0.001$, ** $p\leq0.05$)

IMU position	*Parameter*	*Level of significance 'peak identification' vs 'zero crossing'*	*Estimation of errors: Filtering (s) Level of significance*			
			Filtering within 'peak identification'	*Level of significance for filtering within 'peak identification'*	*Filtering within 'zero crossing'*	*Level of significance for filtering within 'zero crossing'*
Trunk	HS	*	FIR: -0.252, -0.007, 0.002, 0.009,0.252 IIR: 0.006, 0.117, 0.136, 0.155, 0.245 WT: -0.096, 0.033, 0.052, 0.071, 0.214	FIR – IIR * FIR – WT * IIR – WT *	Raw: -0.267,0.024, 0.111, 0.157, 0.282 FIR: -0.268, 0.011, 0.039, 0.058,0.258 IIR: -0.287, 0.092, 0.115, 0.141, 0.240	FIR – IIR * FIR – Raw * IIR – Raw *
	TO	*	WT: -0.228, -0.107, -0.086, -0.053, 0.154	-	FIR: -0.223, -0.077,0.026, 0.089, 0.284 Raw: -0.365, -0.057,0.009,0.073,0.331	FIR – Raw
	Step Time	**	FIR: -0.484, -0.014, -0.001, 0.016, 0.484 IIR: -0.428, -0.009, 0.005, 0.022, 0.155 WT: -0.132, -0.002, 0.008, 0.021, 0.186	FIR – IIR FIR – WT IIR – WT	FIR: -0.237, -0.012,0.009,0.033,0.294 Raw: -0.365, -0.057,0.009,0.073, 0.331	FIR – Raw
	Stance Time	*	WT: -0.314, -0.159, -0.137, -0.105, 0.194	-	FIR: -0.412, -0.119, -0.022,0.067,0.456	-
Shank	HS	-	Raw: -0.128, 0.038, 0.066, 0.079, 0.222 IIR: -0.150, 0.050, 0.076, 0.163, 0.300 WT: -0.112, 0.031, 0.047, 0.067, 0.218	IIR – Raw * IIR – WT * Raw – WT *	-	
	TO		Raw: -0.244, -0.047, -0.002, 0.042, 0.250 IIR: -0.234, -0.017, -0.001, 0.017, 0.206 WT: -0.262, -0.059, -0.048, -0.034, 0.178	IIR – Raw * IIR – WT * Raw – WT *		
	Step Time		Raw: -0.140, -0.005, 0.008, 0.028, 0.212 IIR: -0.280, -0.014, 0.002, 0.017, 0.186 WT: -0.421, -0.008, 0.005, 0.023, 0.230	IIR – Raw ** IIR – WT Raw – WT		
	Stance Time		Raw: -0.283, -0.118, -0.046, -0.018, 0.224 IIR: -0.400, -0.116, -0.092, -0.058, 0.196 WT: -0.240, -0.117, -0.099, -0.072,0.168	IIR – Raw * IIR – WT Raw – WT *		
Foot	HS	*	Raw: -0.191, -0.028, 0.044, 0.059, 0.203 IIR: -0.076, 0.059, 0.080, 0.093, 0.246	IIR – Raw *	IIR: -0.111, 0.083, 0.095,0.102,0.246	-
	TO	*	Raw: -0.256, -0.046, -0.024, 0.009, 0.229 IIR: -0.234, -0.017, -0.001, 0.017, 0.206	IIR – Raw *	IIR: -0.186, 0.021,0.032, 0.045, 0.288	
	Step Time	**	Raw: -0.221, -0.087, -0.010, 0.011, 0.195 IIR: -0.110, 0.016, 0.028, 0.045, 0.218	IIR – Raw *	IIR: -0.143, -0.008, 0.001, 0.009, 0.178	
	Stance Time	-	Raw: -0.261, -0.093, -0.059, 0.001, 0.292 IIR: -0.188, -0.096, -0.081, -0.045, 0.140	IIR – Raw *	IIR: -0.168, -0.075, -0.062, -0.042,0.228	

Discussion

The present study analysed the performance of 17 published algorithms proposed for GE detection from IMU data. The algorithms were selected based on a systematic review and analysed with respect to the influence of IMU position, target variable and computational approach on estimated errors on GEs and derived GTPs.

IMU position

Trunk-based algorithms exhibited a worse performance than shank- and foot-based ones in GE detection. Taking into account the IMU sampling period of 3.5ms, minor differences between the latter two can be considered negligible for HS detection, while foot-based algorithms performed better than shank-based ones both in terms of accuracy and repeatability for TO detection. Generally, error bias resulted in a delay of HS (the largest for trunk-based algorithms, the lowest for

shank- and feet-based algorithms) and an anticipation of TO (the smallest for foot-based algorithms, increasing moving towards shank and trunk) as illustrated in Figure 4. This behaviour justifies the trend observed in the analysed GTPs: step time estimate (derived from HS alone) does not result significantly affected by IMU positioning, while stance time (derived from HS and TO) resulted always underestimated, increasingly from the foot to the trunk. These results provide more detail but are in line with the literature [31,37,38,84].

Target variable

Acceleration-based algorithms: i) resulted more accurate than angular velocity-based ones for TO detection, while differences in accuracy were negligible for HS detection; ii) resulted less repeatable for both HS and TO detection, as supported by the lower values of the intra-class correlation coefficient obtained for shanks and feet acceleration compared to the angular velocity; iii) provided always lower repeatability but better accuracy in stance time and similar accuracy in step time estimation. Jasiewicz et al. [37] found that either linear acceleration or angular velocity of IMUs attached to the foot performed equally in terms of accuracy in GE detection, while Ben Mansour et al. [81], comparing trunk and shank position, showed that shank angular velocity allowed better accuracy for both GEs and GTPs, followed by trunk and shank acceleration for GEs and GTPs, respectively. These differences can be justified considering that their analysis focused only on foot- or shank/trunk- based algorithms, neglecting the influence of different IMU positioning and/or computational approach.

Computational approach

Computational approach resulted to affect performance differently, depending on IMU position. For the computational approach, IMU position have to be taken into account. Considering trunk-based algorithms, ‘peak identification’ with FIR filtering showed the best performance in HS detection, due to the effectiveness of the filter in emphasizing the main acceleration peak associated to HS [28]. For TO detection, ‘peak identification’ with WT filtering resulted the most repeatable while ‘zero crossing’ with FIR filtering resulted the most accurate, in line with the literature [21,29]. No statistically significant difference was found in step time estimation, demonstrating that gait cycle duration can be estimated from the recording of a single IMU, independently from the computational approach [83]. Conversely, stance time was affected by the approach used as observed for TO identification. Considering IMUs positioned on the shanks, the best performance was obtained using ‘peak identification’ with WT filtering for HS and on raw signal for TO detection, in line with the literature [27,86]. Similarly to trunk-based algorithms, computational

approach did not influence step time estimation, while stance estimation varied significantly depending on signal pre-processing: estimation on raw signal resulted to be the most accurate, while a pre-processing with WT filtering provided the best repeatability. Regarding foot positioning, the best accuracy was obtained with 'peak identification' on raw and IIR filtered signal for HS and TO, respectively: this result could be expected, since sharp peaks in angular velocity or acceleration during HS and TO are the more empathized and easy to detect, the closer to the ground the IMU is located [27]. On the other hand, the best repeatability in GE detection was obtained from 'zero crossing' with IIR filtering, which represented a robust way for detecting gait cycles both in healthy and pathological populations [40]. The delay introduced by this approach in HS detection (positive Med), resulted compensated in step estimation (Med 1 ms), exhibiting the best accuracy and reproducibility in the parameter estimation. Conversely, no significant difference was found for stance time estimation between the two approaches.

The potential concurrent influence of different factors was analysed and did not result to affect the performance at the same extent for all analysed factors. Eventual concurrent influence was reported where relevant (e.g. sensor position when discussing computational approach). Most of the algorithms (independently from IMU position, target variable and computational approach) showed comparable performance when estimating step time, while attention is needed for stance duration and GEs. Future studies will address different situations (e.g. ecological conditions, varying walking speed), different sensor type and sampling frequency, as well as populations characterized by altered gait patterns (e.g. children, elderlies, pathological populations) [27,36,87], and will include the assessment of algorithms' specificity and sensitivity, as possible false positive/negatives may occur in these conditions.

In conclusion, all analysed factors resulted to affect GE and GTP estimation. No proposed algorithm can be generally preferred over the others, but the reported results can support researchers in the choice of the most suitable algorithm/algorithms based on experimental condition (e.g. number/type/placement of sensors) and research question (e.g. mean/variability of the selected gait variable). Finally, these results can support future design of novel and more efficient detection algorithms.

2.2

SEGMENTATION OF GAIT IN WATER

The content of this chapter has been published in G. Pacini Panebianco, M.C. Bisi, A.L. Mangia; R. STagni; S. Fantozzi, Gait events estimation using inertial wearable sensors while walking in water, Gait & Posture, 66 (2018), Supplement 1, pp. 28 – 29 and has been submitted to Computer Methods and Programs in Biomedicine as full length article.

Introduction

The water environment plays a relevant role in rehabilitation programs [88]. During aquatic therapy, the buoyancy, the drag force, and the pressure exerted by water reduce the gravitational load on joints, resist motion, and increase proprioception [89–92]. In recent years, Walking in Water (WW) has become extensively used for people with specific gait deviations [88] and represents one of the fundamental motor tasks performed during aquatic therapy [92]. It is recommended for developing and maintaining cardiorespiratory and muscular fitness [93], can be adopted to speed up recovery from minor orthopedic injuries [94], offers clear advantages over the land-based equivalent for populations with high risk of fall such as older adults and neurological patients [95], and can be practiced by individuals without swimming skills [96].

Assessment of motor performance during WW, based on quantitative motion analysis, would support the understanding of water-induced biomechanical modifications and the design and/or monitoring of WW based rehabilitation.

In quantitative motion analysis, the assessment of temporal parameters is of primary importance and requires the correct identification of gait events (GEs, i.e. Foot Contact, FC and Foot Off, FO) [9,97]. Various technologies (i.e. force platforms, instrumented mats, footswitches) can be exploited for identifying GE when Walking on Dry Land (WDL), but no validated instrumentation is available for gait timing identification in the water environment, as highlighted by Matsumoto et al., 2008 [98], relying on video recordings for GE identification. Several studies analysing gait cycle in water exploited a camera-based approach [88,92,93,98], although its drawbacks: i) the limited field of view allowing to analyse only one/two consecutive steps; ii) the time-consuming set-up and post-processing [88,93].

In recent years, the widespread use of IMUs has led to the proposal and implementation of a large number of algorithms for gait segmentation for WDL [9,83]. A recent comprehensive analysis of the available algorithms for GE detection in healthy subjects during WDL [9], highlighted how the specific performance is significantly affected by sensor placement, analysed variable, and computational approach even in ideal conditions. Actually, the design of the available gait segmentation algorithms exploits the identification of specific features that can be identified in the gait pattern of healthy subjects during DLW. The mechanical characteristics of WW, as well as perturbed and pathological conditions, can alter these patterns [88]. Thus, WW can significantly affect the performance of such gait segmentation algorithms. On the other hand, no algorithm was proposed for the segmentation of WW.

The present work was designed to quantify how the alterations of the gait pattern associated to WW affects the performance of 17 different algorithms, designed for GE estimation in WDL.

The results of the present study are meant to support the selection of the most appropriate available algorithm for GE estimation in WW, and to serve the possible design of more efficient ones.

Materials and Methods

Analysed algorithms

17 algorithms for GE and GTP estimation which were reported in the Background for WDL, were here analysed for WW. Following the same approach [9], the algorithms were classified based on:

i) IMU position (i.e. trunk, shanks, feet)
ii) Target variable (i.e. acceleration, angular velocity)
iii) Computational approach: 'peak identification' and 'zero crossing', on raw or filtered target variable (i.e. FIR, IIR, WT filtering).

Experimental analysis

Participants:

Ten young adult healthy participants (5 females, 5 males; age 26.2±3.3 years; height 1.71±0.07 m; weight 65.4±8.6 Kg) were recruited in the study. All participants were physically active and self-reported no musculoskeletal or neurological disorder. The Bioethics Committee of the University of Bologna approved the study on 13/07/2018 with protocol number 99412, and informed consent was signed by all participants.

Data acquisition:

Each participant walked 5 times back and forth along a 10 m straight pathway at self-selected speed in 2 conditions: i) WDL; ii) WW at 1.2m depth with water temperature of 28°C wearing water shoes and keeping the arms on the water surface. No device (e.g. metronome or timer) was used to control the walking speed, not to interfere with the natural walking pattern [99]. Before the WW analysed trial, participants performed an acclimatisation trial.

Five tri-axial IMUs (Cometa, Italy, sf=285 Hz; technical specifications were reported in Chapter 2.1) were attached to the trunk (at L5 level), shanks (about five centimetres above lateral malleolus), and feet (on the dorsal aspect of each shoe) (Figure 6). The walking tasks were also

filmed using a video camera (Hero4, GoPro, USA, sf=240Hz, 848x480 pixels resolution) for GE detection reference. IMU led flashing was video-recorded and used for time-synchronization of IMU and video recording. During WDL trails, ground reaction forces (GRF) were also recorded using two force platforms (Kistler, Winterthur, Switzerland, sf=1000Hz) mounted half-way along the pathway. A trigger signal was generated by IMU system at the beginning of each trial for synchronization with the force platforms.

Figure 6. Attachment of IMU on different body location.

Data analysis:

Average gait speed was calculated from reference video during WDL and WW as the ratio between straight walked distance and time.

For WDL, FC_{GRF} and FO_{GRF} were automatically identified applying a 20 N threshold to the vertical component of the GRF recordings [84]. FC_{GoPro} and FO_{GoPro} denoting the Foot Contact and Foot Off captured by GoPro videos were visually identified for each participant and trial.

The measurement error of video-based assessment was estimated considering the GRF as reference:

$$E_{ref} = GE_{GoPro} - GE_{GRF} \quad (3)$$

For WW, FC_{GoPro} and FO_{GoPro} were visually identified as for WDL, and FC_{IMU} and FO_{IMU} were estimated from IMU measurements using the selected 17 algorithms [9], implemented in MATLAB (MathWorks 2017a, USA).

For each algorithm, the sensitivity in GE identification during WW was calculated, considering in this case the video as reference, as:

$$\frac{\text{Number of GEs identified by algorithm}}{\text{Number of all GEs as identified by video}} \quad (4)$$

For each target variable of the 17 selected algorithms, ICC of the mean stride cycle over the whole sequence of each trial for WW and WDL was calculated to analyse the repeatability of the pattern over the trial in each condition.

ICC of the mean WDL stride cycle over the WW sequence was calculated, to analyse the similarity of the pattern during WW with respect to the one during WDL, assumed as reference for the algorithm design.

For each algorithm and each condition, coefficient of variation (CV) of the analysed target signal was calculated as:

$$\frac{\text{Difference between 75th and 25th percentile over the stride cycle}}{\text{Abs(median of the median value over the stryde cycle)}} \quad (5)$$

Only the algorithms reporting a minimum sensitivity of 81% [83] were considered for further analysis.

GTPs were calculated from GE.

For each algorithm, the error was calculated for GE and GTP, considering the video as reference, as:

$$E_{GE} = GE_{IMU} - GE_{GoPro} \quad (6)$$

$$E_{GTP} = GTP_{IMU} - GTP_{GoPro} \quad (7)$$

Statistical analysis:

For each parameter (FC, FO, Stride Time, Step Time, Stance Time, Swing Time), a linear mixed model [3] was applied to test the dependency of error values on each implementation criterion, with a significance level of 0.05 using R software (R-Core Team 2017, Austria, version 3.4.3). First, the statistical analysis was performed to investigate the influence of IMU position and target variable, alone. Then, the influence of analysed variable and computational approach were investigated separately for each IMU position.

Median value (Med) of the error was calculated to characterize accuracy, and the Dispersion around Med (Dmed, 75^{th} percentile – 25^{th} percentile values of the error) to characterize repeatability.

Results

Gait speed normalised according to Hof [100] resulted 0,33±0,06 for WDL and 0,17±0,08 for WW.

Maximum measurement error of video- versus GRF-reference resulted 0.05 s for both FC and FO.

During WW, 32 FCs and FOs were identified and analysed for each participant, for a total of 320 FCs and FOs.

No algorithm exploiting a sensor on the trunk passed the 81% sensitivity criterion, as well as well as no acceleration-based algorithm, independently from sensor placement, with the exception of two, both exploiting a sensor positioned on the shank and a peak identification approach: i) Khandelwal et al. [101] on WT signal; ii) Lee et al. [102] on a IIR transformed signal.

After the sensitivity analysis, only algorithms exploiting a peak identification approach for shank positioned, and only angular velocity based for foot positioned sensor underwent further error analysis.

Algorithms that passed the 81% sensitivity criterion showed an ICC for WW above or equal to 0.70, with an ICC of WDL stride cycle applied to WW ranging from 0.31 to 0.61. On the other hand, algorithms that did not pass the 81% sensitivity criterion showed an ICC for WW below 0.60, with an ICC of WDL stride cycle applied to WW ranging from 0.10 to 0.34, with the only exception of Trojanello et al. [8], showing an ICC for WW equal to 0.79 but an ICC of WDL stride cycle applied to WW of only 0.11.

No trend was observed for the CV of the variable analysed by each algorithm.

Sensitivity and ICC analysis results are summarised in Table 1.

Table 1: Details of the analysed algorithms classified according to the three criteria (i.e. IMU position, analysed variable and computational approach); sensitivity of algorithms in FC and FO identification; ICC, CV and plots with Median, 25th and 75th percentile of the different target signals in relation to the implementation criterions defined on the normalized stride time and referred to (1) WDL, (2) WW, (3) WDL and WW (thicker lines for WDL plots). The field 'Algorithm information' contains Reference, Imu Position, Target Variable (Direction), Computational Approach.

Algorithm information	***Sensitivity (%)***	***WDL***			***WW***			***WDL and WW***	
	FC FO	***ICC***	***CV***	***Plot***	***ICC***	***CV***	***Plot***	***ICC***	***Plot***
Bugané et al., 2012 • Trunk • Acceleration (AP) • peak identification (IIR)	< 81	0.79	Min: 1.34 Medn: 2.68 Max: 11.27	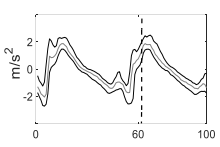	0.33	Min: 3.29 Medn: 4.21 Max: 6.49	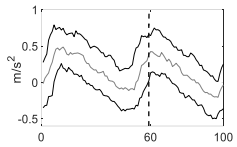	0.24	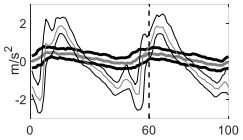
Lee et al., 2009 • Trunk • Acceleration (AP) • peak identification (FIR)		0.79	Min: 1.34 Medn: 2.65 Max: 11.10	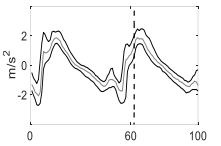	0.33	Min: 3.29 Medn: 4.21 Max: 6.49	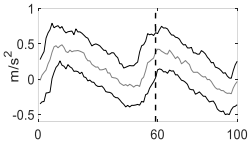	0.23	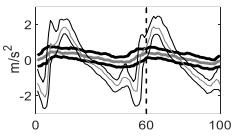
McCamley et al., 2012 • Trunk • Acceleration (V) • peak identification (WT)		0.90	Min: 1.81 Medn: 2.93 Max: 7.92	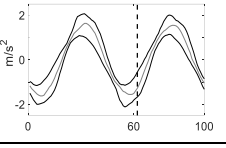	0.37	Min: 164.87 Medn: 229.03 Max: 362.88	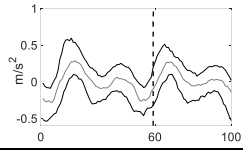	0.10	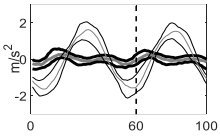
Gonzaléz et al., 2010 • Trunk • Acceleration (AP) • zero crossing (FIR)		0.82	Min: 1.47 Medn: 2.50 Max: 8.97	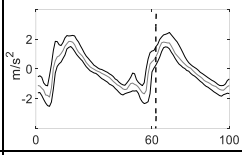	0.34	Min: 3.12 Medn: 3.95 Max: 6.30	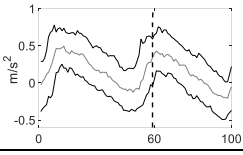	0.23	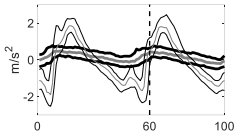
Shin et al., 2011 • Trunk • Acceleration (3D) • zero crossing (Raw)		0.76	Min: 731.96 Medn: 1063.6 Max: 3042.30	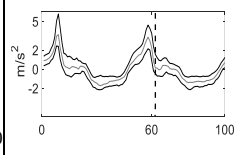	0.19	Min: 4.47 Medn: 6.71 Max: 13.70	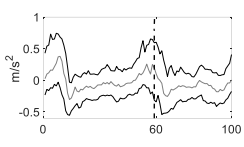	0.15	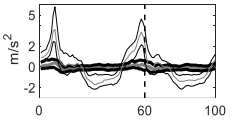
Zijlstra et al., 2003 • Trunk • Acceleration (AP) • zero crossing (IIR)		0.93	Min: 2.91 Medn: 5.28 Max: 8.30	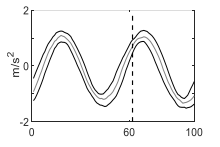	0.44	Min: 2.24 Medn: 3.02 Max: 4.28	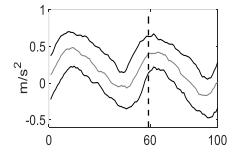	0.34	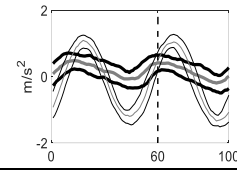
Lee et al., 2010 • Shank • Acceleration (3D) • peak identification (IIR)	98,44 99,69	0.91	Min: 0.79 Medn: 2.17 Max: 6.73	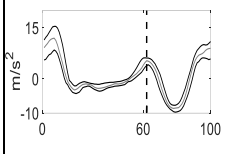	0.70	Min: 30.62 Medn: 154.97 Max: 490.01	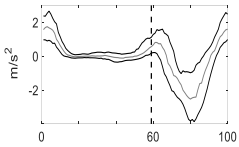	0.31	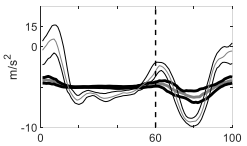
Trojaniello et al., 2014 • Shank • Acceleration (AP) • peak identification (Raw)	< 81	0.75	Min: 1.70 Medn: 5.40 Max: 35.28	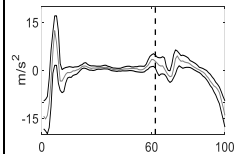	0.79	Min: 4.07 Medn: 6.12 Max: 13.78	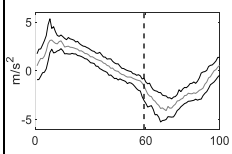	0.11	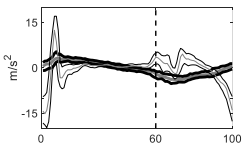
Khandelwal et al., 2014 • Shank • Acceleration (3D) • peak identification (WT)	97,50 99,38	0.91	Min: 2.08 Medn: 14.72 Max: 31.15	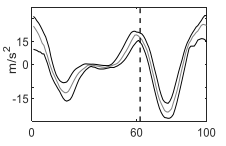	0.76	Min: 4.54 Medn: 17.97 Max: 42.02	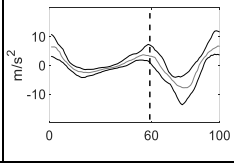	0.56	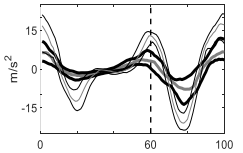

Catalfamo et al., 2010 • Shank • Angular velocity (ML) • peak identification (IIR)	98,13 100	0.97	Min: 0.33 Medn: 1.08 Max: 3.52	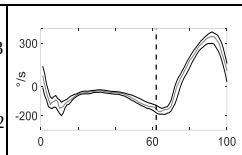	0.86	Min: 0.52 Medn: 1.43 Max: 5.96	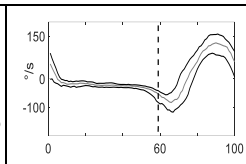	0.61	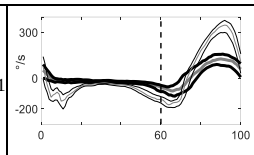
Greene et al., 2010 • Shank • Angular velocity (ML) • peak identification (Raw)	98,13 99,69	0.96	Min: 0.34 Medn: 1.08 Max: 3.45	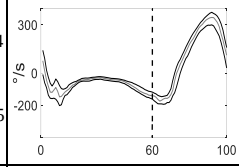	0.86	Min: 0.50 Medn: 1.45 Max: 5.96	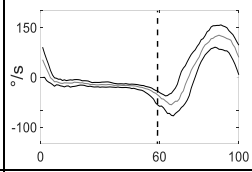	0.61	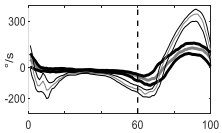
Salarian et al., 2004 • Shank • Angular velocity (ML) • peak identification (Raw)	100 100	0.96	Min: 0.34 Medn: 1.08 Max: 3.45	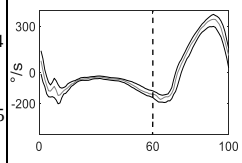	0.86	Min: 0.50 Medn: 1.45 Max: 5.96	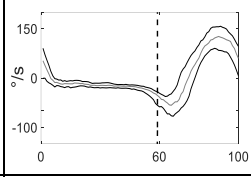	0.61	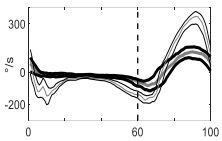
Aminian et al., 2002 • Shank • Angular velocity (ML) • peak identification (WT)	98,13 100	0.96	Min: 0.29 Medn: 1.08 Max: 3.45	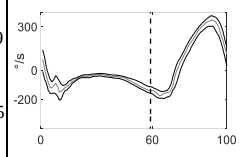	0.86	Min: 0.52 Medn: 1.41 Max: 5.92	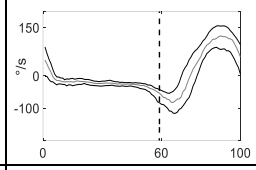	0.61	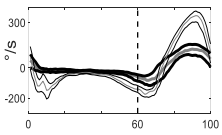
Jasiewicz et al., 2006 • Foot • Acceleration (AP) • peak identification (Raw)	< 81	0.76	Min: 0.47 Medn: 1.57 Max: 15.07	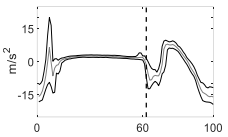	0.56	Min: 5.73 Medn: 15.34 Max: 38.80	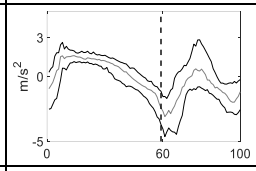	0.19	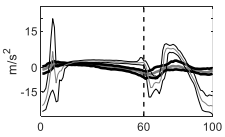
Sabatini et al., 2005 • Foot • Angular velocity (ML) • peak identification (IIR)	99,38 100	0.95	Min: 1.23 Medn: 8.67 Max: 36.37	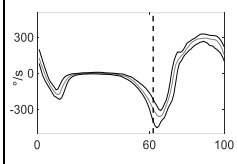	0.82	Min: 1.45 Medn: 4.56 Max: 12.34	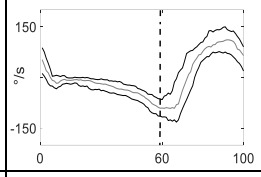	0.56	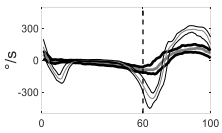
Ferrari et al, 2016 • Foot • Angular velocity (ML) • peak identification (Raw)	93,44 95,31	0.94	Min: 1.28 Medn: 9.13 Max: 41.38	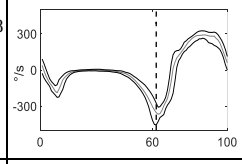	0.82	Min: 1.58 Medn: 4.83 Max: 13.55	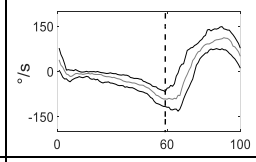	0.54	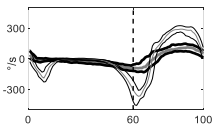
Mariani et al., 2013 • Foot • Angular velocity (ML) • zero crossing (IIR)	98,75 99,69	0.94	Min: 1.31 Medn: 8.91 Max: 38.63	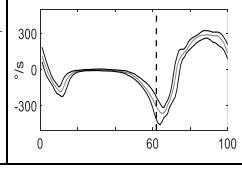	0.82	Min: 1.38 Medn: 4.39 Max: 11.72	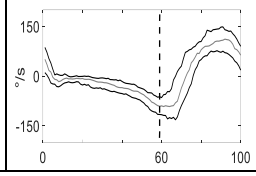	0.55	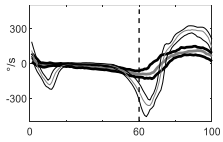

In general, FC and FO estimates resulted delayed, with this delay being compensated in Stride and Step time estimates, while Stance Time was under- and Swing Time over-estimated.

In more detail, considering the different implementation characteristics:

IMU Position

For GE, significant differences were found between Shank- and Foot-based algorithms: Shank-based algorithms resulted equally accurate and repeatable in FC estimation (Med/Dmed: 0.25/0.15 s for both Shank and Foot), but with different error distribution, and equally accurate and more repeatable in FO estimation (Med/Dmed: 0.20/0.20 s and 0.20/0.30 s, for Shank and Foot, respectively) than Foot-based ones.

For GTP, no significant difference was found for Stride and Step time estimates, while Shank-based algorithms resulted equally accurate but more repeatable in Stance Time (Med/Dmed: -0.05/0.25 s and -0.05/0.35 s, for Shank and Foot, respectively) and less accurate but more repeatable in Swing Time estimation (Med/Dmed: 0.05/0.25 s and 0.00/0.35 s, for Shank and Foot, respectively) than Foot-based ones.

Target variable

For GE, Acceleration based algorithms resulted equally accurate but more repeatable for FC (Med/Dmed: 0.25/0.15 s and 0.25/0.20 s, for Acceleration and Angular velocity, respectively), and less accurate and equally repeatable in FO estimation (Med/Dmed: 0.30/0.20 s and 0.15/0.20 s, for Acceleration and Angular velocity, respectively) than Angular velocity-based ones.

For GTP, no significant difference was found in Stride time and Step time estimation, while Acceleration-based algorithms resulted more accurate and equally repeatable in Stance time estimation (Med/Dmed: 0.00/0.25 s and -0.10/0.25 s, for Acceleration and Angular velocity, respectively), and Swing time estimation (Med/Dmed: -0.00/0.25 s and 0.10/0.25 s, for Acceleration and Angular velocity, respectively) than Angular velocity-based ones.

Error characteristics for FC (a), FO (b), Stride- (c), Step- (d), Stance- (e) and Swing time (f) as related to IMU position and target variable are schematically depicted in Figure 7, while error distribution is reported in Table 2.

Figure 7: Box plot (minimum, 25th percentile, median, 75th percentile, maximum values) for FC (a), FO (b), Stride- (c), Step- (d), Stance- (e), and Swing time (f) estimation errors as related to IMU position and target variable. Acceleration-based algorithms are framed in dashes. (* $p < 0.05$)

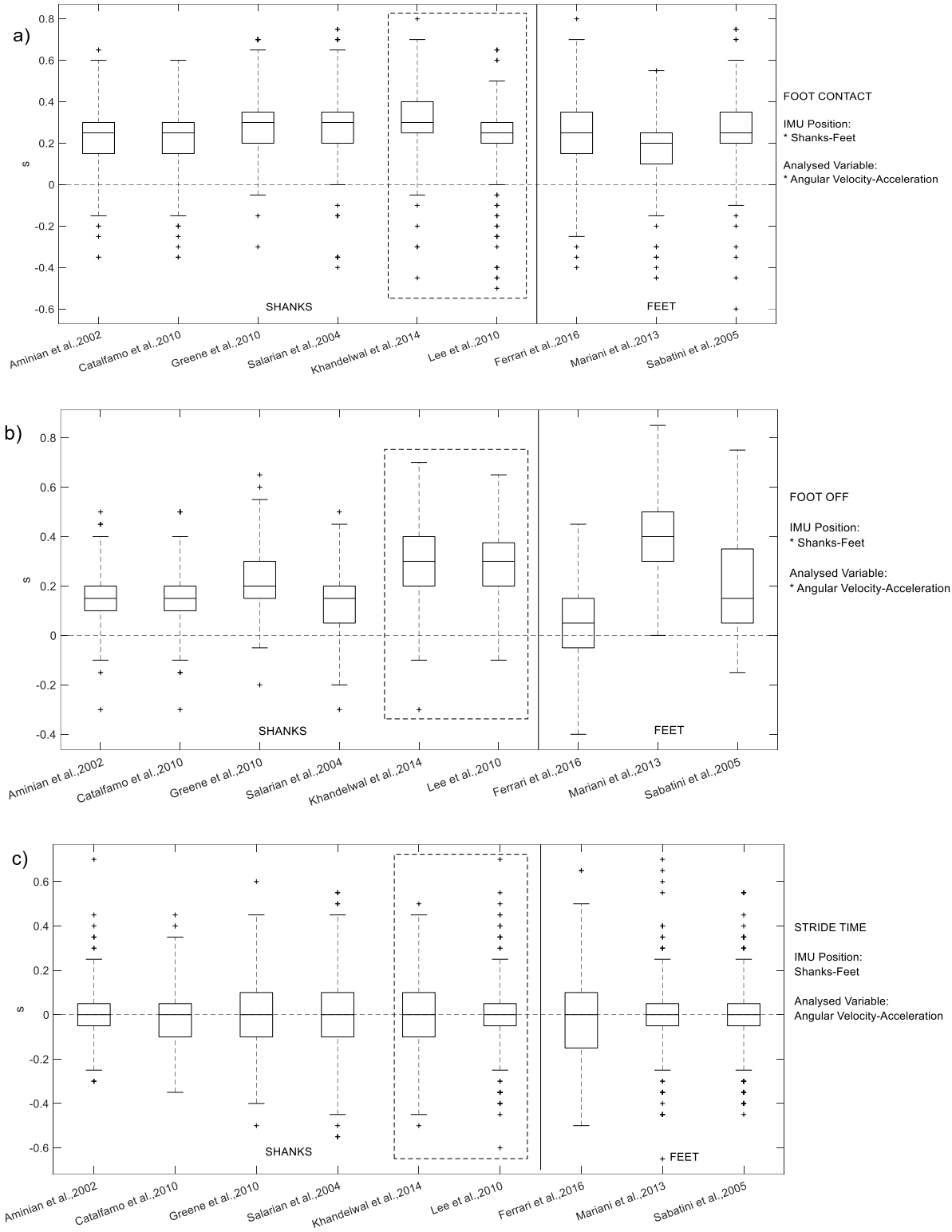

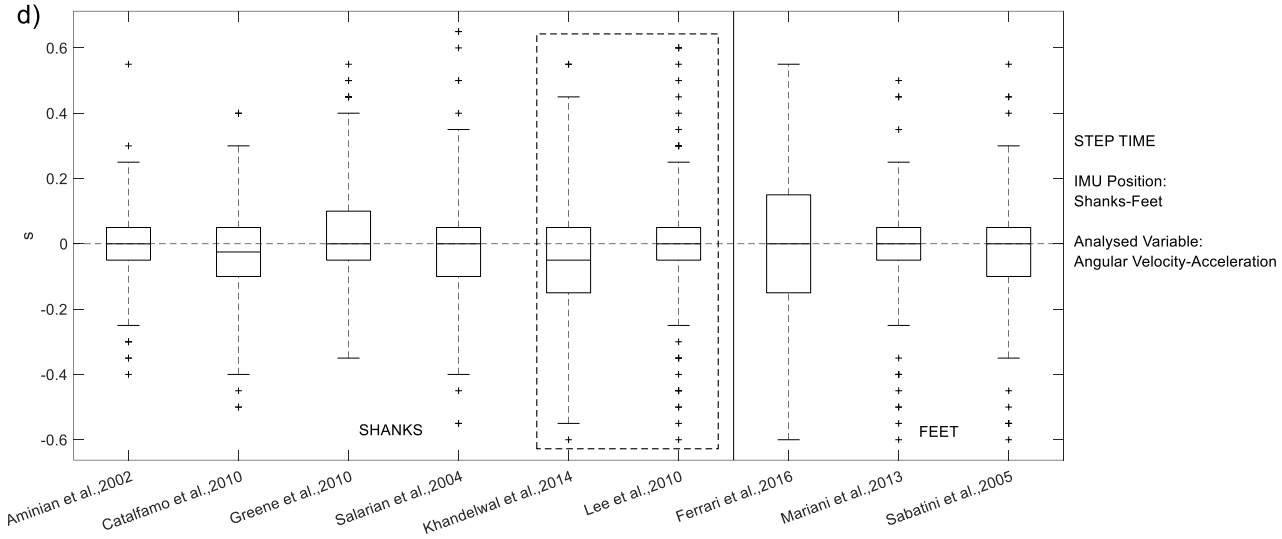
d)
0.6
0.4
0.2
0
-0.2
-0.4
-0.6
s
SHANKS
FEET
STEP TIME
IMU Position:
Shanks-Feet
Analysed Variable:
Angular Velocity-Acceleration
Aminian et al.,2002
Catalfamo et al.,2010
Greene et al.,2010
Salarian et al.,2004
Khandelwal et al.,2014
Lee et al.,2010
Ferrari et al.,2016
Mariani et al.,2013
Sabatini et al.,2005

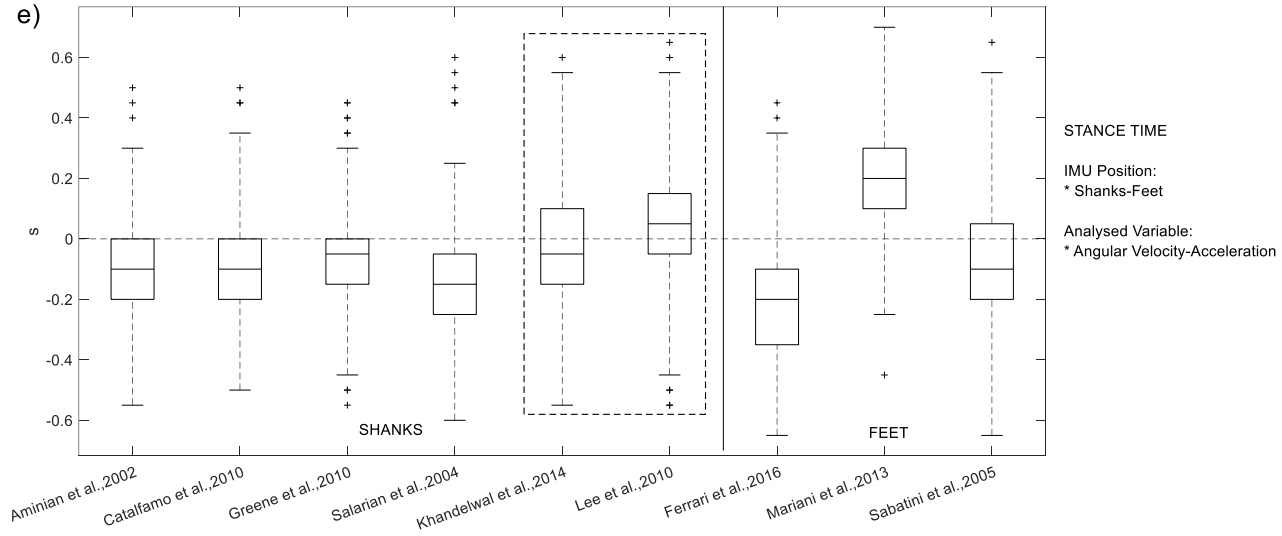
e)
0.6
0.4
0.2
0
-0.2
-0.4
-0.6
s
SHANKS
FEET
STANCE TIME
IMU Position:
* Shanks-Feet
Analysed Variable:
* Angular Velocity-Acceleration
Aminian et al.,2002
Catalfamo et al.,2010
Greene et al.,2010
Salarian et al.,2004
Khandelwal et al.,2014
Lee et al.,2010
Ferrari et al.,2016
Mariani et al.,2013
Sabatini et al.,2005

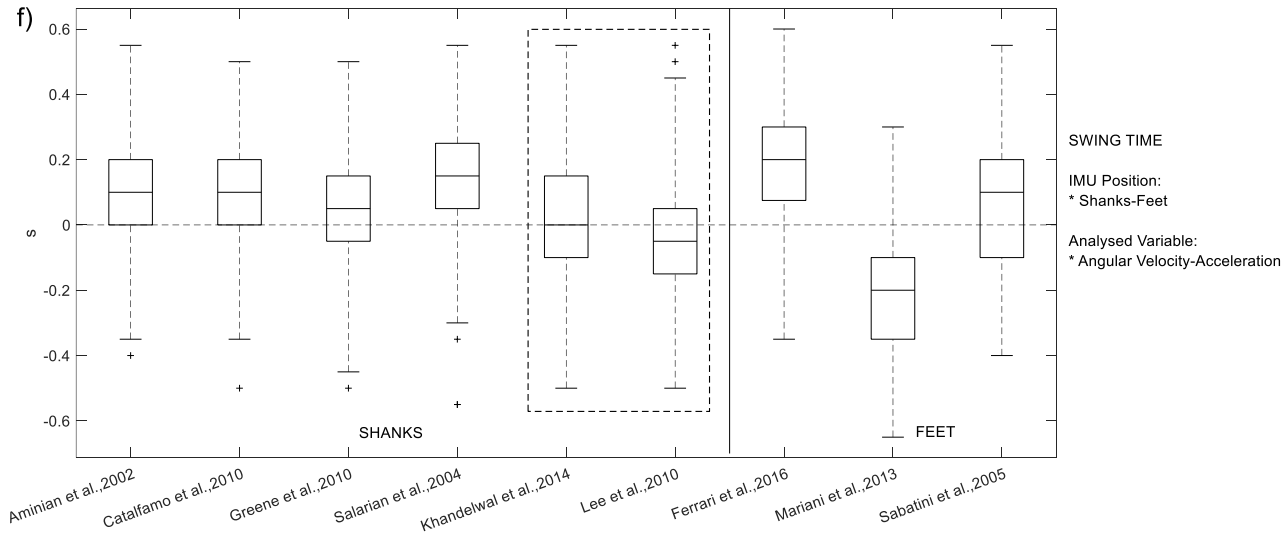
f)
0.6
0.4
0.2
0
-0.2
-0.4
-0.6
s
SHANKS
FEET
SWING TIME
IMU Position:
* Shanks-Feet
Analysed Variable:
* Angular Velocity-Acceleration
Aminian et al.,2002
Catalfamo et al.,2010
Greene et al.,2010
Salarian et al.,2004
Khandelwal et al.,2014
Lee et al.,2010
Ferrari et al.,2016
Mariani et al.,2013
Sabatini et al.,2005

Table 2: Results of statistical analysis for IMU positioning and target variable for WW: 25th quartile, median and 75th quartile of estimation error for FC, FO, stride time, step time, stance time and swing time (* $p<0.05$).

Parameter	***Estimation of errors: IMU position (s)***		***Level of significance***
	Shanks	***Feet***	Shanks – Feet
FC	0.20, 0.25, 0.35	0.15, 0.25, 0.30	*
FO	0.10, 0.20, 0.30	0.05, 0.20, 0.35	*
Stride Time	-0.10, 0.00, 0.05	-0.10, 0.00, 0.05	
Step Time	-0.10, 0.00, 0.05	-0.10, 0.00, 0.10	
Stance Time	-0.20, -0.05, 0.05	-0.20, -0.05, 0.15	*
Swing Time	-0.05, 0.05, 0.20	-0.15, 0.00, 0.20	*
Parameter	***Estimation of errors: target variable (s)***		***Level of significance***
	Acceleration	***Angular velocity***	Angular Velocity – Acceleration
FC	0.20, 0.25, 0.35	0.15, 0.25, 0.35	*
FO	0.20, 0.30, 0.40	0.10, 0.15, 0.30	*
Stride Time	-0.10, 0.00, 0.05	-0.10, 0.00, 0.05	
Step Time	-0.10, 0.00, 0.05	-0.10, 0.00, 0.10	
Stance Time	-0.10, 0.00, 0.15	-0.20, -0.10, 0.05	*
Swing Time	-0.15, 0.00, 0.10	-0.05, 0.10, 0.20	*

Computational approach

Shank-based algorithms exploited only ‘peak identification’ approach. Raw and WT filtering performed equally (Med/DL: 0.30/0.15 s), but less accurate and repeatable than IIR (Med/DL: 0.25/0.10 s) in FC estimation, while IIR and WT performed equally (Med/DL: 0.20/0.20 s), but equally accurate and less repeatable than Raw (Med/DL: 0.20/0.15 s) in FO estimation. Considering GTP, no significant difference was found among Raw, IIR and WT for Stride and Step time estimation in terms of accuracy, with decreasing (Med/DL: 0.00/0.20 s, 0.00/0.15 s, and 0.00/0.10 s, for Raw, IIR and WT, respectively) and equal repeatability (Med/DL: 0.00/0.15 s, for all) for Stride and Step time estimation, respectively; on the other hand, Raw, WT and IIR showed and increasing accuracy, respectively, in Stance and Swing time estimation, but Raw and WT resulted more repeatable than IIR (Med/DL: -0.10/0.20 s, 0.00/0.25 s, and -0.05/0.20 s, for Raw, IIR and WT, respectively for Stance Time; Med/DL: 0.10/0.20 s, 0.00/0.25 s, and 0.05/0.20 s, for Raw, IIR and WT, respectively for Swing Time).

Foot-based algorithms exploited both ‘peak identification’ (both Raw and IIR for filtering) and ‘zero crossing’ (only IIR for filtering) approaches, as applied to angular velocity. ‘zero crossing’ with IIR resulted more accurate in FC, but less accurate in FO estimate than ‘peak identification’, where IIR resulted equally accurate in FC estimate and less accurate in FO estimate than Raw, with comparable repeatability. No significant difference was found in Stride and Step time estimation for both computational approach and filtering technique. On the other hand, ‘zero crossing’ with IIR:

i) delayed and resulted more repeatable, while 'peak identification' anticipated Stance time; ii) anticipated and resulted less accurate, while 'peak identification' delayed' Swing time. For both GTP IIR resulted more accurate than Raw.

Error values and statistical analysis for computational approach are reported in Table 3.

Table 3: Results of statistical analysis for computational approach during WW: 25th quartile, median and 75th quartile of estimation error for FC, FO, stride time, step time, stance time and swing time (* $p<0.05$).

IMU position	Parameter	Level of significance 'peak identification' vs 'zero crossing'	Estimation of errors: Filtering (s) Level of significance			
			Filtering within 'peak identification'	Level of significance for filtering within 'peak identification'	Filtering within 'zero crossing'	Level of significance for filtering within 'zero crossing'
Shank	FC	-	Raw: 0.20, 0.30, 0.35 IIR: 0.20, 0.25, 0.30 WT: 0.20, 0.30, 0.35	IIR – Raw * IIR – WT * Raw – WT	-	
	FO		Raw: 0.10, 0.20, 0.25 IIR: 0.10, 0.20, 0.30 WT: 0.10, 0.20, 0.30	IIR – Raw * IIR – WT Raw – WT *		
	Stride Time		Raw: -0.10, 0.00, 0.10 IIR: -0.10, 0.00, 0.05 WT: -0.05, 0.00, 0.05	IIR – Raw IIR – WT Raw – WT		
	Step Time		Raw: -0.05, 0.00, 0.10 IIR: -0.10, 0.00, 0.05 WT: -0.10, 0.00, 0.05	IIR – Raw * IIR – WT Raw – WT *		
	Stance Time		Raw: -0.20, -0.10, 0.00 IIR: -0.15, 0.00, 0.10 WT: -0.15, -0.05, 0.05	IIR – Raw * IIR – WT * Raw – WT *		
	Swing Time		Raw: 0.00, 0.10, 0.20 IIR: -0.10, 0.00, 0.15 WT: -0.05, 0.05, 0.15	IIR – Raw * IIR – WT * Raw – WT *		
Foot	FC	*	Raw: 0.15, 0.25, 0.35 IIR: 0.20, 0.25, 0.35	IIR – Raw	IIR: 0.10, 0.20, 0.25	-
	FO	*	Raw: -0.05, 0.05, 0.15 IIR: 0.05, 0.15, 0.35	IIR – Raw *	IIR: 0.30, 0.40, 0.50	
	Stride Time		Raw: -0.15, 0.00, 0.10 IIR: -0.05, 0.00, 0.05	IIR – Raw	IIR: -0.05, 0.00, 0.05	
	Step Time		Raw: -0.15, 0.00, 0.15 IIR: -0.10, 0.00, 0.05	IIR – Raw	IIR: -0.05, 0.00, 0.05	
	Stance Time	*	Raw: -0.35, -0.20, -0.10 IIR: -0.20, -0.10, 0.05	IIR – Raw *	IIR: 0.10, 0.20, 0.30	
	Swing Time	*	Raw: 0.10, 0.20, 0.30 IIR: -0.10, 0.10, 0.20	IIR – Raw *	IIR: -0.35 -0.20, -0.10	

Discussion

The analysis of temporal parameters is primary in quantitative gait analysis, therefore, in recent years, the wide spreading use of wearable inertial sensors lead to the design and implementation of a number of different algorithms for the temporal segmentation of gait. A recent paper [9] analysed the performance of these algorithms as applied to the gait of healthy young subjects on dry land. This is the ideal condition for the application of the addressed segmentation algorithms, which are designed to identify specific features in the reference gait pattern of the specific target variable. Still, the performance of the analysed algorithms resulted to be significantly affected by sensor position, target variable, and computational approach [9].

On the other hand, while WW, the load discharge resulting from the thrust of Archimedes and the resistance and inertial effect provided by water determine mechanical conditions leading to an alteration of the gait pattern with respect to WDL [88], thus, potentially affecting the performance of the available segmentation algorithms.

Accordingly, the present work highlighted a significant reduction in the sensitivity of the analysed algorithms for WW. Based on the values of the ICC, sensitivity still resulted over the 81% threshold when the gait pattern of the target variable was sufficiently repeatable (ICC for WW above or equal to 0.70), although differing from the WDL pattern (ICC of WDL over WW from 0.31 to 0.61). On the other hand, sensitivity was below threshold when WW pattern was not repeatable enough (ICC for WW below 0.60), and when it differed too much from the reference WDL one, like for Trojanello et al. [27], showing a repeatable WW pattern (ICC for WW 0.79) but very different from WDL one (ICC of WDL over WW 0.11). According to the reported results, ICC analysis can provide an effective method for the objective preliminary evaluation of performance of a specific algorithm to the segmentation of an altered gait pattern.

In particular, no Trunk-based algorithm passed the sensitivity criterion, while Shank- and Foot-based ones provided better performance, with Shank-based ones performing slightly better in terms of repeatability. The failure of Trunk-based algorithms is associated to the aforementioned drop in WW gait pattern repeatability, but also to the disappearing of the pendulum pattern characterizing the reference WDP pattern [103], while for the shanks and feet, ICC values of WDL pattern over WW result higher due to the still occurring alternate swing of the lower limbs, associated to bi-pedal progression. Nevertheless, due to the alteration of the pattern during WW, Shank- and Foot-based algorithms did no longer perform as differently as for WDL [9].

Considering the influence of target variable, acceleration never passed the sensitivity criterion, with the only exception of 2 Shank-based algorithms [101,102]. Nevertheless, these two resulted slightly more repeatable in FC-, less accurate in FO identification, more accurate in Stance- and Swing-time estimates than Angular-velocity based ones.

For computational approach, no final conclusion can be drawn, given that for Shank-based algorithms only peak identification approach was applied to both acceleration and angular velocity, while both peak identification and zero crossing resulted applied to only angular velocity for Foot-based ones. Therefore, the analysis can hardly evaluate the performance of the computational approach independently from sensor location.

The limited accuracy of the video-based reference for GE identification for WW can be considered a limitation of the present study. On the other hand, no other reference measure was available in the water environment, and the relevant minimal detectable difference was considered in the statistical analysis, supporting the reliability of the results.

In conclusion, according to the results of the present research work: i) no available Trunk-based algorithm is suitable to gait segmentation for walking in water, due to the disappearance of pendulum mechanics; ii) angular velocity based algorithms with sensor located on the shank and feet result more reliable in terms of sensitivity than acceleration based ones, but not in terms of accuracy and repeatability; iii) no final conclusion can be drawn regarding the computational approach, independently form sensor location and target variable. The results of the present work can support the selection of the most appropriate algorithm for specific research questions, and the design of novel segmentation algorithms, better addressing altered gait patterns.

2.3

SEGMENTATION OF GAIT ON A DUMPING SURFACE (SAND)

Part of the content of this chapter has been published in Pacini Panebianco G., Bisi M.C., Mangia A.L., Stagni R., Fantozzi S. 'Analysis of temporal gait parameters during walking on sand using inertial wearable sensors' Gait & Posture 66 (2018), Supplement 1, pp. 29-30, and was submitted to Gait and Posture as full length article.

Introduction

Walking on sand involves metabolic, functional, and biomechanical changes compared to walking on solid ground [104–107]. The energy cost of walking on sand is larger compared to grass [104] or firm surfaces [105]. In particular, walking on sand requires up to 2.5 times more mechanical work than does walking on a hard surface at the same speed [108]: the shifting nature of the soil [106] leads to reduced and variable stiffness [109] and reduced elastic response [110]. While walking on solid surface guarantees an equally distributed and reproducible plantar pressure, maintaining a fluid and regular walking pattern on sand requires an increased control and adaptation associated to increased muscles activity [107] [111] for stabilization and propulsion. The altered walking conditions tend to increase joint range of motion, to strengthen the muscles, to improve balance in injury safe training conditions[111]. Sand training was demonstrated to improve blood lipid profile and to reduce risk of fall in elderly women [106], as well as to improve gait pattern in individuals with multiple sclerosis [112], and to enhance gait endurance in chronic stroke patients [113]. Therefore, walking on sand represents an easily accessible, effective, safe, and inexpensive training and rehabilitative activity [106,112] that has raised significant interest in recent years, requiring a better understanding of its functional and biomechanical characteristics.

Most of the studies assessing walking on sand were performed on the beach, investigating only energy consumption [108,114]. The quantitative analysis of joint kinematics and mechanical work was limited to laboratory controlled conditions using stereophotogrammetry and force platforms, with difficulties in the replication of the sand surface [107,112]. To date, no quantitative analysis has been published, investigating biomechanical aspects of walking on sand in ecological conditions. In this context, one of the fundamental aspects that should be addressed is the objective and quantitative estimation of gait temporal parameters (GTP). Specifically, the measurement of GTP is essential for the assessment of gait abnormalities, the quantitative evaluation of treatment outcomes [18] and the understanding and management of rehabilitation [61,97,115]. However, the quantification of GTP requires, first of all, to identify gait events (GEs, i.e. Foot Contact, FC, and Foot Off, FO)[1]. The correct identification of GEs and related GTP on sand could be adopted to design specific treatments and therapies for injured or pathological people. In this perspective, IMUs represent the optimal solution for the estimation of GEs out of the laboratory, thanks to their

[1] Beyond this point, FC and FO will be used instead of HS and TO, considering possible alteration in GEs due to different environmental constraints.

portability, low costs and limited invasiveness. In fact, a lot of algorithms were implemented and proposed for gait segmentation during over-ground walking using IMUs [9].

To date, no standard methodology for gait segmentation specific for the beach environment is available. Thus, the aim of this work was to provide relevant information for the selection of the most suitable algorithm for estimation of GEs and GTPs from IMU measurements on the sand, starting from the ones proposed for gait segmentation on hard surface.

Materials and Methods

Analysed algorithms

17 algorithms for GE and GTP estimation, previously selected and analysed by Pacini et al. [9] for WDL, were here analysed for WW. Following the same approach [9], the algorithms were classified based on:

iv) IMU position (i.e. trunk, shanks, feet)
v) Target variable (i.e. acceleration, angular velocity)
vi) Computational approach: 'peak identification' and 'zero crossing', on raw or filtered target variable (i.e. FIR, IIR, WT filtering).

Experimental analysis

Participants:

Seven healthy participants (3 females, 4 males; age 31,7±10,0 years; height 1,72±0,04 m; weight 66,9±7,8 Kg) were recruited in the study. All participants were physically active and self-reported no musculoskeletal or neurological disorder. The Bioethics Committee of the University of Bologna approved the study on 9/10/2017 with protocol number 105554, and informed consent was signed by all participants.

Data acquisition:

Each participant walked barefoot 3 times back and forth along a 20 m straight pathway at self-selected speed in 3 conditions: i) hard surface (even concrete blocks); ii) wet sand; iii) dry sand. Measures of angular velocity and acceleration were collected using five tri-axial IMUs (Cometa, Italy, sf=285 Hz) located on the trunk (at L5 level), shanks (about five centimetres above lateral malleolus), and feet (on the dorsal aspect of each shoe) (Figure 8). The walking tasks were also

filmed using a GoPro (Hero4, USA, sf=240Hz, 848x480 pixels resolution) for GE detection reference. IMU led flashing was video-recorded and used for time-synchronization of IMU.

Figure 8. Attachments of IMU on different body locations.

Data analysis:

For each condition, FC_{GoPro} and FO_{GoPro} were visually identified in the frame of the video by the same expert operator using Kinovea (Version 8.27), and FC_{IMU} and FO_{IMU} were estimated from IMU measurements using the selected 17 algorithms [9], implemented in MATLAB (MathWorks 2017a, USA).

For each condition and algorithm, the sensitivity in GE identification was calculated, considering the video as reference, as:

$$\frac{\text{Number of GEs identified by algorithm}}{\text{Number of all GEs as identified by video}} \quad (8)$$

For each target variable of the 17 selected algorithms, ICC of the mean stride cycle over the whole sequence of each trial for each condition (hard surface, wet sand and dry sand) was calculated to analyse the repeatability of the pattern over the trial in each condition (Single ICC). Furthermore, to analyse the similarity of the pattern during wet and dry sand with respect to the hard surface assumed as reference for the algorithm design, ICC of the mean stride cycle of hard surface over the wet sand and dry sand sequence was calculated (Combined ICC).

GTPs, i.e. stride, step, stance and swing time were calculated from GE. For each algorithm, the error was calculated for GE and GTP, considering the video as reference, as:

$$E_{GE} = GE_{IMU} - GE_{GoPro} \quad (9)$$

$$E_{GTP} = GTP_{IMU} - GTP_{GoPro} \quad (10)$$

Statistical analysis:

For each parameter (FC, FO, Stride Time, Step Time, Stance Time, Swing Time), a linear mixed model [3] was applied to test the dependency of error values on each implementation criterion, with a significance level of 0.05 using R software (R-Core Team 2017, Austria, version 3.4.3). First, the statistical analysis was performed to investigate the influence of IMU position and target variable, alone. Then, the influence of analysed variable and computational approach were investigated separately for each IMU position.

To characterize accuracy and repeatability, median value (Med) of the error and the Dispersion around Med (Dmed, 75^{th} percentile – 25^{th} percentile values of the error) were calculated, respectively.

Results

For each condition, 40 FCs and 40 FOs were identified and analysed for each participant, for a total of 280 FCs and 280 FOs.

The sensitivity in GEs identification resulted above 99% for all algorithms and conditions.

For all conditions and independently from IMU positioning, Single ICC showed higher variability for acceleration-based algorithms, ranging from 0,83 to 0,97, while velocity-based algorithms showed values ranging from 0,94 to 0,97. A similar trend was observed for Combined ICC (wet and dry sand versus hard surface), exhibiting values from 0,80 to 0,97 for acceleration-based algorithms and from 0,92 to 0,96 for angular-velocity based ones. Single and Combined ICC values are reported in Table 1.

Table 1. Details of the analysed algorithms classified according to the three criteria (i.e. IMU position, analysed variable and computational approach); Single ICC referred to hard surface, Wet Sand, Dry sand; Combined ICC referred to Hard Surface - Wet Sand, - Dry Sand.

Reference	*Sensor position*	*Target Variable*	*Computational Approach*	*Single ICC*			*Combined ICC*	
				Hard Surface	*Wet Sand*	*Dry Sand*	*Hard Surface - Wet Sand*	*Hard Surface - Dry Sand*
Bugané et al., 2012 [26]	Trunk	Acceleration	'peak identification' (IIR)	0,83	0,87	0,88	0,80	0,80
Lee et al., 2009 [28]	Trunk	Acceleration	'peak identification' (FIR)	0,83	0,87	0,88	0,80	0,80
McCamley et al., 2012 [29]	Trunk	Acceleration	'peak identification' (WT)	0,97	0,97	0,97	0,97	0,97
Gonzaléz et al., 2010 [21]	Trunk	Acceleration	'zero crossing' (FIR)	0,89	0,90	0,90	0,84	0,82
Shin et al., 2011 [30]	Trunk	Acceleration	'zero crossing' (Raw)	0,84	0,89	0,87	0,82	0,80
Zijlstra et al., 2003 [31]	Trunk	Acceleration	'zero crossing' (IIR)	0,96	0,96	0,95	0,93	0,90
Lee et al., 2010 [32]	Shank	Acceleration	'peak identification' (IIR)	0,93	0,95	0,94	0,94	0,90
Trojaniello et al., 2014 [27]	Shank	Acceleration	'peak identification' (Raw)	0,85	0,92	0,92	0,84	0,82
Khandelwal et al., 2014 [33]	Shank	Acceleration	'peak identification' (WT)	0,89	0,94	0,91	0,91	0,85
Catalfamo et al., 2010 [34]	Shank	Angular velocity	'peak identification' (IIR)	0,97	0,98	0,97	0,96	0,94
Greene et al., 2010 [35]	Shank	Angular velocity	'peak identification' (Raw)	0,97	0,98	0,97	0,96	0,94
Salarian et al., 2004 [20]	Shank	Angular velocity	'peak identification' (Raw)	0,97	0,98	0,97	0,96	0,94
Aminian et al., 2002 [36]	Shank	Angular velocity	'peak identification' (WT)	0,97	0,98	0,97	0,96	0,94
Jasiewicz et al., 2006 [37]	Foot	Acceleration	'peak identification' (Raw)	0,85	0,89	0,93	0,84	0,80
Sabatini et al., 2005 [38]	Foot	Angular velocity	'peak identification' (IIR)	0,94	0,94	0,94	0,93	0,92
Ferrari et al, 2016 [39]	Foot	Angular velocity	'peak identification' (Raw)	0,94	0,94	0,93	0,92	0,92
Mariani et al., 2013 [40]	Foot	Angular velocity	'zero crossing' (IIR)	0,94	0,94	0,94	0,93	0,92

IMU Position

For FC, all positioning highlighted higher accuracy on hard surface (showing the same value obtained by the video reference, with Med 0 ms) than on sand (Med 50 ms), with comparable repeatability among conditions for trunk- and foot-based algorithms (Dmed 200 ms). Shank-based algorithms showed lower repeatability on dry sand (Dmed 250 ms) compared to hard surface and wet sand (Dmed 200 ms in both cases). For FO, trunk-based algorithms resulted to be less accurate on hard surface and wet sand (Med of 100 ms and 50 ms, respectively) than on dry sand (Med 0 ms), and less repeatable on hard surface and dry sand (Dmed 200 ms in both cases) compared to wet sand (Dmed 150 ms). For shank- and foot-based algorithms, hard surface showed the highest accuracy (Med 0 ms in both positions), while wet sand showed the highest repeatability (Dmed 150 ms in both positions). In general, comparable accuracy and repeatability were found among different conditions in the estimation of Stride and Step Time, independently from IMU position. In relation to the Stance and Swing Time, a general agreement in accuracy and repeatability of Trunk-based algorithms among conditions was found (Med 10 ms and -10 ms, for Stance and Swing Time, respectively, and Dmed 50 ms in all cases). Instead, Shank- and Foot-based algorithms showed

higher accuracy with comparable repeatability in the estimation of these parameters on sand (Med 0 ms, Dmed 100 ms) compared to hard surface (Med 50 ms, Dmed 100ms).

Target Variable

For GEs identification, the hard surface showed for both angular velocity- and acceleration-based algorithms the highest accuracy (Med 0 ms for FC and FO in both target variables) and repeatability (FC: Dmed 150 ms and 200 ms for angular velocity and acceleration, respectively, FO: Dmed 150 ms for both target signals) among different walking conditions.

Independently from the condition, comparable results were obtained in the estimation of stride time in terms of accuracy and repeatability between Acceleration and Angular Velocity-based algorithms. Similarly, accuracy was comparable among different conditions in the estimation of Step Time, independently from the target variable (Med 0ms in all cases), while lower repeatability was observed for acceleration-based algorithms on hard surface and wet sand compared to Angular-based ones (Dmed 50 ms for angular velocity and 100 ms for acceleration in both conditions). In general, wet and dry sand showed higher accuracy and comparable repeatability in Stance and Swing Time estimation for both Acceleration- and Angular Velocity-based algorithms (Med of 0 ms for wet and dry sand and of 50 ms for hard surfaces, Dmed of 100 ms in all conditions).

Error characteristics for FC, FO, Stride-, Step-, Stance- and Swing time as related to IMU position and target variable are schematically depicted in Figure 9, while numerical values of the errors are reported in Table 2.

Figure 9: Box plot (minimum, 25th percentile, median, 75th percentile, maximum values) for FC (a), FO (b), Stride- (c), Step- (d), Stance- (e), and Swing time (f) estimation errors as related to IMU position and target variable on hard surface (top), wet (centre) and dry (bottom) sand. Angular velocity-based algorithms are framed in dashes.

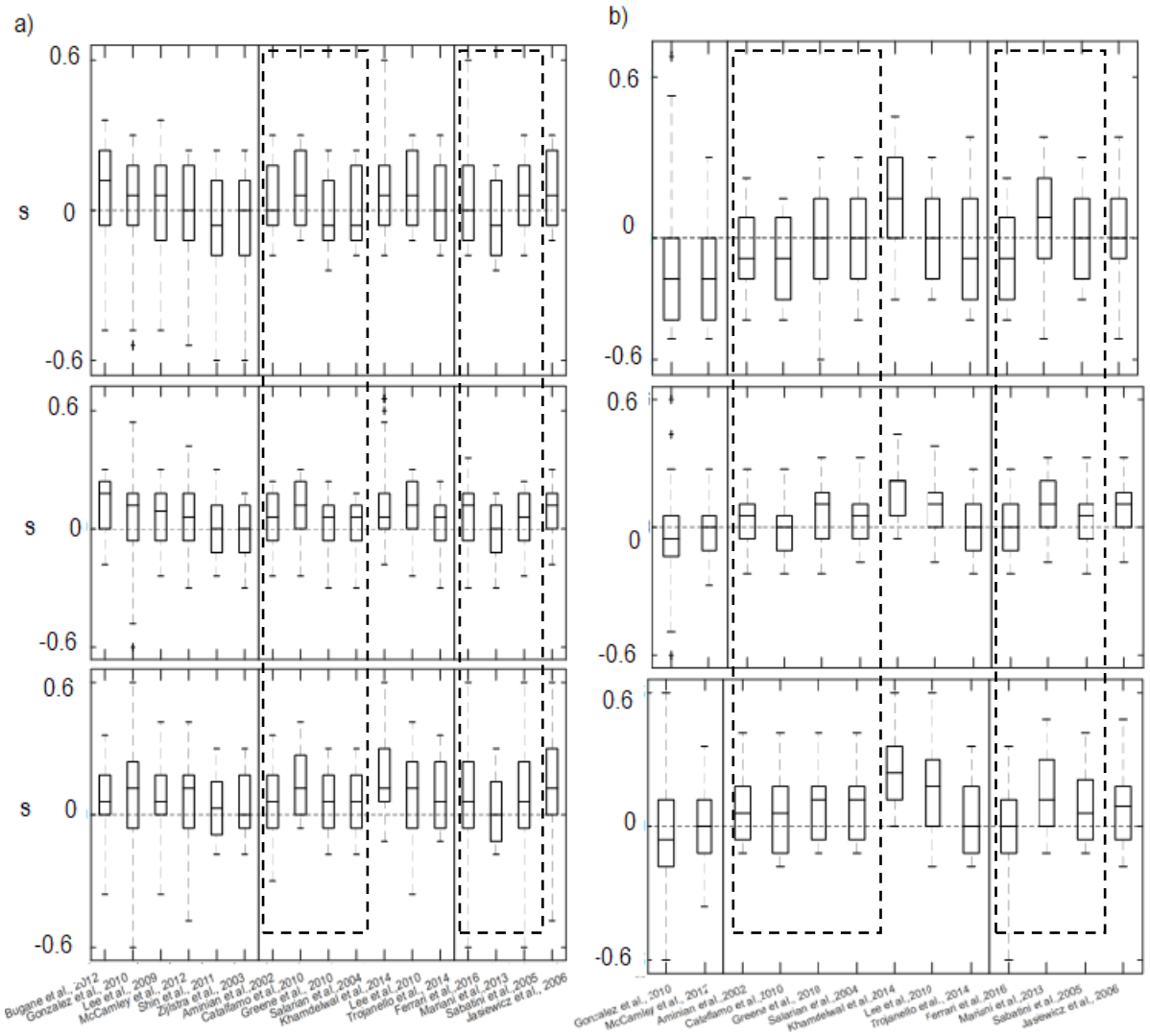

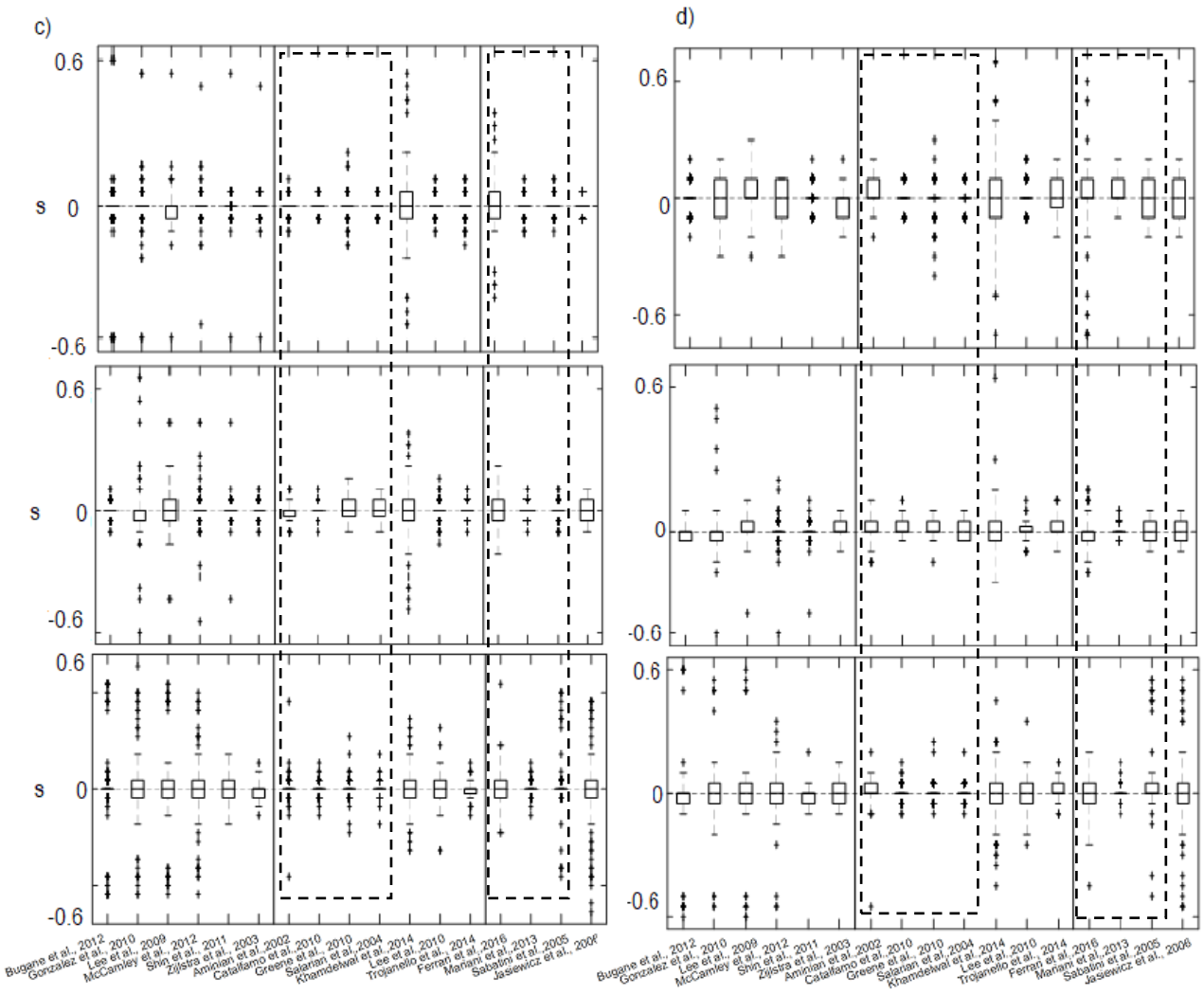
c)
d)
0.6
0
-0.6
s
Buggane et al., 2012
Gonzalez et al., 2010
Lee et al., 2009
McCamley et al., 2012
Shin et al., 2011
Zijlstra et al., 2003
Aminian et al.,2002
Catalfamo et al., 2010
Greene et al., 2010
Salarian et al.,2004
Khamdelwal et al., 2014
Lee et al., 2010
Trojaniello et al., 2014
Ferraji et al., 2016
Mariani et al., 2013
Sabatini et al.,2005
Jasiewicz et al., 2006

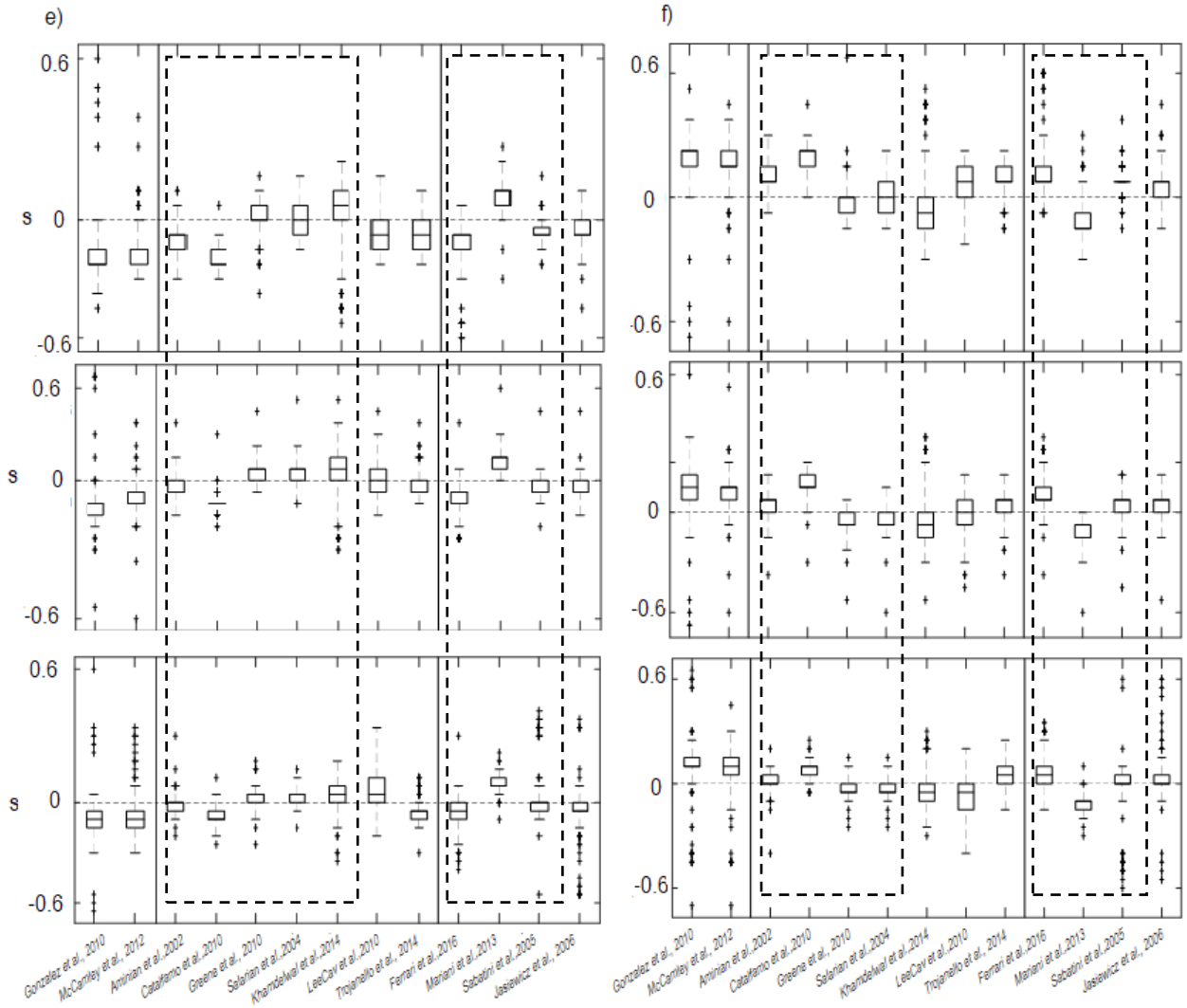
e)
f)
0.6
0
-0.6
s
Gonzalez et al., 2010
McCarthey et al., 2012
Aminian et al.,2002
Catalfamo et al.,2010
Greene et al., 2010
Salarian et al.,2004
Khandelwal et al.,2014
LeeCavi et al.,2010
Trojanello et al., 2014
Ferrari et al.,2016
Mariani et al.,2013
Sabatini et al.,2005
Jasiewicz et al., 2006

Table 2: Results of statistical analysis for IMU position and target variable: minimum, 25th quartile, median, 75th quartile and maximum of estimation error for FC, FO, stride time, step time, stance time and swing time (* $p<0.05$) across different walking conditions, i.e. hard surface (HSf), wet sand (WS) and dry sand (DS).

Parameter		***Estimation of errors: IMU position (s)***			***Level of significance***
		Trunk	***Shanks***	***Feet***	
FC	**HSf**	-0.50; -0.05; 0.00; 0.15; 0.30	-0.20; -0.05; 0.00; 0.15; 0.50	-0.20; -0.10; 0.00; 0.10; 0.50	Trunk-Shanks HSf* WS* DS* Trunk-Feet WS* DS* Shanks-Feet HSf* DS*
	WS	-0.50; -0.05; 0.05; 0.15; 0.45	-0.25; -0.05; 0.05; 0.15; 0.55	-0.25; -0.05; 0.05; 0.15; 0.30	
	DS	-0.50; -0.05; 0.05; 0.15; 0.50	-0.30; -0.05; 0.05; 0.20; 0.50	-0.50; -0.05; 0.05; 0.15; 0.50	
FO	**HSf**	-0.25; -0.20; -0.10; 0.00; 0.45	-0.30; -0.10; 0.00; 0.10; 0.30	-0.25; -0.05; 0.00; 0.10; 0.25	Trunk-Shanks HSf* WS* DS* Trunk-Feet HSf* WS* DS* Shanks-Feet HSf* DS*
	WS	-0.55 -0.10 -0.05 0.05 0.55	-0.20; -0.05; 0.05; 0.10; 0.40	-0.20; -0.05; 0.05; 0.10; 0.30	
	DS	-0.50 -0.10 0.00 0.10 0.50	-0.15; -0.05; 0.10; 0.20; 0.50	-0.50; -0.05; 0.05; 0.15; 0.40	
Stride time	**HSf**	-0.50; 0.00; 0.00; 0.00; 0.55	-0.45; 0.00; 0.00; 0.00; 0.50	-0.35; 0.00; 0.00; 0.00; 0.35	Trunk-Shanks Trunk-Feet Shanks-Feet WS*
	WS	-0.55; 0.00; 0.00; 0.00; 0.60	-0.45; 0.00; 0.00; 0.00; 0.35	-0.20; 0.00; 0.00; 0.00; 0.20	
	DS	-0.60; -0.05; 0.00; 0.05; 0.70	-0.50; 0.00; 0.00; 0.00; 0.50	-0.70; -0.05; 0.00; 0.00; 0.60	
Step Time	**HSf**	-0.55; -0.05; 0.00; 0.00; 0.15	-0.35; 0.00; 0.00; 0.05; 0.35	-0.35; 0.00; 0.00; 0.05; 0.30	Trunk-Shanks HSf* WS* Trunk-Feet Shanks-Feet WS* DS*
	WS	-0.50; 0.00; 0.00; 0.05; 0.60	-0.25; 0.00; 0.00; 0.05; 0.75	-0.20; -0.05; 0.00; 0.05; 0.20	
	DS	-0.60; -0.05; 0.00; 0.05; 0.60	-0.55; 0.00; 0.00; 0.05; 0.45	-0.55; 0.00; 0.00; 0.05; 0.55	
Stance Time	**HSf**	-0.30; -0.15; -0.15; -0.10; 0.55	-0.35; -0.10; -0.05; 0.00; 0.20	-0.40 -0.05 -0.05 0.05 0.25	Trunk-Shanks HSf* WS* DS* Trunk-Feet HSf* WS* DS* Shanks-Feet HSf* WS* DS*
	WS	-0.60; -0.10; -0.10; -0.05; 0.45	-0.30; -0.05; 0.00; 0.05; 0.35	-0.25; -0.05; 0.00; 0.05; 0.40	
	DS	-0.65; -0.15; -0.10; -0.05; 0.80	-0.35; -0.05; 0.00; 0.05; 0.45	-0.55; -0.05; 0.00; 0.05; 0.55	
Swing time	**HSf**	-0.45; 0.10; 0.10; 0.15; 0.35	-0.20; 0.00; 0.05; 0.10; 0.45	-0.20; -0.05; 0.05; 0.05; 0.40	Trunk-Shanks HSf* WS* DS* Trunk-Feet HSf* WS* DS* Shanks-Feet HSf* WS* DS*
	WS	-0.45; 0.05; 0.10; 0.10; 0.55	-0.40; -0.05; 0.00; 0.05; 0.30	-0.40; -0.05; 0.00; 0.05; 0.30	
	DS	-0.70; 0.05; 0.10; 0.15; 0.65	-0.40; -0.05; 0.00; 0.05; 0.30	-0.60; -0.05; 0.00; 0.05; 0.60	

Parameter		***Estimation of errors: Target Variable (s)***		***Level of significance***
		Angular Velocity	***Acceleration***	
FC	HSf	-0.20; -0.05; 0.00; 0.10; 0.50	-0.50; -0.05; 0.00; 0.15; 0.50	Angular Velocity - Acceleration HSf* WS* DS*
	WS	-0.25; -0.05; 0.05; 0.15; 0.30	-0.50; -0.05; 0.05; 0.15; 0.55	
	DS	-0.50; -0.05; 0.05; 0.15; 0.50	-0.50; -0.05; 0.05; 0.20; 0.50	
FO	HSf	-0.30; -0.10; 0.00; 0.05; 0.25	-0.25; -0.10; 0.00; 0.05; 0.45	Angular Velocity - Acceleration WS*
	WS	-0.20; -0.05; 0.05; 0.10; 0.30	-0.55; -0.05; 0.05; 0.10; 0.55	
	DS	-0.50; -0.05; 0.05; 0.15; 0.40	-0.50; -0.05; 0.05; 0.15; 0.50	
Stride time	HSf	-0.35; 0.00; 0.00; 0.00; 0.35	-0.50; 0.00; 0.00; 0.00; 0.55	Angular Velocity - Acceleration
	WS	-0.20; 0.00; 0.00; 0.00; 0.20	-0.55; 0.00; 0.00; 0.00; 0.60	
	DS	-0.50; 0.00; 0.00; 0.00; 0.60	-0.70; -0.05; 0.00; 0.05; 0.70	
Step Time	HSf	-0.35; 0.00; 0.00; 0.05; 0.30	-0.55; -0.05; 0.00; 0.05; 0.35	Angular Velocity - Acceleration
	WS	-0.20; 0.00; 0.00; 0.05; 0.20	-0.50; 0.00; 0.00; 0.05; 0.75	
	DS	-0.55; 0.00; 0.00; 0.05; 0.55	-0.60; -0.05; 0.00; 0.05; 0.60	
Stance Time	HSf	-0.40; -0.10; -0.05; 0.05; 0.25	-0.35; -0.10; -0.05; 0.00; 0.55	Angular Velocity - Acceleration HSf* WS* DS*
	WS	-0.25; -0.05; 0.00; 0.05; 0.40	-0.60; -0.10; -0.05; 0.00; 0.45	
	DS	-0.55; -0.05; 0.00; 0.05; 0.55	-0.65; -0.10; -0.05; 0.05; 0.80	
Swing time	HSf	-0.20; -0.05; 0.05; 0.10; 0.45	-0.45; 0.00; 0.05; 0.10; 0.35	Angular Velocity - Acceleration HSf* WS* DS*
	WS	-0.40; -0.05; 0.00; 0.05; 0.30	-0.45; 0.00; 0.05; 0.10; 0.55	
	DS	-0.60; -0.05; 0.00; 0.05; 0.60	-0.70; -0.05; 0.05; 0.10; 0.65	

Computational approach

For all IMU positions, algorithms showed statistically significant differences between the two approaches in GEs, Stance and Swing estimation. Instead, the estimation of Stride and Step Time showed comparable accuracy and repeatability among different walking conditions, independently from IMU position and computational approach. Numerical values of error characteristics for GE and GTP as related to computational approach are reported in Table 3.

Table 3. Results of statistical analysis for computational approach: minimum, 25th quartile, median, 75th quartile and maximum of estimation error for HS, TO, stride time, step time, stance time and swing time (* $p<0.05$) across different walking conditions, i.e. Hard Surface (HSf), Wet Sand (WS) and Dry Sand (DS).

IMU position	Parameter	Level of significance 'peak identification' vs 'zero crossing'	Estimation of errors: Filtering (s) Level of significance				
				Filtering within 'peak identification'	Level of significance for filtering within 'peak identification'	Filtering within 'zero crossing'	Level of significance for filtering within 'zero crossing'
Trunk	HS	HSf* WS* DS*	HSf	FIR: -0.40; -0.10; 0.05; 0.15; 0.30 IIR: -0.40; -0.05; 0.10; 0.20; 0.30 WT: -0.45; -0.10; 0.00; 0.15; 0.20	FIR – IIR* FIR – WT* IIR – WT *	Raw: -0.50; -0.15; -0.05; 0.10; 0.20 FIR: -0.45; -0.05; 0.05; 0.15; 0.25 IIR: -0.50; -0.15; 0.00; 0.10; 0.20	FIR – IIR* FIR – Raw IIR – Raw
			WS	FIR: -0.20; -0.05; 0.05; 0.15; 0.25 IIR: -0.15; 0.00; 0.15; 0.20; 0.25 WT: -0.25; -0.05; 0.05; 0.15; 0.35	FIR – IIR* FIR – WT* IIR – WT *	Raw: -0.20; -0.10; 0.00; 0.10; 0.25 FIR: -0.50; -0.05; 0.10; 0.15; 0.45 IIR: -0.25; -0.10; 0.00; 0.10; 0.15	FIR – IIR* FIR – Raw* IIR – Raw
			DS	FIR: -0.30; 0.00; 0.05; 0.15; 0.35 IIR: -0.30; 0.00; 0.05; 0.15; 0.30 WT: -0.40; -0.05; 0.10; 0.15; 0.35	FIR – IIR* FIR – WT IIR – WT	Raw: -0.15; -0.06; 0.05; 0.10; 0.25 FIR: -0.50; -0.05; 0.10; 0.20; 0.50 IIR: -0.30; 0.00; 0.05; 0.15; 0.30	FIR – IIR * FIR – Raw* IIR – Raw
	TO	DS*	HSf	WT -0.25; -0.20; -0.10; 0.00; 0.20	-	FIR -0.25; -0.20; -0.10; 0.00; 0.45	-
			WS	WT: -0.25; -0.10; 0.00; 0.05; 0.25		FIR: -0.55; -0.10; -0.05; 0.05; 0.55	
			DS	WT: -0.30; -0.10; 0.00; 0.10; 0.30		FIR: -0.50; -0.15; -0.05; 0.10; 0.50	
	Stride time	HSf WS DS	HSf	FIR -0.50; -0.05; 0.00; 0.00; 0.50 IIR -0.10; 0.00; 0.00; 0.00; 0.55 WT -0.15; 0.00; 0.00; 0.00; 0.15	FIR – IIR FIR – WT IIR – WT	FIR -0.20; 0.00; 0.00; 0.00; 0.15 IIR -0.10; 0.00; 0.00; 0.00; 0.05 Raw -0.10; 0.00; 0.00; 0.00; 0.05	FIR – IIR FIR – Raw IIR – Raw
			WS	FIR -0.40; -0.05; 0.00; 0.05; 0.40 IIR -0.10; 0.00; 0.00; 0.00; 0.10 WT -0.50; 0.00; 0.00; 0.00; 0.40	FIR – IIR FIR – WT IIR – WT	FIR -0.55; -0.05; 0.00; 0.00; 0.60 IIR -0.10; 0.00; 0.00; 0.00; 0.10 Raw -0.40; 0.00; 0.00; 0.00; 0.40	FIR – IIR FIR – Raw IIR – Raw
			DS	FIR: -0.60; -0.05; 0.00; 0.05; 0.60 IIR -0.60; 0.00; 0.00; 0.00; 0.60 WT -0.60; -0.05; 0.00; 0.05; 0.55	FIR – IIR FIR – WT IIR – WT	FIR -0.60; -0.05; 0.00; 0.05; 0.70 IIR -0.15; -0.05; 0.00; 0.00; 0.15 Raw -0.20; -0.05; 0.00; 0.05; 0.20	FIR – IIR FIR – Raw IIR – Raw
	Step Time	HSf WS DS	HSf	FIR -0.15; 0.00; 0.00; 0.05; 0.15 IIR -0.55; 0.00; 0.00; 0.00; 0.10 WT -0.15; -0.05; 0.00; 0.05; 0.05	FIR – IIR FIR – WT IIR – WT	FIR -0.15; -0.05; 0.00; 0.05; 0.10 Raw -0.05; 0.00; 0.00; 0.00; 0.10	FIR – Raw
			WS	FIR -0.40; 0.00; 0.00; 0.05; 0.15 IIR -0.05; -0.05; 0.00; 0.00; 0.10 WT -0.50; 0.00; 0.00; 0.00; 0.25	FIR – IIR FIR – WT IIR – WT	FIR -0.50; -0.05; 0.00; 0.00; 0.60 Raw: -0.40; 0.00; 0.00; 0.00; 0.15	FIR – Raw
			DS	FIR -0.60; -0.05; 0.00; 0.05; 0.60 IIR -0.60; -0.05: 0.00: 0.00; 0.60 WT -0.55; -0.05; 0.00; 0.05; 0.35	FIR – IIR FIR – WT IIR – WT	FIR: -0.55; -0.05; 0.00; 0.05; 0.55 Raw: -0.10; -0.05; 0.00; 0.00; 0.20	FIR – Raw
	Stance time	HSf* WS*	HSf	WT -0.20; -0.15; -0.10; -0.10; 0.35	-	FIR -0.30; -0.15; -0.15; -0.10; 0.55	-
			WS	WT -0.60; -0.10 -0.10 -0.05 0.25		FIR -0.55; -0.15; -0.10; -0.10; 0.45	
			DS	WT -0.30; -0.15; -0.10; -0.05; 0.45		FIR -0.65; -0.15; -0.10; -0.05; 0.80	
	Swing Time	HSf* WS*	HSf	WT -0.40; 0.10; 0.10; 0.15; 0.30	-	FIR: -0.45; 0.10; 0.15; 0.15; 0.35	-
			WS	WT -0.40; 0.10; 0.10; 0.15; 0.30		FIR: -0.45; 0.10; 0.15; 0.15; 0.35	
			DS	WT -0.70; 0.05; 0.10; 0.15; 0.45		FIR: -0.70; 0.10; 0.10; 0.15; 0.65	
Shank	HS	-	HSf	Raw -0.20; -0.10; 0.00; 0.15; 0.25 IIR -0.10; -0.05; 0.05; 0.20; 0.25 WT -0.15; -0.05; 0.05; 0.15; 0.50	IIR – Raw* IIR – WT Raw – WT*	-	
			WS	Raw -0.25; -0.05; 0.05; 0.10; 0.20 IIR -0.20; 0.00; 0.10; 0.20; 0.25 WT -0.20; 0.00; 0.05; 0.15; 0.55	IIR – Raw* IIR – WT Raw – WT*		
			DS	Raw -0.30; 0.00; 0.05; 0.15; 0.35 IIR -0.30; 0.00; 0.05; 0.15; 0.30 WT -0.40; -0.05; 0.10; 0.15; 0.35	IIR – Raw* IIR – WT* Raw – WT*		
	TO		HSf	Raw -0.30; -0.10; 0.00; 0.10; 0.25 IIR -0.20; -0.10; -0.05; 0.05; 0.20 WT -0.20; -0.05; 0.05; 0.10; 0.30	IIR – Raw* IIR – WT* Raw – WT*		
			WS	Raw -0.20; -0.05; 0.05; 0.10; 0.30 IIR -0.20; -0.10; 0.05; 0.10; 0.35 WT -0.20; -0.05; 0.10; 0.20; 0.40	IIR – Raw IIR – WT* Raw – WT*		
			DS	Raw -0.15; -0.05; 0.05; 0.15; 0.35 IIR -0.15; -0.05; 0.05; 0.20; 0.50 WT -0.10; 0.05; 0.10; 0.20; 0.50	IIR – Raw* IIR – WT* Raw – WT*		
	Stride time		HSf	Raw -0.15; 0.00; 0.00; 0.00; 0.20 IIR -0.10; 0.00; 0.00; 0.00; 0.10 WT -0.45; 0.00; 0.00; 0.05; 0.50			
			WS	Raw -0.10; 0.00; 0.00; 0.00; 0.15 IIR -0.15; 0.00; 0.00; 0.00; 0.15 WT -0.45; -0.05; 0.00; 0.05; 0.35	IIR – Raw IIR – WT Raw – WT		
			DS	Raw -0.25; 0.00; 0.00; 0.00; 0.30 IIR -0.35; -0.00; 0.00; 0.05; 0.35 WT -0.50; -0.05; 0.00; 0.05; 0.50			
	Step Time		HSf	Raw -0.20; 0.00; 0.00; 0.00; 0.15 IIR -0.05; 0.00; 0.00; 0.00; 0.10 WT -0.35; 0.00; 0.00; 0.05; 0.35	IIR – Raw IIR – WT Raw – WT		

			WS	Raw -0.15; 0.00; 0.00; 0.05; 0.15 IIR -0.10; 0.00; 0.00; 0.05; 0.15 WT -0.25; -0.05; 0.00; 0.05; 0.75			
			DS	Raw -0.10; 0.00; 0.00; 0.00; 0.25 IIR -0.25; 0.00; 0.00; 0.05; 0.35 WT -0.55; -0.05; 0.00; 0.05; 0.45			
	Stance time		HSf	Raw -0.25; -0.05; 0.00; 0.05; 0.15 IIR -0.20; -0.15; -0.10; -0.05; 0.15 WT -0.35; -0.10; -0.05; 0.05; 0.20	IIR – Raw HSF* WS* IIR – WT HSF* WS* DS* Raw – WT		
			WS	Raw -0.10; -0.05; 0.00; 0.05; 0.35 IIR -0.20; -0.10; -0.10; 0.00; 0.30 WT -0.30; -0.05; 0.00; 0.05; 0.35			
			DS	Raw -0.30; -0.05; 0.00; 0.05; 0.25 IIR -0.25; -0.10; -0.05; 0.05; 0.45 WT -0.35; -0.05; 0.00; 0.05; 0.40			
	Swing Time		HSf	Raw -0.10; -0.05; 0.00; 0.05; 0.45 IIR -0.15; 0.05; 0.10; 0.15; 0.30 WT -0.20; -0.05; 0.05; 0.10; 0.35	IIR – Raw HSF* WS* IIR – WT HSF* WS* DS* Raw – WT HSF* WS*		
			WS	Raw -0.10; -0.05; 0.00; 0.05; 0.45 IIR -0.15; 0.05; 0.10; 0.15; 0.30 WT -0.20; -0.05; 0.05; 0.10; 0.35			
			DS	Raw -0.25; -0.05; 0.00; 0.05; 0.25 IIR -0.40; -0.05; 0.05; 0.10; 0.25 WT -0.40; -0.05; 0.00; 0.05; 0.30			
Foot	HS	HSf* WS* DS*	HSf	Raw -0.15; -0.05; 0.05; 0.15; 0.50 IIR -0.15; -0.05; 0.05; 0.15; 0.25	IIR – Raw WS* DS*	IIR -0.20; -0.15; -0.05; 0.10; 0.15	-
			WS	Raw -0.25; 0.00; 0.10; 0.15; 0.30 IIR -0.20; -0.05; 0.05; 0.15; 0.20		IIR -0.25; -0.10; 0.00; 0.10; 0.15	
			DS	Raw -0.50; 0.00; 0.05; 0.20; 0.50 IIR -0.50; -0.05; 0.05; 0.20; 0.50		IIR -0.15; -0.10; 0.00; 0.10; 0.25	
	TO	HSf* WS* DS*	HSf	Raw -0.25; -0.10; 0.00; 0.10; 0.25 IIR -0.15; -0.10; 0.00; 0.10; 0.20	IIR – Raw	IIR -0.25; -0.05; 0.05; 0.15; 0.25	
			WS	Raw -0.20; -0.05; 0.05; 0.10; 0.30 IIR -0.20; -0.05; 0.05; 0.10; 0.30		IIR -0.15; 0.00; 0.10; 0.20; 0.30	
			DS	Raw -0.50; -0.05; 0.05; 0.15; 0.40 IIR -0.10; -0.05; 0.05; 0.15; 0.35		IIR -0.10; 0.00; 0.10; 0.25; 0.40	
	Stride time	HSf WS DS	HSf	Raw -0.35; 0.00; 0.00; 0.00; 0.35 IIR -0.10; 0.00; 0.00; 0.00; 0.10	IIR – Raw	IIR -0.10; 0.00; 0.00; 0.00; 0.10	
			WS	Raw -0.20; -0.05; 0.00; 0.05;0.20 IIR -0.10; 0.00; 0.00; 0.00; 0.10		IIR -0.10; 0.00; 0.00; 0.00; 0.10	
			DS	Raw -0.70; -0.05; 0.00; 0.05; 0.60 IIR -0.50; 0.00; 0.00; 0.00; 0.55		IIR -0.15; 0.00; 0.00; 0.00; 0.15	
	Step Time	HSf WS DS	HSf	Raw -0.35; 0.00; 0.00; 0.05; 0.30 IIR -0.10; -0.05; 0.00; 0.05; 0.10	IIR – Raw DS*	IIR -0.05; 0.00; 0.00; 0.05; 0.10	
			WS	Raw -0.20; -0.05; 0.00; 0.05; 0.20 IIR -0.10; -0.05; 0.00; 0.05; 0.10		IIR -0.05; 0.00; 0.00; 0.00; 0.10	
			DS	Raw -0.55; -0.05; 0.00; 0.05; 0.55 IIR -0.50; 0.00; 0.00; 0.05; 0.55		IIR -0.10; 0.00; 0.00; 0.00; 0.15	
	Stance time	HSf* WS* DS*	HSf	Raw -0.40; -0.10; -0.05; 0.00; 0.10 IIR -0.15; -0.05 -0.05 -0.05; 0.15	IIR – Raw WS* DS*	IIR -0.20; 0.05; 0.10; 0.10; 0.25	
			WS	Raw -0.25; -0.10; -0.05; 0.00; 0.30 IIR -0.20; -0.05; -0.05; 0.00; 0.30		IIR 0.00; 0.05; 0.10; 0.10; 0.40	
			DS	Raw -0.55; -0.10; -0.05; 0.00; 0.50 IIR -0.55; -0.05; 0.00; 0.00; 0.55		IIR -0.10; 0.10; 0.10; 0.15; 0.30	
	Swing Time	HSf* WS* DS*	HSf	Raw -0.10; 0.00; 0.05; 0.10; 0.40 IIR -0.10; 0.05; 0.05; 0.05; 0.25	IIR – Raw DS*	IIR -0.20; -0.10; -0.10; -0.05; 0.20	
			WS	Raw -0.10; 0.00; 0.05; 0.10; 0.40 IIR -0.10; 0.05; 0.05; 0.05; 0.25		IIR -0.20; -0.10; -0.10; -0.05; 0.20	
			DS	Raw -0.55; 0.00; 0.05; 0.05; 0.60 IIR -0.60; 0.00; 0.00; 0.05; 0.60		IIR -0.30; -0.15; -0.10; -0.10; 0.10	

Discussion

The present study analysed the performance of 17 algorithms originally designed for GE detection in healthy people during walking on hard surface when applied to gait on dry and wet sand. In both conditions, all the algorithms showed over-threshold sensitivity, suggesting the possibility to extend their application in the marine context. The high sensitivity can be explained by the results obtained in the similarity of the gait pattern across different conditions, assessed by ICC. In the literature, ICC theory was already adopted for the analysis of multivariate categorical data [116] and later proposed by other authors to evaluate the reproducibility in the acceleration pattern of the trunk during walking [117]. In this work, Single and Combined ICC showed excellent reproducibility of signal features on wet and dry sand, alone, and also compared with the hard surface, adopted as reference for algorithm implementation. More in details, algorithms exploiting angular velocity of shanks and feet showed excellent reproducibility across different environments, with minimum value of Single and Combined ICC of 0.92. Also, good reproducibility was observed for the acceleration-based algorithms, independently from IMU position, with minimum value of Single and Combined ICC of 0.80. An example of reproducibility in the gait pattern within the single condition was reported in Figure 10, showing a representative signal derived from trunk acceleration during walking on (a) hard surface, (b) wet and (c) dry sand, with values of Single ICC of 0.83, 0.87 and 0.88, respectively.

Figure 10. Plots with Median, 25th and 75th percentile of a representative target signals from trunk acceleration on the normalized stride time and referred to (a) hard surface, (b) wet sand, (c) dry sand.

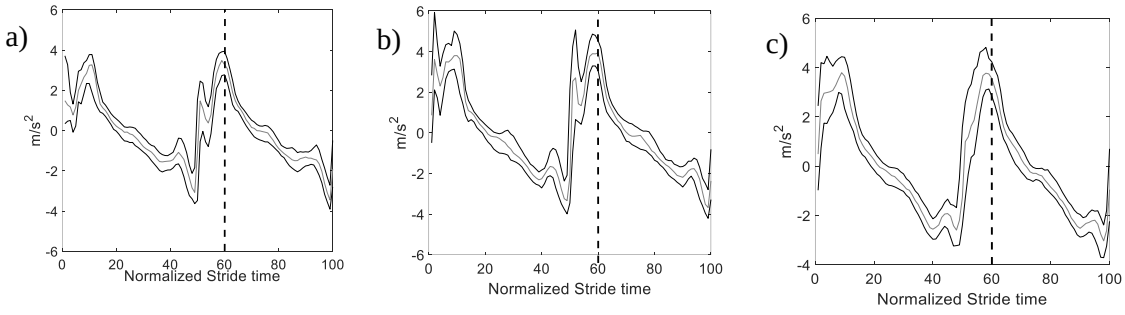

Also, the similarity of the gait pattern on sand compared to the hard surface was represented in Figure 11, where specific features of the target signal were comparable among different conditions, with values of Combined ICC of 0.80 in both wet and dry sand versus hard surface.

Figure 11. Plots with Medians of a representative target signals from trunk acceleration on the normalized stride time referred to hard surface, wet and dry sand.

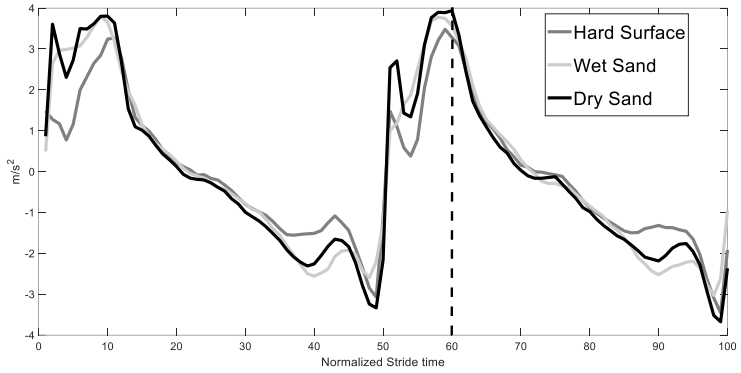

Different accuracy and repeatability were observed in the estimation of GE, Stance and Swing time across different walking conditions. Independently from different IMU position and target variable, hard surfaces and wet sand showed a general greater accuracy and comparable repeatability in GE estimation compared to dry sand. On the other hand, higher accuracy and comparable repeatability were highlighted in the estimation of Stance and Swing Time for wet and dry sand compared to hard surface (Table 2), suggesting that bias occurring during FC detection on sand tended to be compensated by bias introduced with FO more than in hard surface. Considering the computational approach, an indicatory conclusion can be hardly proposed, because different results were obtained in relation to the different sensor location. Across different conditions, all algorithms showed delay or anticipation in the estimation of FC compared to the Gold Standard (Figure 1). These biases were generally compensated in the estimation of Stride and Step time (derived from HS alone), thus these parameters resulted not to be significantly affected by different implementation characteristics and walking conditions.

From these results, overall better performances were obtained in GE and GTP estimation for segmentation algorithms applied to wet sand both in terms of accuracy and repeatability. Since the original algorithms were implemented based on inertial data of people walking on solid surfaces and dressing comfortable shoes, wet sand might play the same biomechanical role associated to

footwear [118], possibly justifying the better results obtained for this latter condition.

In conclusion, results of this study suggested that the physical characteristics of the sand terrains (i. e. shifting nature, reduced elastic response and different stiffness) did not substantially modify acceleration and angular velocity patterns derived from different IMU position during walking, thus assuring overall good performance of algorithms in the estimation of GEs and GTPs. The main limitation of the study is represented by the low number of participants. Thus, further analyses will extend the number of analysed subjects to provide consistent guidelines for the assessment of appropriate segmentation algorithms in the marine environment.

2.4

NON- LINEAR METRICS OF GAIT IN WATER

Part of the content of this chapter has been published in Pacini Panebianco, Giulia; Bisi, Maria Cristina; Giovanardi, Andrea; Stagni, Rita; Fantozzi, Silvia, 'Gait performance of walking in or out of the water: Objective and interpretative observation using variability and stability indices', Gait & Posture 49s (2016), 7 – 8, and was submitted to Gait and Posture as full length article.

Introduction

The water environment has been promoted for rehabilitative motor activities of people with impaired locomotion [88,92]. Aquatic therapies are beneficial in the management of patients with musculoskeletal disorders, neurological problems and cardiopulmonary pathology [91]. More specifically, walking in water represents one of the most effective motor tasks in the rehabilitation programs and can be performed by individuals without swimming skill [88,92,96]. In this context, the selection of the proper level of immersion is essential for the effectiveness of the therapy. In fact, walking tasks in the aquatic rehabilitation should be performed at various water depths (progressing from deeper to shallower), in order to enable the removal of a proportion of body weight to facilitate optimal gait patterns, as needed [119]. Despite its recognised clinical relevance, a limited number of studies quantitively analysed the biomechanical and functional characteristics of gait in water [88,92,120,121], usually limiting the analysis to metabolic and physiological effects on the motor performance and considering fixed level of immersion [91,122–125]. Thus, it is still a challenge to explain and understand the reasons for the clinical efficacy of the walking therapy in this environment from a functional and biomechanical point of view.

In recent years, the assessment of motor control during over-ground walking have been performed using specific parameters, such as variability of the stride time (PSD1, PSD2, SD) and non-linear metrics (e.g. RQA and MSE), proposed in the literature to quantify variability, regularity and complexity of the gait pattern [44,46,51] (see Paragraph 1.2 of the Background for more details). Some studies analysed methodological aspects related to the potential use of these metrics in the clinical practice and the development of the base research [43,46,51,126]. In particular, Riva et al. [44] investigated the minimum number of strides to assess the reliability of non-linear metrics calculation during over-ground walking. Due to the different motor pattern observed during gait in water (see Paragraph 2.2 of Section 1), the results obtained by Riva et al. [44] for over-ground walking cannot be extended to the water environment. In order to provide relevant information of motor control for rehabilitation in water and aquatic therapy, methodological aspects in relation to the implementation of the non-linear metrics during walking in the water at different levels of immersion were investigated. Thus, the aims of the present study were to i) assess the minimum number of strides required for a reliable application of non-linear metrics; ii) characterize the influence of different level of immersion.

Materials and methods

Participants

Fourteen healthy participants (8 females, 6 males; 23.4± 4.0 years; 1.7 ± 0.1m; 63.9 ± 11.8 Kg) were recruited in the study. All participants were physically active and self-reported no known history of physical or mental impairments. The study was approved on 18/08/2018 with protocol number 1831 by The School of Education and Sport Ethics Sub-Committee of the University of Edinburgh and written informed consent was reviewed and signed by all participants.

Data acquisition

Each participant was measured during walking in water at three different levels of immersion, i.e. knee, pelvis and xiphoid process, with a temperature of 28°C. For each condition, participants walked barefoot back and forth along a 10 m straight pathway at self-selected speed for three minutes, after completing a three-minutes acclimatization trial. Although arm movement was not restricted, participants were not permitted to use their arms for propulsion. Two tri-axial synchronized IMUs (Cometa, Italy, sf=285 Hz) equipped with accelerometer and gyroscope were attached to the trunk (at the level of the fifth lumbar vertebra) and the right shank.

Data analysis

Stride time was estimated from shank angular velocities [20] and used to calculate variability metrics (i.e. SD and PSD1/PSD2) to quantify timing variability [44], while trunk acceleration measures were exploited to calculate non-linear variability and stability metrics (i.e. RQA and MSE) on vertical (V), medio-lateral (ML) and anterior– posterior (AP) directions to quantify pattern regularity and motor complexity [44,51].

Statistical analysis

According to the literature [44], metrics were calculated on windows of decreasing length, from 150 to 10 strides, with 1 stride increment. Interquartile range, median value of variability and stability metrics were calculated for each number of strides over the analyzed subjects. Then, percent interquartile range/median ratio (IMR) was calculated, starting from the 150 strides window, which gave the lowest ratio, and proceeding backwards [44]. Thresholds for the IMR were fixed at 10%, 20%, 30%, 40% and 50%. The required number of strides was defined as the smallest one at which the ratio remained below the lowest possible threshold. The minimum number of strides was first calculated per index and per subject, then for each index the largest number of strides over

subjects was selected. Successively, the influence of different environments on non-linear metrics was tested with one-way ANOVA with minimum level of significance of 5%, considering 150 strides per subject, since this was the maximum number of strides considered for the analysis. Median, 25th and 75th percentile values of non-linear metrics were hence calculated for each condition.

Results

All metrics required a number of strides higher than 105 across different level of immersion even for the 50% threshold. Comparable results with previous studies on dry land were obtained only for RQA (V Max, Div) that never reached steady values in the analysed range in any of the three conditions (Table 1). During walking in water, the same behaviour was observed also for ML and AP direction of RQA (ML and AP Max, Div) for all levels of immersion. On dry land, 10 strides were sufficient to reach a 10% threshold for MSE V (τ=1, …, 4) and RQA (AP rr, det, avg, ML rr and V rr, det, avg). Conversely, a number of strides higher than 145 was associated to all these latter metrics during walking in water, independently from the level of immersion. Detailed results are shown in Table 1.

Table 1. Number of required strides for each measure at each threshold as related to previous work on Dry Land (DL) and current analysis during walking in water at Knee (K), Pelvis (P) and Xiphoid Process (XP) level.

	Threshold																			
	10%				**20%**				**30%**				**40%**				**50%**			
	DL	**K**	**P**	**XP**	**DL**	**K**	**P**	**XP**	**DL**	**K**	**P**	**XP**	**DL**	**K**	**P**	**XP**	**DL**	**K**	**P**	**XP**
RQA V (rr)	10	144	147	146	10	138	145	145	10	137	142	141	10	131	131	137	10	124	127	134
RQA V (Det)	10	149	146	143	10	148	144	133	10	142	139	125	10	138	136	122	10	135	132	120
RQA V (Avg)	10	143	148	147	10	137	141	144	10	134	133	138	10	133	129	131	10	132	125	124
RQA V (Max)	150	150	150	150	150	150	150	150	150	150	150	150	150	150	150	150	150	150	150	150
RQA V (Div)	150	150	150	150	150	150	150	150	150	150	150	150	150	150	150	150	150	150	150	150
RQA ML (rr)	10	149	146	145	10	148	140	140	10	143	133	131	10	135	128	127	10	120	124	126
RQA ML (Det)	78	145	146	148	10	137	136	140	10	128	131	131	10	118	113	129	10	105	111	124
RQA ML (Avg)	55	147	141	145	10	145	131	138	10	144	122	136	10	139	114	129	10	138	111	124
RQA ML (Max)	136	150	150	150	129	150	150	150	73	150	150	150	29	150	150	150	29	150	150	150
RQA ML (Div)	136	150	150	150	135	150	150	150	79	150	150	150	29	150	150	150	29	150	150	150
RQA AP (rr)	10	146	148	149	10	143	146	142	10	141	145	140	10	137	143	138	10	129	140	137
RQA AP (Det)	10	149	147	146	10	146	143	139	10	139	139	136	10	138	123	131	10	137	117	127
RQA AP (Avg)	10	147	148	145	10	141	145	139	10	137	143	138	10	128	141	136	10	119	138	127
RQA AP (Max)	121	150	150	150	75	150	150	150	74	150	150	150	37	150	150	150	36	150	150	150
RQA AP (Div)	107	150	150	150	95	150	150	150	74	150	150	150	74	150	150	150	74	150	150	150
SE V τ=1	10	145	146	147	10	139	143	145	10	139	139	134	10	139	135	134	10	139	105	134
SE V τ=2	10	147	148	147	10	144	146	143	10	139	142	135	10	139	136	135	10	139	129	135
SE V τ=4	10	149	147	148	10	140	141	142	10	136	139	135	10	134	136	135	10	131	133	135
SE V τ=6	15	148	149	148	10	143	146	135	10	141	143	135	10	135	135	135	10	118	134	135
SE V τ=8	-	147	148	149	-	144	143	144	-	138	141	138	-	129	136	135	-	125	134	135
SE V τ=10	-	147	148	147	-	140	142	146	-	139	141	144	-	135	140	143	-	122	139	141
SE V τ=12	-	146	146	145	-	136	141	139	-	132	138	135	-	125	136	135	-	121	135	135
SE ML τ=1	10	146	146	146	10	143	144	145	10	141	141	140	10	139	135	133	10	115	121	123
SE ML τ=2	30	148	148	146	10	144	146	142	10	140	144	135	10	136	140	131	10	131	137	128
SE ML τ=4	31	147	149	144	10	144	148	136	10	132	147	130	10	122	146	128	10	113	145	111
SE ML τ=6	32	148	146	147	10	147	142	145	10	122	136	140	10	121	134	134	10	120	133	121
SE ML τ=8	-	147	146	146	-	141	144	144	-	139	141	142	-	132	136	131	-	129	132	128
SE ML τ=10	-	144	145	144	-	133	144	142	-	128	140	141	-	126	126	131	-	124	119	129
SE ML τ=12	-	147	148	148	-	141	140	145	-	135	137	137	-	125	136	133	-	120	131	132
SE AP τ=1	19	147	148	148	10	136	145	139	10	128	142	136	10	123	138	131	10	122	131	131
SE AP τ=2	19	147	148	147	10	145	145	140	10	144	142	139	10	139	138	138	10	129	131	138
SE AP τ=4	15	148	149	146	10	143	148	142	10	140	135	136	10	136	131	133	10	127	129	133
SE AP τ=6	17	146	148	146	10	136	146	136	10	128	135	135	10	123	133	135	10	118	131	134
SE AP τ=8	-	148	148	148	-	141	144	140	-	135	140	135	-	129	133	134	-	122	130	134
SE AP τ=10	-	148	146	146	-	137	141	139	-	131	119	133	-	129	114	132	-	126	113	131
SE AP τ=12	-	148	143	143	-	146	137	136	-	146	129	133	-	145	120	132	-	144	116	130
SD	125	148	145	147	59	143	142	143	20	138	141	129	15	136	140	124	10	131	139	119
PSD1	127	143	148	149	52	142	145	147	16	142	143	145	15	141	132	142	10	140	131	139
PSD2	120	146	146	149	106	143	142	147	74	138	141	146	25	132	141	139	19	121	140	129

Considering 150 strides and comparing results among different levels of immersion, significant differences were observed between knee and pelvis for RQA V (rr, Det and Avg), and

between knee and xiphoid process for RQA V (rr, Det and Avg), ML (rr and Avg) and AP (rr and Avg), with increasing values from knee to xiphoid process level (Table 2). Figure 12 showed Median, 25th and 75th percentiles of RQA (V, ML and AP) in the three conditions. For SE (Figure 13), a significant decreasing of values (Table 2) was observed between knee and xiphoid process in V direction (τ=4, 6, 8). In AP direction, differences were found both between knee and xiphoid process (τ=1, 2) and between pelvis and xiphoid process (τ=1), increasing from knee to xiphoid process (Table 2). All variability measures (Figure 14) significantly increased and tended to double from knee to xiphoid process, except for PSD2, that showed no difference between knee and pelvis.

Figure 12. Median, 25th and 75th percentiles of RQA with asterisks indicating p_value < 5% for the three walking conditions (K, P and XP).

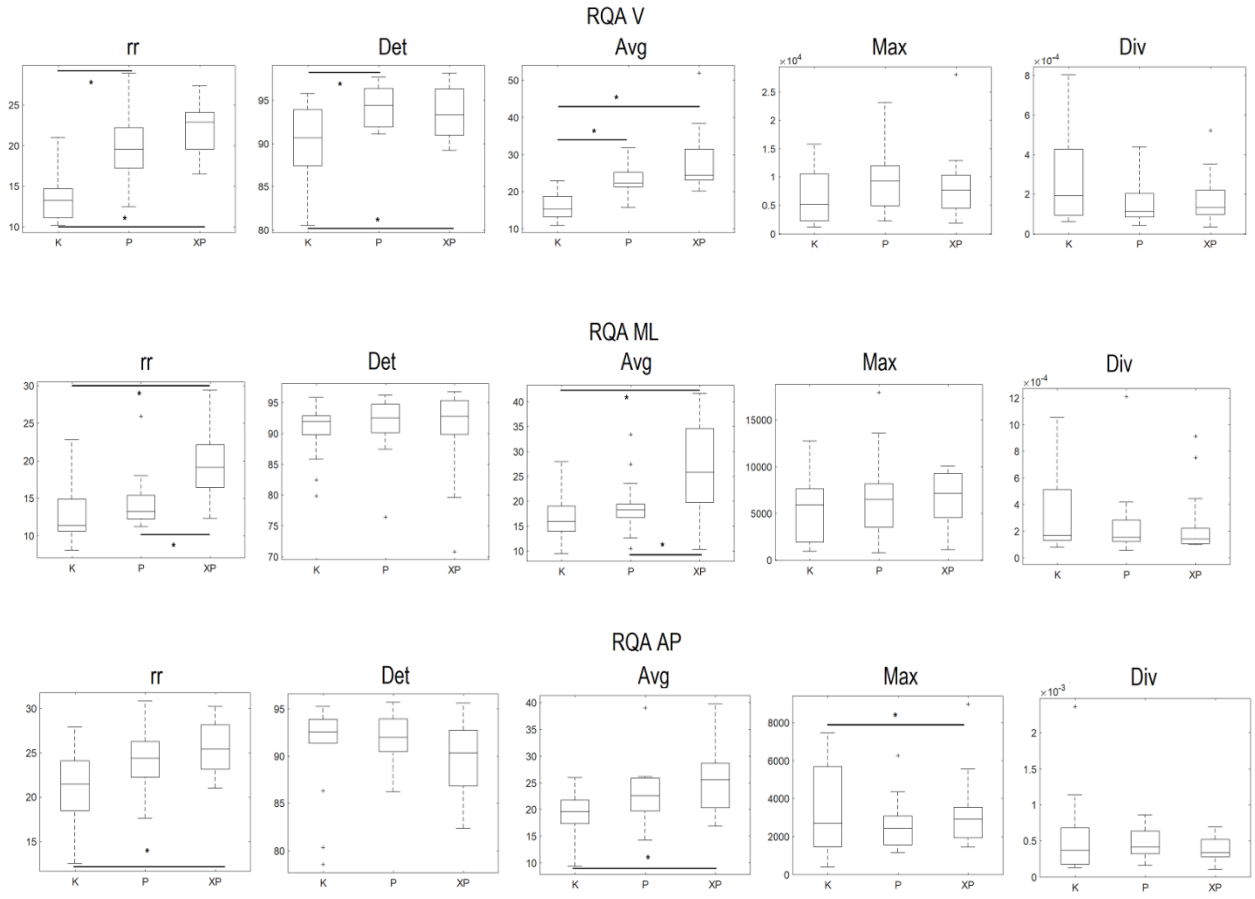

Figure 13. Median, 25th and 75th percentiles of SE with asterisks indicating p_value < 5% for the three walking conditions (K, P and XP).

Figure 14. Median, 25th and 75th percentiles of SD, PSD1 and PSD2 with asterisks indicating p_value < 5% for the three walking conditions (K, P and XP).

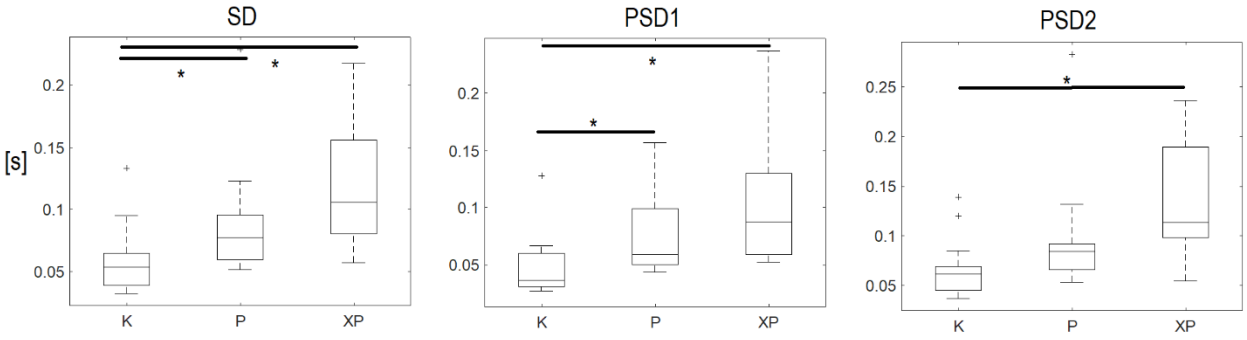

Table 2. Detailed values (median, 25th and 75th percentiles) of each parameter in all directions (V, ML and AP) as related to different level of immersion, i.e. Knee (K), Pelvis (P) and Xiphoid Process (XP).

Level of immersion	K			P			XP		
Parameter	**Median**	**25th**	**75th**	**Median**	**25th**	**75th**	**Median**	**25th**	**75th**
RQA V (rr)	13,30	11,11	14,73	19,55	17,20	22,22	22,90	19,56	24,11
RQA V (Det)	90,67	87,40	93,94	94,43	91,94	96,40	93,35	90,98	96,32
RQA V (Avg)	15,26	13,34	18,73	22,38	21,27	25,21	24,49	23,14	31,45
RQA V (Max)	5196,50	2333,00	10545,00	9293,00	4918,00	11982,00	7673,00	4540,00	10295,00
RQA V (Div)	0,00	0,00	0,00	0,00	0,00	0,00	0,00	0,00	0,00
RQA ML (rr)	11,37	10,60	14,89	13,24	12,25	15,38	19,14	16,41	22,18
RQA ML (Det)	91,94	89,81	92,86	92,53	90,13	94,77	92,85	89,90	95,35
RQA ML (Avg)	15,93	13,94	19,02	18,28	16,70	19,43	25,90	19,76	34,65
RQA ML (Max)	5914,50	1951,00	7617,00	6496,00	3528,00	8143,00	7122,50	4521,00	9266,00
RQA ML (Div)	0,00	0,00	0,00	0,00	0,00	0,00	0,00	0,00	0,00
RQA AP (rr)	21,49	18,46	24,12	24,42	22,28	26,30	25,45	23,20	28,16
RQA AP (Det)	92,55	91,40	93,91	91,98	90,50	93,92	90,37	86,86	92,74
RQA AP (Avg)	19,63	17,36	21,70	22,62	19,71	25,95	25,65	20,29	28,70
RQA AP (Max)	2698,50	1461,00	5684,00	2435,00	1568,00	3079,00	2921,00	1928,00	3534,00
RQA AP (Div)	0,00	0,00	0,00	0,00	0,00	0,00	0,00	0,00	0,00
SE V τ=1	0,28	0,23	0,30	0,26	0,24	0,30	0,29	0,23	0,33
SE V τ=2	0,42	0,35	0,44	0,38	0,35	0,40	0,40	0,35	0,44
SE V τ=4	0,65	0,57	0,70	0,58	0,55	0,66	0,58	0,53	0,63
SE V τ=6	0,84	0,75	0,89	0,75	0,69	0,85	0,75	0,67	0,79
SE V τ=8	0,98	0,88	1,05	0,90	0,82	0,98	0,89	0,78	0,93
SE V τ=10	1,11	0,98	1,22	1,02	0,93	1,12	1,03	0,88	1,07
SE V τ=12	1,22	1,09	1,32	1,12	1,02	1,24	1,16	0,97	1,21
SE ML τ=1	0,29	0,27	0,33	0,29	0,27	0,35	0,30	0,27	0,38
SE ML τ=2	0,45	0,39	0,49	0,45	0,39	0,47	0,42	0,38	0,48
SE ML τ=4	0,73	0,63	0,77	0,70	0,65	0,76	0,64	0,58	0,72
SE ML τ=6	0,96	0,83	1,03	0,91	0,87	1,02	0,83	0,71	0,92
SE ML τ=8	1,14	1,03	1,25	1,11	1,08	1,27	1,01	0,84	1,12
SE ML τ=10	1,32	1,21	1,44	1,30	1,24	1,45	1,17	1,00	1,30
SE ML τ=12	1,46	1,38	1,65	1,47	1,41	1,62	1,33	1,13	1,48
SE AP τ=1	0,23	0,20	0,30	0,29	0,23	0,38	0,39	0,30	0,50
SE AP τ=2	0,33	0,31	0,36	0,38	0,33	0,49	0,45	0,39	0,51
SE AP τ=4	0,48	0,44	0,53	0,55	0,47	0,60	0,53	0,52	0,68
SE AP τ=6	0,61	0,56	0,71	0,67	0,57	0,73	0,65	0,61	0,76
SE AP τ=8	0,71	0,66	0,85	0,76	0,68	0,85	0,77	0,67	0,85
SE AP τ=10	0,79	0,75	0,94	0,87	0,77	0,97	0,87	0,73	0,93
SE AP τ=12	0,86	0,80	1,02	0,97	0,86	1,07	0,95	0,80	1,02
SD [s]	0,05	0,04	0,06	0,08	0,06	0,10	0,11	0,08	0,16
PSD1	0,04	0,03	0,06	0,06	0,05	0,10	0,09	0,06	0,13
PSD2	0,06	0,05	0,07	0,08	0,07	0,09	0,11	0,10	0,19

Discussion

The gait pattern of young healthy adults was analysed during walking in water at different level of immersion (knee, pelvis and xiphoid process) to investigate the minimum number of strides to assess the reliability of non-linear metrics calculation during walking. Moreover, given the maximum number of available strides equal to 150, a characterization of the influence of water on gait performance at different level of immersion was performed.

Overall discrepancy was found between the minimum number of strides identified by previous authors for walking over-ground [44] and the results obtained from the present study. In fact, the great majority of the parameters need more than 120 strides to obtain a reliable measure of variability measures and non-linear metrics, independently from the level of immersion. Instead, measures reached steady values for lower numbers of strides considering over-ground walking: less than 63 strides were sufficient for MSE in the three directions and RQA in V and AP directions, while variability measures (SD, PSD1 and PSD2) need more than 127 strides to obtained a reliable application. For healthy people, walking on dry land represented an automatic and well controlled task, which has been learnt from the firs years of life [127] and can be performed with minimal use of attention-demanding executive control resources [128]. On the contrary, the physical characteristics of the water introduced different testing conditions, that altered the traditional gait pattern and motor control, thus requiring the identification of new gait strategies to perform the walking task in this environment. As a consequence, the great number of strides might be justified with the need of making many attempts to familiarize with the environment, learn and automatize movements. These observations were confirmed by the fact that both variability measures, associated to the specific gait pattern, and the non-linear metrics (RQA and SE), related to the underlying motor control, exhibited a great number of strides to obtain reliable measures [43], thus resulting to be influenced the environment constraints. Possible limitations for the comparison between dry land and water are related to the differences in the length of walking path. In fact, previous analyses on dry land considered gait on 250 m long dead-end road (about 180 strides) [44]. In this work, only central strides of the walking tasks were considered, even if constraints related to pool length of 10 m might influence the calculation of non-linear metrics, in terms of acceleration and deceleration.

Considering a fix number of 150 strides, no significant differences were found between pelvis and xiphoid process level among the analysed metrics, suggesting that gait patterns and motor control were not influenced by the presence of the water in the trunk region. Conversely, most of the metrics significantly varied between knee and the other level of immersions, suggesting that the

disappearing of the pendulum pattern characterizing the over-ground walking resulted to be more effective from the pelvis to higher level. In particular, the differences observed in SD between knee and the other level of immersions indicated that stride time variability changes significantly when water reached the pelvis level. This behaviour was further confirmed by PSD1 and PSD2 values: increasing trend from knee to xiphoid process highlighted how both short- and long-term variability of stride times should be interpreted with caution when analysing data from different environments, confirming the observations defined by previous authors [43]. Also, another factor that influence gait variability is represented by possible differences in the length of the path across different walking conditions, as suggested for older subjects [129] and healthy adults walking in different environments and testing conditions [43]. Increasing in RQA (rr) in all direction from knee to xiphoid process suggested that gait is more regular with the increasing of the level of immersion, and also slower, as highlighted by increasing values of RQA (Avg). In the literature, the complexity of gait on the sagittal plane was quantified by SE and provided relevant parameter for characterizing the maturation of gait [130]. In the current study, no differences were found among different condition for SE in ML direction, suggesting that the stability of trunk acceleration in the sagittal plane during gait in water is not influenced by different level of immersions in young healthy adults. Moreover, for all directions, higher SE values for increasing τ were observed. This trend is in accordance to those reported in the literature [43,130,131].

In conclusion, this study assessed the minimum number of strides to obtain a reliable calculation of non-linear metrics during gait in water at different levels of immersion. Higher number of strides (above 140) were observed in all conditions compared to results obtained by other authors on dry land where variable number of strides in relation to the considered measures were found (from 10 strides for RQA V and AP to more than 120 strides for SD, PSD1 and PSD2). These results suggest carefulness when drawing conclusions about gait variability and stability obtained from short walking trials in the water. In this environment, a number of strides coherent with the indications illustrated in Table 2 should always be considered. Moreover, water environment affected gait performance in terms of variability of the gait pattern and motor control response. In general, these results cannot be generalized to other populations, assuming that the physical characteristics of the water affected gait performance of elderly and/or pathologic subjects in the same way.

Synthesis of the findings

In this section, the influence of extrinsic factors (i.e. different walking surfaces: solid ground and sand; different environment such as water) was assessed during gait of healthy people to evaluate the performance of gait segmentation algorithms and to determine the minimum number of strides for a reliable application of non-linear metrics in the water environment.

All algorithms for gait segmentation applied during walking on solid ground in a controlled laboratory condition were able to correctly identify gait events and temporal parameters. Different accuracy and repeatability were found depending on the implementation characteristics, i.e. sensor position, analysed variable, and computational approach. High similarity in the gait patterns between solid ground and (wet and dry) sand was found for all the analysed variables, explaining the efficiency of algorithms for gait segmentation in the marine environment. On the other hand, gait patterns resulted to be different for walking in the water, especially for signals provided from the sensor attached to the trunk. This finding explained the failure of specific gait segmentation algorithms when applied to walking in water, mostly due to the disappearing of the pendulum mechanics. Moreover, the water environment influenced the motor control response, resulting in a greater number of strides for the application of non-linear metrics in this ambient compared to the results obtained for solid ground.

3.

SECTION 2

INFLUENCE OF INTRINSIC FACTORS ON THE PERFORMANCE OF GAIT ALGORITHMS: ANALYSIS OF PATHOLOGICAL SUBJECTS (PARKINSON'S DISEASE)

Overview

In addition to the extrinsic factors, several elements peculiar of the single person and independent from the environment constraints can affect gait pattern. These intrinsic factors include gender, muscle strength or muscle power, balance, peripheral sensation (proprioception, vibration sense, tactile sensitivity), cognition, and diseases. Although the analysis of the effect of the single factor on the gait performance could be of primary importance in sports and clinical contexts, it was barely reported in the literature, especially for gait in ecological condition.

In this section, the effect of pathology on algorithms for gait segmentation and FOG automatic detection was assessed in PDP during gait on solid grounds. The gait segmentation and FOG detection algorithms were identified from two separate systematic literature reviews and previously explained in the Background.

3.1

SEGMENTATION OF GAIT ON SOLID GROUND IN PEOPLE WITH PARKINSON'S DISEASE

The content of this chapter has been published as abstract in Proceedings of SIAMOC conference 2019 (Bologna) and will be submitted to Gati and Posture as full length article.

Introduction

Patients suffering from Parkinson's disease (PDPs) manifest gait impairments that affect motor behaviour and compromise the quality of life [132]. Objective measures of the gait temporal parameters (GTPs) allow to define the level of impairment and to characterize functional gait performance, which can serve as a biomarker of mobility [14]. The computation of GTP requires the identification of the gait events (GEs), i.e. foot contact (FC) and foot off (FO). These parameters are typically estimated using inertial measurement units (IMUs) given their reliability, limited cost, possibility to exploit in ecological conditions, and limited invasiveness [9]. A number of different algorithms have been proposed for the identification of FC and FO in healthy people, showing excellent sensitivity as well as high accuracy and repeatability when applied to the gait of healthy subjects in controlled laboratory conditions [9,82].

On the other hand, PDPs exhibited gait characteristics that are markedly different from healthy ones [133], such as: i) flat foot strike and toe-to-heel walking [134], ii) reduced foot lifting during the swing phase of gait [135]; iii) higher relative loads in the forefoot regions combined with a load shift towards medial foot areas[136]. These PD specific characteristics of the gait resulted in alterations of the traditional signal patterns provided from IMUs [14,97]. In particular, some authors reported differences in the angular velocity and acceleration of the shank [86,137,138], the foot [39,97,138,139] and the trunk [140] between PDPs and healthy people. Such modifications of the gait signals involved a general degradation of the algorithm performance, highlighting higher error in the identification of GE in PDP [97,137]. Therefore, the algorithm performance for healthy gait cannot be generalized to PD population. Furthermore, a recent study assessed the performances of available algorithms for gait segmentation during walking of healthy people, highlighting differences in the identification of GE in relation to the implementation criterions, i.e. sensor placement, analysed variable, and computational approach [9]. Considering the altered signals pattern in PDP and the influence of the implementation characteristics on the accuracy and repeatability of the algorithms, a comprehensive evaluation of the performance specific to the pathology is necessary.

The present work aimed to fill in this gap analysing the performance of 17 algorithms for GE estimation in PDP patients and taking into account the differences in the signal patterns with respect to healthy subjects for which the algorithms were designed for. The results were intended as the bases for the selection criteria of the most appropriate algorithm for the specific pathology under evaluation.

Materials and Methods

Analysed algorithms

Seventeen algorithms representative of the state of art in the estimation of GE and GTP for healthy subjects [9], were here analysed for PDP. As reported by the author in the original paper [9], the algorithms were classified based on:

i) IMU position (i.e. trunk, shanks, feet)

ii) Target variable (i.e. acceleration, angular velocity)

iii) Computational approach: 'peak identification' and 'zero crossing', on raw or filtered target variable (i.e. finite impulse response (FIR), infinite impulse response (IIR), wavelet transform (WT) filtering).

Experimental analysis

Participants:

The study population consisted of 20 PDPs (12 females ,8 males; 67.2±9.1 years old; 1.65±0.12 m; 67.3±13.1 Kg) at Hoehn and Yahr stage III, of which 10 with a diagnosis of freezing. All patients were in the medication ON state and were able to walk without aids (e.g. canes) and/or helped by operators or physiotherapists. The study was approved by the local scientific committee and institutional review board (Comitato Etico Interaziendale delle Provincie di Lecco, Como, Sondrio) and was in accordance with the Code of Ethics of the World Medical Association (Declaration of Helsinki, 1967). A complete explanation of the study protocol was provided to the patients and written informed consent was obtained before their participation in the study. This trial was registered on ClinicalTrials.gov NCT03015714.

Data acquisition:

Each participant performed a six-minutes walking test along a 15 m straight pathway at self-selected speed wearing own comfortable footwear. Five tri-axial IMUs (OPAL, Apdm, sf=128 Hz) were attached to the trunk (at L5 level), shanks (about five centimetres above lateral malleolus), and feet (on the dorsal surface of each shoe). The walking tasks were also filmed using a GoPro (Hero4, USA, sf=240Hz). Three IMUs impacts were video-recorded and used for time-synchronization of IMUs and video recording.

Data Analysis:

Elaboration 1: Validation with respect to video without freezing episodes, limited to 12 central steps of straight walking.

To test the performance of the algorithms in GE and GTP estimation against the video reference, only the central steps of the straight walking path were considered. Therefore, any freezing episode as well as turning, resting periods, first and last steps of each walked path were excluded. Finally, 12 central steps of 4 straight walking paths were considered, for a total of 48 FC and 48 FO analysed for each patient. FC_{GoPro} and FO_{GoPro} were visually identified from the videos and used as reference. FC_{IMU} and FO_{IMU} were then estimated form IMU measurements using the selected 17 algorithms [9], implemented in MATLAB (MathWorks 2017a, USA).

For each algorithm, the Sensitivity in GE identification was calculated as:

$$\frac{\text{Number of GEs identified by algorithm}}{\text{Number of all GEs as identified by video}} \quad (11)$$

For both acceleration and angular velocity components, depending on the variable analysed by each of the 17 selected algorithms, ICC of the mean stride cycle over the whole sequence of the trial for each participant (Single ICC_{E1}) was calculated to analyse the repeatability of the curves.

GTPs were calculated from GE only for the patients reporting a minimum Sensitivity of 81% [83] for all algorithms. Then, the measurement errors for GE and GTP were estimated for each algorithm as follows:

$$E_{GE} = GE_{IMU} - GE_{GoPro} \quad (12)$$

$$E_{GTP} = GTP_{IMU} - GTP_{GoPro} \quad (13)$$

Since in the original work the performance of the algorithms in GE identification was analysed considering ground reaction forces as reference, the maximum measurement error of video versus ground reaction force was estimated to be equal to 0,05s (see Paragraph 2.2 of Section 1).

For each parameter (FC, FO, Stride Time, Step Time, Stance Time, Swing Time), a linear mixed model [85] was applied to test the dependency of error values on each implementation criterion, with a significance level of 0.05 using R software (R-Core Team 2017, Austria, version 3.4.3). First, the statistical analysis was performed to investigate the influence of IMU position and target

variable, alone. Then, the influence of analysed variable and computational approach were investigated separately for each IMU position.

Median value (Med) of the error was calculated to characterize accuracy, and the Dispersion around Med (Dmed, 75^{th} percentile – 25^{th} percentile values of the error) to characterize repeatability.

Elaboration 2: Performance comparison analysis with freezing episodes, considering 6 minutes walking without turnings.

The signals acquired during the whole six-minute walking test were here considered. Turnings and resting periods were segmented and excluded from the analysis [43,137,141].

Average gait speed was calculated separately for each subject as the ratio between straight walked distance and time.

GEs identified from the angular velocity around the medio-lateral axis of the leg adopting the algorithm by Salarian et al. [137] was used as a Gold Standard as it was already validated for GE detection of PDP [137] and exhibit excellent performance in gait segmentation of healthy subjects [9]. Sensitivity of the algorithms was then calculated as:

$$\frac{\text{Number of GE identified by algorithm}}{\text{Number of all GE as identified by Salarian}}$$

ICC of the mean stride cycle over the whole sequence of the trial for each participant was calculated (Single ICC_{E2}) to analyse the repeatability of the curves. ICC of the mean stride cycle of the signals exploited for the implementation of the algorithms over the curve representative of the gait pattern of healthy people (Combined ICC_{E2}) was calculated to analyse the similarity of PDP curve with respect to the healthy ones, assumed as reference for the algorithm implementation.

Results

Although 10 of the 20 patients were diagnosed with freezing, only 5 presented the symptoms during the experiment.

Elaboration 1

For 2 of the 20 patients, the visual identification of FC and FO was compromised because one foot covered the other during the whole walking test, thus they were not considered in Elaboration 1. For each of the remaining 18 participants, 48 FCs and FOs were identified and analysed during the six minutes walking test, for a total of 864 FCs and FOs.

All the algorithms passed the 81% Sensitivity criterion for all the subjects, with the exception of one patient. In this case, algorithms that failed in GE detection exploited:

i) angular velocity of the shank, i.e. Catalfamo et al. 2010 [34] and Greene et al. 2010 [35], and the foot, i.e. Ferrari et al. 2010 [39], showing Single ICC_{E1} values of 0.94, 0.93 and 0.89, respectively;

ii) acceleration of the shank, i.e. Khamdelwal et al. 2014 [33], and the foot, i.e. Jasiewicz et al. 2006 [37], reporting Single ICC_{E1} of 0,46 and 0,65, respectively.

Results from Elaboration 1 of Sensitivity and Single ICC_{E1} are summarised in Table 1.

Table 1. Sensitivity (expressed as a percentage) as related to the estimation of GEs below 81% were punctually reported; Single ICC_{E1} (highlighted in light grey) of the different target signals in relation to the implementation criterions defined on the normalized stride time. Algorithms showing ICC below 81% are pointed out in dark grey.

Algotithm	Subject																	
	1	2	3	4	5	6	8	9	10	11	12	13	15	16	17	18	19	20
	Sensitivity FC/FO ICC																	
Bugané et al. 2012	>81																	
	0.81	0.95	0.91	0.97	0.95	0.89	0.97	0.92	0.95	0.97	0.88	0.85	0.90	0.96	0.94	0.86	0.98	0.95
Lee et al. 2009	>81																	
	0.88	0.93	0.87	0.97	0.92	0.85	0.96	0.87	0.93	0.96	0.85	0.80	0.86	0.95	0.92	0.83	0.98	0.94
McCamley et al. 2012	>81																	
	0.93	0.98	0.96	0.97	0.98	0.97	0.99	0.95	0.97	0.98	0.95	0.61	0.97	0.98	0.96	0.95	0.98	0.95
Gonzalez et al. 2010	>81																	
	0.93	0.97	0.93	0.98	0.97	0.92	0.98	0.94	0.97	0.98	0.91	0.88	0.95	0.97	0.96	0.89	0.98	0.96
Shin et al. 2011	>81																	
	0.86	0.93	0.93	0.96	0.95	0.92	0.98	0.87	0.96	0.97	0.91	0.64	0.86	0.96	0.94	0.87	0.97	0.94
Zijlstra et al. 2003	>81																	
	0.94	0.99	0.92	0.99	0.99	0.97	0.99	0.94	0.98	0.98	0.97	0.71	0.97	0.99	0.97	0.97	0.99	0.99
Lee et al. 2010	>81																	
	0.98	0.99	0.97	0.99	0.98	0.96	0.99	0.98	0.97	0.99	0.97	0.88	0.98	0.98	0.99	0.97	0.99	0.98
Trojanello et al. 2014	>81											89/73	>81					
	0.84	0.82	0.79	0.87	0.94	0.82	0.96	0.81	0.73	0.88	0.91	0.46	0.71	0.93	0.9	0.6	0.91	0.92
Khandelwal et al. 2014	>81																	
	0.95	0.99	0.95	0.99	0.98	0.87	0.98	0.97	0.96	0.98	0.94	0.86	0.96	0.97	0.96	0.95	0.98	0.96
Catalfamo et al. 2010	>81											100/75	>81					
	0.99	0,99	0.98	0.99	0.91	0.99	0.99	0.99	0.98	1	0.99	0.94	0.99	0.99	0.99	0.98	0.99	0.99
Greene et al. 2010	>81											60/58	>81					
	0.99	0.99	0.98	0.99	0.99	0.99	0.99	0.99	0.99	0.99	0.99	0.93	0.99	0.99	0.99	0.98	0.99	0.99
Salarian et al. 2004	>81																	
	0.99	0.99	0.98	0.99	0.99	0.99	0.99	0.99	0.99	0.99	0.99	0.93	0.99	0.99	0.99	0.98	0.99	0.99
Aminian et al. 2002	>81																	
	0.98	0.99	0.98	0.99	0.99	0.99	0.99	0.99	0.98	0.99	0.99	0.93	0.99	0.99	0.99	0.98	0.99	0.99
Jasiewicz et al. 2006	>81											75/81	>81					
	0.93	0.90	0.89	0.95	0.93	0.84	0.96	0.90	0.83	0.85	0.92	0.65	0.89	0.93	0.93	0.78	0.94	0.92
Sabatini et al. 2005	>81																	
	0.98	0.99	0.97	0.99	0.98	0.98	0.99	0.99	0.97	0.99	0.97	0.92	0.98	0.99	0.99	0.96	0.99	0.99
Ferrari et al. 2016	>81											83/79	>81					
	0.98	0.99	0.97	0.99	0.98	0.98	0.99	0.98	0.97	0.99	0.97	0.89	0.98	0.99	0.99	0.96	0.99	0.99
Mariani et al. 2013	>81																	
	0.98	0.99	0.97	0.99	0.98	0.98	0.99	0.99	0.97	0.99	0.97	0.92	0.98	0.99	0.99	0.96	0.99	0.99

The characterization of the errors in GE detection was conducted for all the patients that passed the 81% Sensitivity criterion. It is reported in more detail here below, considering the different implementation characteristics.

IMU Position

Considering GE, significant differences were found among different IMU position. In particular, FC identification resulted more accurate for Foot- and Shank- based algorithms than Trunk-based ones (Med 0.05 s for both Shank and Foot, 0.10 s for Trunk) and more repeatable for Shank-based algorithms, followed by Foot- and Trunk-based ones (DMed 0.05s for Shank, 0.10s for Foot and Trunk). As for FO, Foot-based algorithms showed the best accuracy, with Med 0.05s, while Shank-based highlighted the best repeatability, with DMed 0,05s. For GTP, similar performance was found for Stride and Step time estimates among the three IMU position, while Foot-based algorithms showed the best accuracy and repeatability for Stance and Swing time (Med of -0.05s and 0.05s for Stance and Swing, respectively, and DMed of 0.10s for both parameters).

Target variable

Angular velocity-based algorithms resulted equally repeatable but more accurate for FC (Med/Dmed: 0.05/0.10 s and 0.10/0.10 s, for Angular velocity and Acceleration, respectively), and less accurate and more repeatable in FO estimation (Med/Dmed: -0,05/0.05 s and 0.00/0.15 s, for Angular velocity and Acceleration, respectively) than Acceleration-based ones. For GTP, comparable results were found in Stride time, Step time and Stance Time estimation, while Acceleration-based algorithms resulted less repeatable and equally accurate in Swing time estimation (Med/Dmed: 0.10/0.15 s and 0.10/0.10 s, for Acceleration and Angular velocity, respectively).

Error characteristics for FC (a), FO (b), Stride- (c), Step- (d), Stance- (e) and Swing time (f) as related to IMU position and target variable are schematically depicted in Figure 1, while numerical values of the errors are reported in Table 2.

Table 2: Results of statistical analysis for IMU position and target variable: 25th quartile, median and 75th quartile of estimation error for FC, FO, stride time, step time, stance time and swing time (* $p<0.05$).

Parameter	***Estimation of errors: IMU position (s)***			***Level of significance***
	Trunk	***Shanks***	***Feet***	Shanks – Feet
FC	0.05; 0.10; 0.15	0.05; 0.05; 0.10	0.00; 0.05; 0.10	Trunk - Shanks * Trunk - Feet * Shanks - Feet *
FO	-0.15; -0.10; -0.05	-0.05; -0.05; 0.00	-0.05; 0.00; 0.05	Trunk - Shanks * Trunk - Feet * Shanks - Feet *
Stride Time	-0.05; 0.00; 0.05	0.00; 0.00; 0.00	0.00; 0.00; 0.00	Trunk - Shanks Trunk - Feet Shanks - Feet
Step Time	-0.05; 0.00; 0.05	-0.05; 0.00; 0.05	-0.05; 0.00; 0.05	Trunk - Shanks * Trunk - Feet * Shanks - Feet
Stance Time	-0.25; -0.20; -0.15	-0.15; -0.10; -0.05	-0.10; -0.05; 0.00	Trunk - Shanks * Trunk - Feet * Shanks - Feet *
Swing Time	0.15; 0.20; 0.25	0.05; 0.10; 0.15	0.00; 0.05; 0.10	Trunk - Shanks * Trunk - Feet * Shanks - Feet *
Parameter	***Estimation of errors: target variable (s)***			***Level of significance***
	Acceleration	***Angular velocity***		Angular Velocity – Acceleration
FC	0.00; 0.05; 0.10	0.05; 0.10; 0.15		*
FO	-0.05; -0.05; 0.00	-0.10; 0.00; 0.05		*
Stride Time	0.00; 0.00; 0.00	-0.05; 0.00; 0.05		
Step Time	-0.05; 0.00; 0.05	-0.05; 0.00; 0.05		*
Stance Time	-0.15; -0.10; -0.05	-0.15; -0.10; -0.05		*
Swing Time	0.05; 0.10; 0.15	0.05; 0.10; 0.20		*

Figure 15: Box plot (minimum, 25th percentile, median, 75th percentile, maximum values) for FC (a), FO (b), Stride- (c), Step- (d), Stance- (e), and Swing time (f) estimation errors as related to IMU position and target variable. Angular velocity-based algorithms are framed in dashes.

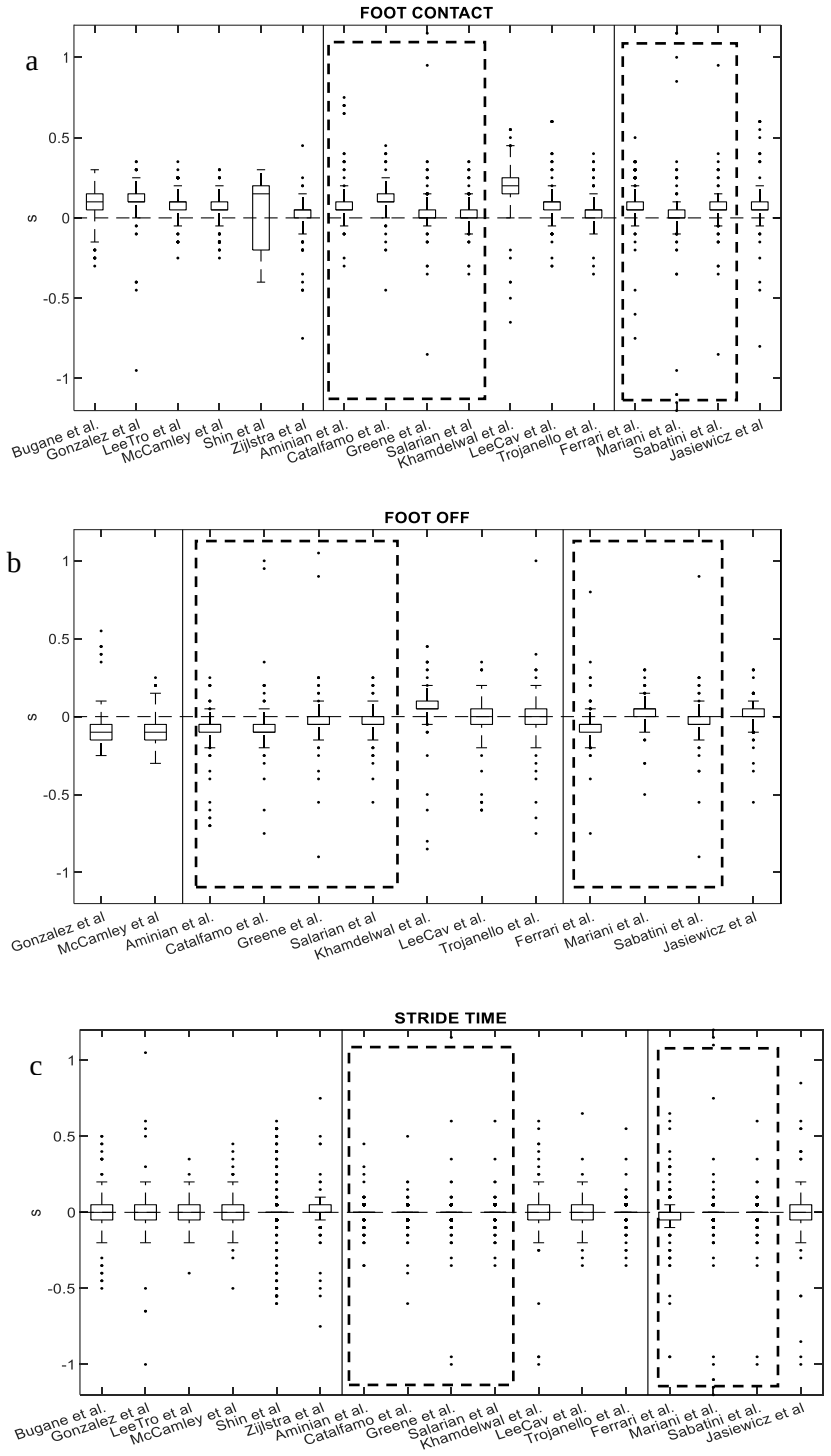

d

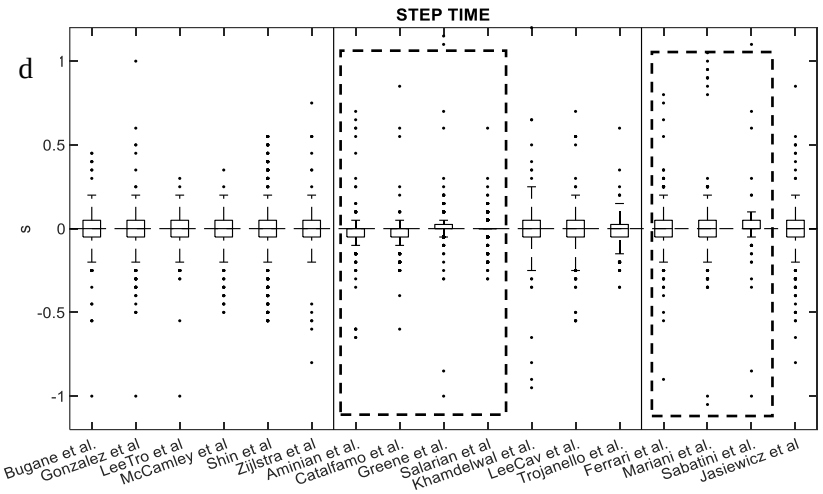
STEP TIME
s
1
0.5
0
-0.5
-1
Bugane et al.
Gonzalez et al
LeeTro et al
McCamley et al
Shin et al
Zijlstra et al
Aminian et al.
Catalfamo et al.
Greene et al.
Salarian et al
Khamdelwal et al.
LeeCav et al.
Trojanello et al.
Ferrari et al.
Mariani et al.
Sabatini et al.
Jasiewicz et al

e

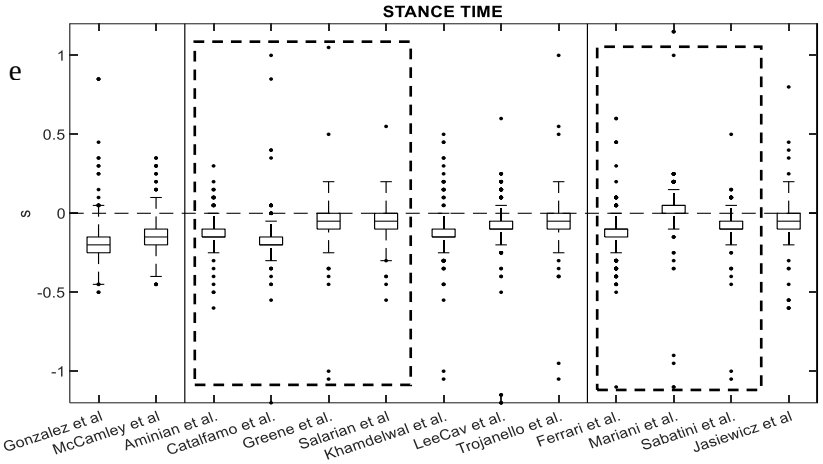
STANCE TIME
s
1
0.5
0
-0.5
-1
Gonzalez et al
McCamley et al
Aminian et al.
Catalfamo et al.
Greene et al.
Salarian et al
Khamdelwal et al.
LeeCav et al.
Trojanello et al.
Ferrari et al.
Mariani et al.
Sabatini et al.
Jasiewicz et al

f)

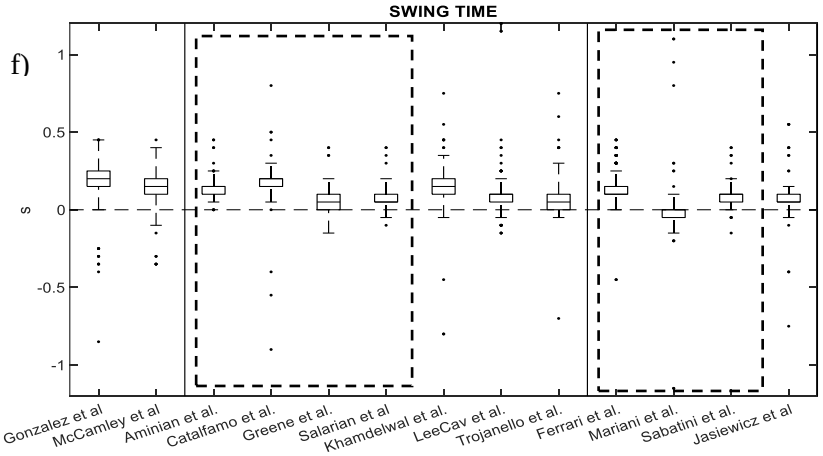
SWING TIME
s
1
0.5
0
-0.5
-1
Gonzalez et al
McCamley et al
Aminian et al.
Catalfamo et al.
Greene et al.
Salarian et al
Khamdelwal et al.
LeeCav et al.
Trojanello et al.
Ferrari et al.
Mariani et al.
Sabatini et al.
Jasiewicz et al

Computational approach

GEs.

Considering the trunk-based algorithms, 'peak identification' with WT and 'zero crossing' with IIR filtering resulted to be the most accurate and repeatable for FC identification, with Med/Dmed equal to 0.05s0.05s. Similar accuracy and repeatability were observed for FO detection among different computational approaches (Med/Dmed -0.10/-0.10s both for 'peak identification' with WT filtering and 'zero crossing' with FIR filtering). Shank-based algorithms exploited only 'peak identification' approach: Raw signal reported the highest accuracy and repeatability in FC detection (Med/Dmed of 0,05/0,05s) as well as the best repeatability in FO detection (Dmed 0.05s), while WT filtering showed the best accuracy (Med 0.00s). For Foot-based algorithms, independently from the computational approach and filtering, similar results were obtained for GE estimation in terms of repeatability (Dmed equal to 0.05s in all cases), while 'zero crossing' with IIR and 'peak detection' of Raw signal resulted the most accurate for FC and FO estimation, respectively, with Med of 0.00s.

GTPs.

In general, the estimation of Stride and Step time showed similar accuracy and repeatability independently from the implementation characteristics, while significant differences are observed among different computational approaches for Stance and Swing time. Error values and statistical analysis for computational approach are reported in Table 3.

Table 3: Results of statistical analysis for computational approach: 25th quartile, median and 75th quartile of estimation error for FC, FO, stride time, step time, stance time and swing time (* $p<0.05$).

IMU position	Parameter	Level of significance 'peak identification' vs 'zero crossing'	Estimation of errors: Filtering (s) Level of significance			
			Filtering within 'peak identification'	Level of significance for filtering within 'peak identification'	Filtering within 'zero crossing'	Level of significance for filtering within 'zero crossing'
Trunk	FC	*	FIR: 0.05; 0.10; 0.10 IIR: 0.05; 0.10; 0.15 WT: 0.05; 0.05; 0.10	FIR – IIR * FIR – WT IIR – WT *	Raw: -0.20; 0.15; 0.20 FIR: 0.10; 0.10; 0.15 IIR: 0.00; 0.05; 0.05	FIR – IIR * FIR – Raw * IIR – Raw
	FO	*	WT: -0.15; -0.10; -0.05	-	FIR: -0.15; -0.10; -0.05	-
	Stride	-	FIR: -0.05; 0.00; 0.05 IIR: -0.05; 0.00; 0.05 WT: -0.05; 0.00; 0.05	FIR – IIR FIR – WT IIR – WT	FIR: -0.05; 0.00; 0.05 IIR: 0.00; 0.00; 0.05 Raw: 0.00; 0.00; 0.00	FIR – Raw FIR – IIR IIR – Raw
	Step	-	FIR: -0.05; 0.00; 0.05 IIR: -0.05; 0.00; 0.05 WT: -0.05; 0.00; 0.05	FIR – IIR FIR – WT IIR – WT	FIR: -0.05; 0.00; 0.05 IIR: -0.05; 0.00; 0.05 Raw: -0.05; 0.00; 0.05	FIR – Raw FIR – IIR IIR – Raw
	Stance	*	WT: -0.20; -0.15; -0.10	-	FIR: -0.25; -0.20; -0.15	-
	Swing	*	WT: 0.10; 0.15; 0.20	-	FIR: 0.15; 0.20; 0.25	-
Shank	FC	-	Raw: 0.00; 0.05; 0.05 IIR: 0.05; 0.10; 0.15 WT: 0.05; 0.10; 0.20	IIR – Raw * IIR – WT * Raw – WT *	-	

	FO		Raw: -0.05; -0.05; 0.00 IIR: -0.10; -0.05; 0.00 WT: -0.05; 0.00; 0.05	IIR – Raw * IIR – WT * Raw – WT *		
	Stride		IIR: 0.00; 0.00; 0.00 Raw: 0.00; 0.00; 0.00 WT: 0.00; 0.00; 0.00	IIR – Raw IIR – WT Raw – WT		
	Step		Raw: 0.00; 0.00; 0.00 IIR: -0.05; 0.00; 0.05 WT: -0.05; 0.00; 0.05	IIR – Raw IIR – WT Raw – WT *		
	Stance		Raw: -0.10; -0.05; 0.00 IIR: -0.20; -0.15; -0.10 WT: -0.15; -0.15; -0.10	IIR – Raw * IIR – WT Raw – WT *		
	Swing		IIR: 0.10; 0.15; 0.20 Raw: 0.00; 0.05; 0.10 WT: 0.10; 0.15; 0.15	IIR – Raw * IIR – WT Raw – WT *		
Foot	FC	*	Raw: 0.05; 0.05; 0.10 IIR: 0.05; 0.05; 0.10	IIR – Raw *	IIR: 0.00; 0.00; 0.05	-
	FO	*	Raw: -0.05; 0.00; 0.00 IIR: -0.05; -0.05; 0.00	IIR – Raw *	IIR: 0.00; 0.05; 0.05	
	Stride	-	IIR: 0.00; 0.00; 0.00 Raw: -0.05; 0.00; 0.05	IIR – Raw	IIR: 0.00; 0.00; 0.00	
	Step	-	Raw: -0.05; 0.00; 0.05 IIR: 0.00; 0.00; 0.05	IIR – Raw	IIR: -0.05; 0.00; 0.05	
	Stance	*	Raw: -0.15; -0.10; -0.05 IIR: -0.10; -0.10; -0.05	IIR – Raw	IIR: 0.00; 0.05; 0.05	
	Swing	*	IIR: 0.05; 0.10; 0.10 Raw: 0.05; 0.10; 0.15	IIR – Raw	IIR: -0.05; 0.00; 0.00	

Elaboration 2

For each subject, a mean (±standard deviation, SD) of 195 (± 71) strides was obtained. Gait speed normalised according to Hof [100] ranged from 0.03±0.01 to 0.49±0.05.

In 3 subjects, some of the algorithms for GE identification showed values below 81% Sensitivity. In particular, algorithms that failed in GE detection exploited:

i) angular velocity of the shank, i.e. Catalfamo et al. 2010 [34], and the foot, i.e. Ferrari et al. 2010 [39] and Mariani et al. 2013 [40]. Single ICC_{E2} values were between 0.83 and 0.94 for the shank, and between 0.68 and 0.88 for the foot, while Combined ICC_{E2} values were between 0.50 and 0.69 for the shank, and between 0.17 and 0.51 for the foot.

ii) acceleration of the shank, i.e. Khandelwal et al. 2014 [33], and the foot, i.e. Jasiewicz et al. 2006 [37], reporting Single ICC_{E2} from 0.64 and 0.67 for shank and of 0.56 for foot. Combined ICC_{E2} values were between 0.12 and 0.35 for the shank, and 0.37 for the foot.

Results of average Gait speed, Sensitivity, Single and Combined ICC_{E2} for the single subject are summarised in Table 4.

Table 4. Sensitivity (expressed as a percentage) as related to the estimation of GEs; Single and Combined ICC_{E2} (S- and C-ICC, highlighted in light grey) of the different target signals in relation to the implementation criterions defined on the normalized stride time. Algorithms showing ICC below 81% are pointed out in dark grey.

		Subject																			
		1	**2**	**3**	**4**	**5**	**6**	**7**	**8**	**9**	**10**	**11**	**12**	**13**	**14**	**15**	**16**	**17**	**18**	**19**	**20**
Gait speed/ Algorithm	**Mean**	0.22	0.49	0.31	0.47	0.45	0.29	0.07	0.40	0.41	0.41	0.45	0.21	0.11	0.03	0.44	0.43	0.27	0.36	0.46	0.37
	Std	0.01	0.05	0.06	0.05	0.03	0.01	0.02	0.03	0.03	0.02	0.04	0.02	0.08	0.01	0.04	0.03	0.02	0.03	0.04	0.04
Bugane et al. 2012	**FC/FO**	>81																			
	S-ICC	0,83	0,97	0,87	0,97	0,93	0,87	0,77	0,97	0,94	0,97	0,93	0,88	0,72	0,79	0,96	0,97	0,92	0,93	0,98	0,94
	C-ICC	0,56	0,65	0,71	0,65	0,66	0,66	0,39	0,79	0,68	0,86	0,71	0,48	0,58	0,5	0,83	0,65	0,79	0,8	0,88	0,87
Lee et al. 2009	**FC/FO**	>81																			
	S-ICC	0,77	0,95	0,83	0,95	0,9	0,83	0,76	0,96	0,92	0,96	0,91	0,86	0,67	0,73	0,94	0,95	0,89	0,92	0,97	0,93
	C-ICC	0,53	0,59	0,68	0,59	0,6	0,64	0,39	0,77	0,66	0,82	0,68	0,48	0,57	0,5	0,79	0,6	0,77	0,79	0,86	0,85
McCamley et al. 2012	**FC/FO**	>81																			
	S-ICC	0,80	0,99	0,97	0,99	0,98	0,97	0,82	0,99	0,97	0,99	0,97	0,92	0,32	0,74	0,99	0,99	0,94	0,98	0,99	0,98
	C-ICC	0,17	0,93	0,95	0,87	0,61	0,65	0,08	0,69	0,77	0,85	0,85	0,23	0,09	0,09	0,93	0,93	0,65	0,85	0,88	0,89
Gonzalez et al. 2010	**FC/FO**	>81																			
	S-ICC	0,89	0,98	0,9	0,98	0,96	0,90	0,80	0,98	0,95	0,98	0,95	0,91	0,77	0,81	0,97	0,98	0,94	0,95	0,98	0,96
	C-ICC	0,63	0,73	0,85	0,68	0,87	0,66	0,34	0,85	0,83	0,89	0,86	0,51	0,58	0,44	0,91	0,73	0,71	0,74	0,89	0,80
Shin et al. 2011	**FC/FO**	>81																			
	S-ICC	0,86	0,95	0,92	0,95	0,93	0,91	0,66	0,97	0,93	0,97	0,93	0,89	0,47	0,51	0,93	0,95	0,89	0,95	0,97	0,93
	C-ICC	0,19	0,48	0,77	0,52	0,58	0,58	0,13	0,72	0,49	0,72	0,74	0,41	0,02	0,13	0,73	0,48	0,75	0,6	0,75	0,81
Zijlstra et al. 2003	**FC/FO**	>81																			
	S-ICC	0,92	0,99	0,89	0,99	0,97	0,96	0,92	0,99	0,94	0,98	0,97	0,96	0,65	0,85	0,98	0,99	0,97	0,98	0,99	0,98
	C-ICC	0,59	0,83	0,69	0,92	0,78	0,86	0,4	0,91	0,55	0,9	0,84	0,5	0,32	0,57	0,81	0,83	0,84	0,79	0,97	0,93
Lee et al. 2010	**FC/FO**	>81																			
	S-ICC	0,97	0,99	0,97	0,99	0,98	0,97	0,82	0,97	0,99	0,98	0,98	0,97	0,75	0,82	0,99	0,99	0,96	0,98	0,99	0,98
	C-ICC	0,88	0,91	0,86	0,93	0,88	0,86	0,39	0,91	0,92	0,85	0,91	0,83	0,58	0,61	0,94	0,91	0,83	0,94	0,96	0,89
Trojanello et al. 2014	**FC/FO**	>81						89/58	>81					90/67	>81						
	S-ICC	0,94	0,97	0,86	0,96	0,95	0,91	0,75	0,97	0,97	0,95	0,94	0,95	0,68	0,69	0,96	0,97	0,93	0,96	0,97	0,94
	C-ICC	0,75	0,65	0,67	0,7	0,77	0,7	0,53	0,59	0,78	0,74	0,74	0,82	0,65	0,56	0,68	0,65	0,79	0,72	0,89	0,86
Khandelwal et al. 2014	**FC/FO**	>81						71/100	>81					92/49	>81						
	S-ICC	0,94	0,98	0,95	0,98	0,96	0,91	0,67	0,98	0,98	0,98	0,95	0,95	0,64	0,63	0,98	0,98	0,91	0,97	0,98	0,94
	C-ICC	0,64	0,72	0,61	0,68	0,69	0,35	0,12	0,6	0,75	0,59	0,58	0,44	0,35	0,24	0,69	0,72	0,41	0,66	0,62	0,45
Catalfamo et al. 2010	**FC/FO**	>81						92/80	>81					100/69	96/77	>81					
	S-ICC	0,99	0,99	0,98	0,99	0,99	0,99	0,94	0,99	0,99	0,99	0,99	0,99	0,83	0,87	0,99	0,99	0,98	0,99	0,99	0,99
	C-ICC	0,82	0,98	0,94	0,97	0,97	0,97	0,57	0,94	0,97	0,97	0,97	0,87	0,50	0,69	0,95	0,98	0,96	0,98	0,98	0,98
Greene et al. 2010	**FC/FO**	>81																			
	S-ICC	0,99	0,99	0,98	0,99	0,99	0,99	0,94	0,99	0,99	0,99	0,99	0,99	0,83	0,87	0,99	0,99	0,98	0,99	0,99	0,99
	C-ICC	0,82	0,97	0,94	0,97	0,97	0,97	0,57	0,94	0,97	0,97	0,97	0,87	0,5	0,69	0,95	0,97	0,96	0,98	0,98	0,98
Salarian et al. 2004	**FC/FO**	Gold Standard																			
	S-ICC	0,99	0,99	0,98	0,99	0,99	0,99	0,94	0,99	0,99	0,99	0,99	0,99	0,83	0,87	0,99	0,99	0,98	0,99	0,99	0,99
	C-ICC	0,82	0,97	0,94	0,97	0,97	0,97	0,57	0,94	0,97	0,97	0,97	0,87	0,50	0,69	0,95	0,97	0,96	0,98	0,98	0,98
Aminian et al. 2002	**FC/FO**	>81																			
	S-ICC	0,99	0,99	0,98	0,99	0,99	0,99	0,94	0,99	0,99	0,99	0,99	0,99	0,83	0,87	0,99	0,99	0,99	0,99	0,99	0,99
	C-ICC	0,82	0,97	0,94	0,97	0,97	0,97	0,57	0,94	0,97	0,97	0,97	0,87	0,5	0,69	0,95	0,97	0,96	0,98	0,98	0,98
Jasiewicz et al. 2006	**FC/FO**	>81												69/73	>81						
	S-ICC	0,92	0,93	0,89	0,96	0,87	0,86	0,78	0,97	0,93	0,96	0,93	0,91	0,56	0,75	0,93	0,93	0,86	0,95	0,95	0,89
	C-ICC	0,83	0,67	0,81	0,73	0,77	0,77	0,46	0,71	0,85	0,76	0,81	0,72	0,37	0,53	0,78	0,66	0,79	0,83	0,87	0,83
Sabatini et al. 2005	**FC/FO**	>81																			
	S-ICC	0,97	0,99	0,97	0,99	0,98	0,97	0,88	0,99	0,99	0,99	0,99	0,97	0,69	0,79	0,99	0,99	0,98	0,99	0,99	0,98
	C-ICC	0,8	0,92	0,92	0,93	0,96	0,91	0,34	0,87	0,97	0,93	0,94	0,7	0,17	0,52	0,92	0,92	0,93	0,95	0,96	0,97
Ferrari et al. 2016	**FC/FO**	>81						21/21	>81					67/65	62/61	>81					
	S-ICC	0,97	0,98	0,96	0,99	0,98	0,97	0,88	0,99	0,99	0,99	0,98	0,97	0,69	0,78	0,99	0,98	0,97	0,99	0,99	0,98
	C-ICC	0,81	0,92	0,9	0,93	0,96	0,9	0,32	0,88	0,97	0,93	0,94	0,7	0,18	0,51	0,9	0,92	0,92	0,95	0,95	0,96
Mariani et al. 2013	**FC**	>81						64/100	>81					81/99	79/100	>81					
	S-ICC	0,97	0,98	0,97	0,99	0,98	0,97	0,88	0,99	0,99	0,99	0,99	0,97	0,68	0,79	0,99	0,98	0,98	0,99	0,99	0,98
	C-ICC	0,8	0,92	0,91	0,93	0,96	0,9	0,33	0,87	0,97	0,93	0,94	0,7	0,17	0,52	0,92	0,92	0,92	0,95	0,96	0,97

Discussion

The present study analysed the performance of 17 algorithms originally designed for GE detection in healthy people when applied to the inertial data collected from six-minutes walking test in PDP. More specifically, the influence of the implementation characteristics (IMU position, target variable and computational approach) on the accuracy was investigated. Furthermore, a performance comparison between the algorithms was exploited taking into account the specific altered signal pattern of the pathologic population under analysis.

In order to characterize the performance of the algorithms in term of accuracy and repeatability in GE and GTP detection and considering the video-camera as reference, only central strides of straight paths were considered. In these conditions, all the algorithms showed over-threshold Sensitivity, with the exception of one subject, that was not considered in the error characterization. According to the results obtained from previous analysis on healthy subjects [9], performance of algorithms in GE detection, Stance and Swing time estimation significantly depends on the implementation characteristics, i.e. sensor position, analysed variable and computational approach. In particular, Shank- and Foot-based algorithms resulted to be preferable than Trunk-based one. This behaviour was already observed in healthy people [9], and then confirmed in pathological populations [97]. In fact, as a general rule, the closer the sensor is to the point of impact the higher are the chances of correctly detecting the GE [142]. In relation to the analysed variable, angular velocity-based algorithms performed slightly better than Acceleration-based one. This trend might be associated to the general lower repeatability in the gait pattern of algorithms exploiting accelerations compared to angular velocities, showing minimum Single ICC_{E1} of 0.46 and 0.89, respectively. Considering the computational approach, an indicatory conclusion can be hardly proposed, because different results were obtained in relation to the different sensor location. On the other hand, any bias introduced in FC detection was compensated in Stride and Step time estimation, resulting unaffected by different implementation criterions. Then, to identify algorithms suitable for possible applications in ecological settings, e.g. routinely clinic evaluation or daily walking at home, an uninterrupted walking trial of six minutes was considered.

The vast majority of the algorithms showed over-threshold Sensitivity in GE identification, with the exception of three subjects, reporting a Sensitivity lower than 81% for both Acceleration and Angular Velocity of Shank- and Foot-based algorithms (i.e. Trojanello et al. [97], Khamdelwal et al. [33], Catalfamo et al. [34], Jasiewicz et al. [37], Ferrari et al. [39], Mariani et al. [40]). In these cases, the features associated to the single target variable resulted to be pretty reproducible (Single

ICC_{E2} ranging from 0.56 to 0.94), although substantially differing from the reference gait pattern of healthy subjects (Combined ICC_{E1} ranging from 0.17 to 0.69).

Relying on previous findings, to characterize the suitability of algorithms for GE detection in PDP, a decisional flow-chart based on Sensitivity, Single and Combined ICC values can be defined (Figure 2). In particular, Single and Combined ICC were evaluated for each patient to test the repeatability of the gait pattern over the walking trial as excellent ($0.8 < ICC < 1$), good ($0.6 < ICC < 0.8$), fair ($0.4 < ICC < 0.6$), poor ($0.2 < ICC < 0.4$), and bad ($ICC < 0.2$). This classification was firstly proposed by Landis and Koch [116], and later adopted by other authors in the evaluation of the repeatability of trunk acceleration during gait [117].

Figure 2. Decisional flow-chart based on Sensitivity and ICC values for the assessment of suitable algorithms in GE detection of PDP.

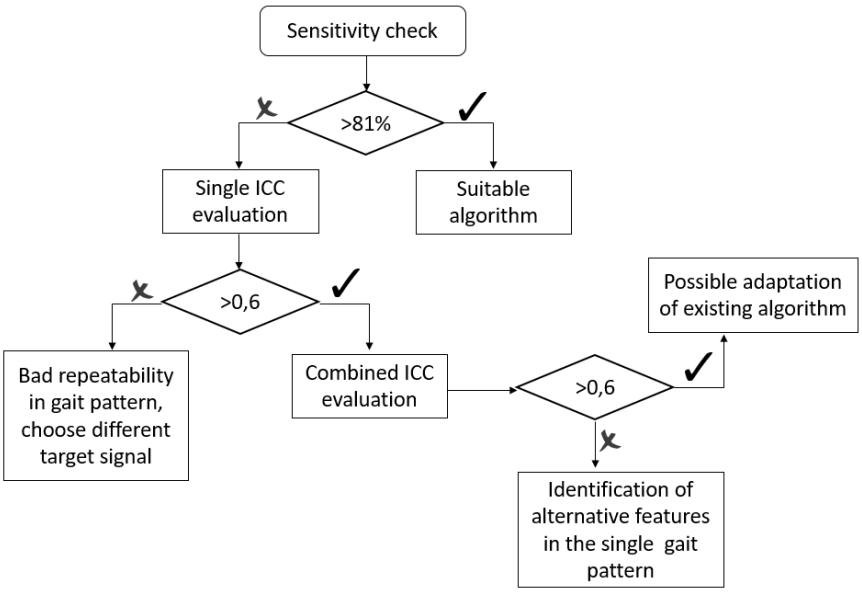

Single ICC values of the target variable for algorithms that showed Sensitivity below the threshold was evaluated: values lower than 0.6 denoted fair reproducibility of the gait pattern during the six minutes walking test, suggesting the absence of repetitive features in the specific target variable. In this case, the algorithm resulted to be unsuitable for gait segmentation in PDP. In case Single ICC resulted greater than 0.6, but Combined ICC did not, the target variable was sufficiently repeatable

within the same walking trial, although differing from the gait pattern of healthy people, assumed as reference for the implementation of the segmentation algorithms. In this case, possible alternative features in the gait pattern should be defined, in order to design subject-specific algorithms. On the other hand, Single and Combined ICC above threshold suggested that the gait pattern of the target variable was sufficiently repeatable both within the same subject and compared to the reference gait pattern of healthy people. In this case, possible adaptation of existing algorithms should be considered. For example, considering the algorithm proposed by Catalfamo et al. [34], Subject 14 reported a Single ICC_{E1} of 0.87 and a Combined ICC of 0.69 (Figure 3). In this case, features characterizing the specific target variable, i.e. angular velocity of the shank in the medio-lateral direction, are repeatable both within different strides of the walking trial and also similar to the healthy reference pattern, suggesting a possible adaptation of specific thresholds for a reliable GE detection.

Figure 3. Plots with i) Median, 25th and 75th percentile as related to Subject 14 (thin solid lines) and ii) Median as related to reference pattern of healthy subjects (thick dashed line) of Angular velocity from Shank on the medio-lateral direction defined on the normalized stride time.

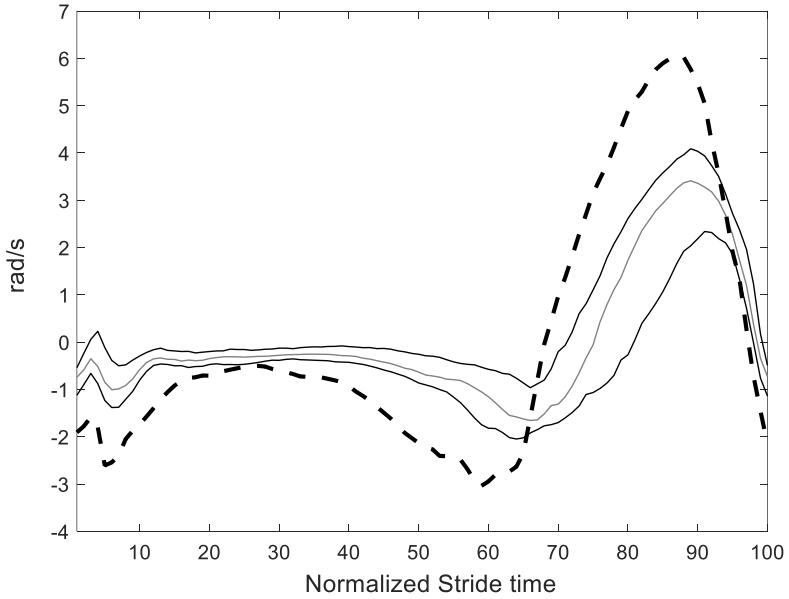

The algorithm proposed by Salarian et al. [137] and adopted as gold standard for the identification of GE represents a possible limitation of the study. However, in order to establish an operator-

independent criterion for the assessment of algorithm suitability when walking in ecological condition, the video-reference should be replaced by a sensor-based approach. In this context, the algorithm implemented by Salarian et al. [137] represent a possible solution because it exhibited excellent performances in gait segmentation of heathy subjects [9] and was already validated in PDP [20]. Moreover, it was recently adopted as reference by other authors to validate a GE detection algorithm in children with cerebral palsy [143].

In this work, all patients were tested in the medication ON state, thus the outcomes of the study should not be extended to PDP during OFF state of medication, neither to different pathological populations.

In conclusion, considering the error assessment, all analysed factors resulted to affect GE and GTP estimation, as previously observed in healthy people. Given inertial measures of six minutes walking, Sensitivity and ICC analyses represent possible solutions for the selection of the most suitable algorithm for gait segmentation in PDP. Moreover, the assessment of these parameters will allow future studies to adapt existing algorithms, if possible, and/or support the design of novel and more efficient detection algorithms in PDP.

3.2

DETECTION OF FREEZING EVENTS DURING GAIT ON SOLID GROUND IN PEOPLE WITH PARKINSON'S DISEASE

Introduction

FOG is a disabling symptom for PDP [144]. It is defined as a unique and disabling clinical phenomenon characterised by brief episodes of inability to step or by extremely short steps that typically occur on initiating gait or on turning while walking [145]. The correct identification of FOG episodes is of primary importance for understanding the causes of the motor impairments and personalizing the treatment [146]. Usually, FOG is observationally assessed by expert operators during medical examinations in a clinical context. This type of assessment is characterizes by low reproducibility and operator-dependent evaluation [147], but also by how little the behaviour of the patient during clinical observation represents FOG manifestation in real life conditions. To overcome the limited reliability of subjective observation, several quantitative instrumental methods for FOG assessment were proposed, using EMG, stereophotogrammetry, force platforms, goniometers and footswitches [67,148,149]. More recently, with the purpose of going towards quantitative ecological evaluation, automatic detection of FOG from wearable inertial sensors has been proposed, allowing the monitoring of FOG episodes during daily life of PDPs: several published works proposed and tested [72–74] the performance of specific algorithms, exploiting different sensor placement, processing signals in different domains with different approaches, but no work addressed the direct comparison of the performance on these algorithms.

This study was designed to fill in this gap, aiming to comparatively analyse the performance of algorithms proposed for the automatic identification of FOG in gait, addressing the influence of the different implementation characteristics, to provide information to support the selection of the most suitable algorithm for specific applications.

Material and methods

Participants

Ten PDPs with a diagnosis of freezing (5 females, 5 males; 68±6 years old; 1.69±0.1 m; 69.4±15.1 Kg; Hoehn-Yahr stage III) were enlisted in this study. The study was approved by the local scientific committee and institutional review board (Comitato Etico Interaziendale delle Provincie di Lecco, Como, Sondrio) and was in accordance with the Code of Ethics of the World Medical Association (Declaration of Helsinki, 1967). A complete explanation of the study protocol was provided to the patients and written informed consent was obtained before their participation in the study. This trial was registered on ClinicalTrials.gov NCT03015714.

Data acquisition:

Each participant performed a six-minute walking test along a 15 m straight pathway at self-selected speed wearing own comfortable footwear. Five tri-axial IMUs (OPAL, Apdm, sf=128 Hz; technical specifications were reported in Chapter 3.1) were attached to the trunk (at L5 level), shanks (about five centimetres above lateral malleolus), and feet (on the dorsal surface of each shoe). The walking tasks were also filmed using a GoPro (Hero4, USA, sf=240Hz, 848x480 pixels resolution). Three impacts on IMU sensors were video-recorded and used for time-synchronization between the two measurement systems.

Data analysis

FOG episodes were visually detected by one trained operator for each subject using Kinovea (Version 8.27). Then, the 7 algorithms derived from a literature review and reported in detail in the Paragraph 1.3 of the Background were classified based on: Domain (i.e. frequency, time-frequency, time) and IMU position (i.e. lower trunk, shank, foot)
Of the 7 algorithms:

- 5 were implemented in the frequency domain, exploiting acceleration from trunk ([75]), shank ([73,75–78]) and foot ([75,76]);
- 1 was implemented in the time-frequency domain, exploiting angular velocity of the shank ([79]);
- 1 was implemented in the time domain, exploiting acceleration of the trunk ([80]) and the shank ([80]).

The 7 algorithms were implemented in MATLAB (MathWorks 2017a, NATHSK, USA) and FOG events were estimated from IMU data for each participant with each algorithm.

Sensitivity and Specificity were calculated as following:

$$\text{Sensitivity} = \frac{\text{Number of FOG correctly identified by algorithm}}{\text{Number of all FOG as identified by video}} * 100 \quad (14)$$

$$\text{Specificity} = \frac{\text{Number of all FOG identified by algorithm} - \text{Number of all FOG as identified by video}}{\text{Number of all FOG as identified by video}} * 100 \quad (15)$$

Results

Most of the algorithms showed a different combination of Windows and Thresholds, as resulting from the specific implementation rules, driving to different results in terms of Sensitivity and Specificity. According to the literature, algorithms showing a Sensitivity below 78% and a Specificity above 20% were not considered for further analyses [73]. Details of implementation characteristics, Sensitivity and Specificity of algorithms are reported in Table 2.

Table 2. Details of algorithms identified from the literature review and classified according to the implementation characteristics (i.e. Domain, IMU position, Target variable); Windows and Thresholds adopted for the implementation; results for Sensitivity and Specificity in FOG detection as related to each algorithm. Algorithms showing a Sensitivity above 78% and a Specificity below 20% were highlighted in light grey. To assist the reader, results obtained for Moore et al. 2013 were reported below the table.

Reference	Domain	IMU position	Target variable (component)	Window (in seconds)	Threshold	Sensitivity	Specificity
Moore et al. 2008 [73]	Frequency	Shank	Acceleration (V)	6	2.9	12	0
Jovanov et al. 2009 [76]	Frequency	Shank	Acceleration (V)	4	Manual	78	0
				6		71	0
		Foot	Acceleration (V)	4		78	0
				6		83	0
Mancini et al. 2012 [77]	Frequency	Shank	Acceleration (AP)	5	2.9	58.5	0
Morris et al. 2012 [78]	Frequency	Shank	Acceleration (V)	4	2	63	0
				6	2	24.1	0
				10	2	19	0
Moore et al. 2013 [75]	Frequency	Trunk Shank Foot	Acceleration (V)	From 2.5 to 10 with 2.5 increment	From 0.5 to 7 with 0.5 increment	*	
Djiuric et al. 2014 [79]	Time - Frequency	Shank	Angular velocity (ML)	-	-	100	25
Rezvanian et al. 2016 [80]	Time	Trunk	Acceleration (AP)	4	58.9	100	54
			Acceleration (ML)	4	59.1	100	55
			Acceleration (V)	4	66	100	57
		Shank	Acceleration (AP)	4	58.9	100	52
			Acceleration (ML)	4	59.1	100	46
			Acceleration (V)	4	66	100	59

*

Window	2.5		5															7.5									10								
Threshold	0.5	from 1 to 7	0.5	1	1.5	2	2.5	3	3.5	4	4.5	5	5.5	6	6.5	7	0.5	1	1.5	2	2.5	3	3.5	4	from 4.5 to 7	0.5	1	1.5	2	2.5	3	3.5	4	from 4.5 to 7
Sensitivity	2.5	0	100	95	63	32	24	19.5	17	14.5	14.5	14.5	9.8	7.3	7.3	7.3	68	54	37	17	9.8	7.3	7.3	7.9	0	63	54	29	12	9.6	9.6	2.4	2.4	0
Specificity	0	0	11	0	0	0	0	0	0	0	0	0	0	0	0	0	0	0	0	0	0	0	0	0	0	0	0	0	0	0	0	0	0	0

Window	2.5		5							7.			10							2.5			5										
Threshold	0.5	from 1 to 7	0.5	1	1.5	2	2.5	3	3.5-7	0.5	1	from 1.5 to 7	0.5	1	1.5	2	2.5	3	3.5-7	0.5	1	from 1.5 to 7	0.5	1	1.5	2	2.5	3	3.5	4	4.5	5	from 5.5 to 7
Sensitivity	2.4	0	71	68	9.75	7.3	7.3	4.5	0	77	44	0	58.5	39	7.3	4.8	2.4	2.4	0	100	37	0	24	97.5	100	80	100	19.5	12	7.3	4.9	4.9	4.9
Specificity	0	0	0	0	0	0	0	0	0	0	0	0	0	0	0	0	0	0	0	46	0	0	0	0	2.4	0	0	0	0	0	0	0	0

Window	7.5									10								
Threshold	0.5	1	1.5	2	2.5	3	3.5	4	from 4.5 to 7	0.5	1	1.5	2	2.5	3	3.5	4	from 5 to 7
Sensitivity	36.5	100	100	100	83	56	44	44	0	22	34	46	29	17	7.3	2.4	2.4	0
Specificity	0	4.7	44.5	16	0	0	0	0	0	0	0	0	0	0	0	0	0	0

Among the 7 algorithms, only two passed the Sensitivity and Specificity criterion, i.e. Jovanov et al. 2009 [76] and Moore et al. 2013 [75], with some specific combinations of Windows and Thresholds (Table 2). In Jovanon et al. [76], comparable results were obtained for the windows of 4 seconds, both for shank and foot, with 78% of Sensitivity and no false positive events (Specificity 0%). Instead, Windows of 6 seconds provided 83% of Sensitivity for foot position, but only 71% for the shank, with no false events in both cases. For Moore et al. [75], preliminary results showed that window of 5 seconds provided the best results both for shank (Sensitivity of 100% and 95%, and Specificity of 11% and 0% for threshold of 0.5 and 1, respectively) and foot position of IMU (Sensitivity of 97.5% and 100%, and Specificity of 0% for threshold of 1 and 2.5, respectively).

Concerning specific implementation characteristic, only algorithms implemented in the frequency domain passed the Sensitivity and Specificity criterion, while both time and time-frequency domains showed values of Sensitivity of 100% in all cases, but also Specificity always greater than 25%.

In relation to the positioning, trunk-based algorithms reported no false positive events, but Sensitivity always lower than 78%. Among algorithms that passed the Sensitivity and Specificity criterion, preliminary results showed similar values of these measures for Shank- and Foot-based algorithms (Table 2).

Discussion

This study aimed to assess the performance of 7 published algorithms proposed for FOG detection from IMU data. The algorithms were selected and implemented after a systematic literature review and then analysed based on Sensitivity and Specificity values with respect to the influence of the domain of implementation and IMU position.

Preliminary results showed that only two algorithms resulted to be suitable for FOG identification in the considered population, both implemented in the frequency domain and exploiting acceleration from Shank and Foot positioning. Independently from implementation characteristics, values of Windows and Threshold resulted to be relevant in the assessment of the performance of the single algorithm. More specifically, acceptable performances were obtained with

Widow sizes varying from 4 seconds to 7 seconds and Threshold varying from 0.5 to 2.5 or manually set, according to previous studies [73,75]. In fact, window sizes should be at least of the same time length of the FOG episodes, but shorter than 10 seconds, to avoid a low pass filter effect that tended to average short FOG events [73].

Preliminary results showed that Shank and Foot positionings obtained both better performance than trunk-based algorithms. This result is in agreement with a previous study by Moore et al., who demonstrated that objective FOG identification based on the frequency characteristics of lower body motion can achieve a strong correspondence with the clinical assessment [75].

In general, frequency-based algorithms seemed to provide better results than time and time-frequency based ones. This behaviour might be explained with the reported high correlation between the identification of FOG episodes and FI index, on which frequency domain algorithms are based on [73,75,76]. However, more effort should be performed to explain the failure of most of the algorithms proposed in this study.

These results should be interpreted as preliminary. In fact, previous authors underlined that the reliability of clinical video assessment was not robust in the identification of FOG events across multiple Parkinson's disease centres [78], suggesting that visual observation introduced low objectivity and reliability, also among clinicians. In this study, each subject was analysed by one single trained operator: next analyses will extend the identification of FOG episodes from videos to a larger number of trained operators, to improve the reliability of the gold standard identification. Moreover, despite all 10 subjects reported a clinical history of FOG, only 5 experienced freezing during the six-minute walking task, possibly due to the controlled environment of a research study that may have reduced the likelihood of FOG episodes [73,150]. Thus, further study should assess the performance of the proposed algorithms in a greater number of PDP.

Since the automatic detection of FOG assumes a fundamental role in the prediction of falls [146], the current study sets the stage for a conscious choice of the proper algorithm for the specific patient and situation. Moreover, it supports the effectiveness of IMUs for the health-professionals' evaluation of PDP symptoms, improving treatment, and augmenting self-management of patients [151].

Synthesis of findings

In this section, the assessment of algorithms for gait segmentation and FOG detection in PDPs was provided.

In accordance with the results obtained for healthy people, implementation characteristics (i.e. sensor position, analysed variable and computational approach) affected the performance of algorithms in gait timing estimation. Indicatory conclusions for the selection of subject-specific algorithm were proposed based on the similarity between gait pattern of healthy individuals, adopted as reference for algorithms implementation, and PDP ones.

The performance of the algorithms for FOG automatic detection varied depending on different implementation domain (frequency, time and time-frequency) and sensor position (trunk, shanks, feet). According to the literature, frequency-based algorithms seemed to provide better results than time and time-frequency based ones.

Conclusion

In recent years, the widespread use of inertial wearable sensors has opened the possibility for the quantitative assessment of gait in ecological conditions, for the objective characterization of specific gait patterns, with the aim to support and guide clinical decision and treatment definition.

The significant interest in finding effective methods for the quantification of specific parameters for clinical led to a proliferation of novel methods for gait analysis. Most of these methods were partially tested on the gait of healthy subjects and/or of specific pathologic populations in laboratory conditions, without considering the influence of intrinsic or extrinsic factors altering the reference gait pattern. Therefore, the aim of the present project was to comparatively analyze the influence of said extrinsic (e.g. walking surface and environment) and intrinsic (i.e. gait alterations related to pathological conditions) factors on the performance of the numerous algorithms proposed for the quantification of specific characteristics (i.e. timing, variability/stability) and alterations (i.e. freezing) of gait.

Section 1 addressed the assessment of the influence of extrinsic factors on algorithms for the quantification of gait timing and of non-linear metrics of gait variability/stability on healthy subjects. First, the performance of the algorithms available in the literature for gait timing estimation were assessed during walking of healthy people in controlled laboratory conditions, to analyse the influence of different implementation characteristics (i.e. sensor position, target variable and computational approach). Then, the same evaluation was performed in ecological conditions, considering different environmental constraints, i.e. walking in water and on sand.

Analyzing the gait of healthy subjects on solid ground, which represents the reference gait pattern for the implementation of the analyzed algorithms, significant differences were found in the estimation of gait timing in relation to the implementation characteristics. In general, shank- and foot-based algorithms performed better than lower trunk-based ones, as well as angular velocity-based algorithms compared to the acceleration-based ones, while the performance of different computational approaches varied depending on sensor positioning. Analyzing gait in water, no trunk-based algorithms as well as no acceleration-based one, with the exception of two exploiting a shank positioned sensor, rose above the required minimum Sensitivity threshold of 81%, thus resulting unsuitable for gait event detection; this ineffective performance was associated to significant differences in the pattern of the specific variables during walking in water as compared

to walking on dry land. In fact, sensitivity was below threshold when walking in water pattern was not repeatable enough (ICC for walking in water below 0.60), and when it differed too much from the reference WDL one (ICC of walking on dry land over walking in water below 0.31). Analyzing the sand environment, all algorithms resulted suitable for gait events identification, with threshold of Sensitivity above 81% for all algorithms and conditions, as the pattern of the specific variables did not change significantly with respect to the reference condition. From a comparison with solid ground walking, considered the reference pattern for algorithm implementation, ICC values were always greater than 0.8, both in wet and dry sand. Independently from the environmental constraints, delays/anticipation in gait events estimation were found in relation to the specific implementation characteristics, with a general lower accuracy and repeatability on dry sand compared to hard surface and wet sand, leading to a compensation of this error in the estimate of Stride and Step time, and a general underestimation/overestimation of Stance- and Swing-time, respectively.

These works allowed to identify reference values of comparative performance in terms of sensitivity, accuracy and repeatability of the different algorithms in different operative conditions, supporting: 1) the selection of most appropriate algorithm for specific applications; 2) the development/optimization of more effective algorithms. In this context, future studies should investigate the performance of algorithms for gait segmentation based on innovative and advanced machine learning techniques e.g. neural networks, hidden Markov models, and Gaussian mixture models [23–25], adopting the datasets provided by the current dissertation.

The application of non-linear metrics to walking in water requires the identification of reference criteria for a reliable implementation, thus the evaluation of the minimum number of strides was assessed among different level of immersion (i.e. knee, pelvis and xiphoid process), showing higher number of strides in all conditions (above 140) also for the 50% threshold compared to results obtained by other authors on dry land.

Section 2 addressed the assessment of the influence of intrinsic factors, i.e. pathological condition in Parkinson's disease patients, on algorithms for the quantification of gait timing and automatic identification of freezing events. The gait segmentation algorithms, already tested in Section 1 for extrinsic factors, are firstly evaluated excluding turnings, rest periods and freezing episodes, resulting to be suitable in the identification of gait events (Sensitivity above 81%) for all the analysed subjects with the exception of one patient. The characterization of the errors showed comparable accuracy and repeatability in the estimation of Stride and Step time, independently from the implementation characteristics. Conversely, GEs, Stance and Swing time resulted underestimated or overestimated, depending on the implementation rules.

Then, whole walking tasks were considered, including possible freezing episodes. In this case, some of the algorithms exploiting angular velocity and acceleration of the shanks and the feet, showed Sensitivity below the 81% for 3 of the 20 considered subjects. To define possible rules for a reliable application of gait segmentation algorithms during walking of PDPs, reproducibility of the target variable within the single walking task (Single ICC) and compared to the gait pattern of healthy subjects (Combined ICC) was evaluated. In particular, when the single target variable presents repetitive features (Single ICC greater than 0.6) and is sufficiently similar to gait pattern of healthy people (Combined ICC greater than 0.6), the application of existing segmentation algorithms should be considered. Otherwise, possible definition of new methods or adaptation of the existing ones should be considered.

Finally, the performance of the available algorithms for freezing of gait detection was investigated starting from a systematic review to identify the different proposed methods. The aim was to provide relevant information for the selection of the most suitable algorithm for specific applications in relation to the implementation characteristics (i.e. implementation domain and IMU position). Preliminary results showed that frequency-based algorithms perform better than time and time-frequency based ones, and algorithms exploiting signals from shanks and feet are preferable than trunk-based ones.

Even though not exhaustive, these results provide essential methodological reference for the reliable adoption of IMU for the characterization of biomechanical and functional aspects of gait across different environments and surfaces, both in healthy and pathological people. Future developments will extend the same methods to different environmental constraints and populations, in order to overcome the main limitations of this dissertation, namely the possibility to generalize (when and if possible) the obtained results to other populations.

In conclusion, the present Thesis outlines a systematic approach for the assessment of the performance of algorithms proposed for the quantification of specific characteristics of gait from inertial measures, taking into account and highlighting the influence of intrinsic and extrinsic influencing factors. The results provide relevant information for the evidence-based selection of the most appropriate approach, if available, for the specific application, and for the development of more effective algorithms for the assessment of ecological gait in healthy and pathologic subjects.

Appendix

MUSCLE ACTIVATION DURING WALKING IN PARKINSON'S DISEASE PATIENTS

The content of this chapter has been published in G. Pacini Panebianco, M. Fonsato, G. Frazzitta, R. Stagni, S. Fantozzi, 'EMG activation during walking in Parkinson's disease patients', Gait & Posture 74 (2019) S1–S39

Introduction

During gait, gastrocnemius (GS) and tibialis anterior (TA) play a fundamental role in forward progression [152,153]. Perry et al. reported different phases of activation in the gait cycle for these antagonist muscles, i.e. GS active from loading response to terminal stance, and TA from pre-swing to the following initial contact [18]. However, a recent assessment by Di Nardo et al. [154] of the activation patterns of gastrocnemius lateralis (GL) and TA during gait showed large variability in the number of activations, in their occurrence rate, and in the on-off timing, over different strides of the same gait trial. For each muscle, the assessment of the different patterns of activation allowed to identify a scheme, allowing to characterize the behaviour of muscles during normal gait, improving the interpretation of EMG signals in physiological and pathological conditions. In particular, the pattern of GL activation was centred in two phases of the gait cycle: the transition between flat foot contact and push-off and the final swing. Similarly, two phases characterized EMG pattern of TA: from pre-swing to following loading response, and the mid-stance [154]. In recent studies, the same authors also addressed the quantification of the asymmetric behaviour of ankle-muscle recruitment during walking in type I hemiplegic children, in order to describe control strategies and support clinicians and physical therapists in planning treatment approaches [155] and the assessment of the co-contraction patterns of gastrocnemius ad vastus lateralis in healthy people to better understand their role in controlling joints mechanics [156].

In the last decades, the analysis of the muscle activation has assumed considerable significance in the diagnosis, prognosis and monitoring of neuromuscular pathologies [157]. In particular, it represents a fundamental aspect in the evaluation of motor disorders in people with Parkinson's Disease (PDPs) [158]. Gait dysfunctions in PDP are often associated with abnormal muscular activaty [67], as demonstrated by the quantification of the rhythmicity and variability of the EMG pattern during gait in PDP in general, and as associated to freezing in particular [67,150,159]. Studies concerning EMG assessment of PDP during walking on a treadmill showed reduced GM activity, overactivation of TA [151] and greater co-activation of antagonist leg muscles during the support phase [152] compared with healthy controls. Analyses performed on walking on solid ground highlighted muscle activity asymmetry between right and left leg [160], premature and relatively prolonged activity of GS [150], anticipated activity and reduced or absent push-off peak in GM, absent or reduced activity around ground contact phase in TA [155]. Moreover, Nieuwboer et al., [150] demonstrated that overall reciprocity between GS and TA was preserved during walking on solid surfaces.

Although of primary importance in the clinical context to design subject-specific treatments, the assessment of different activation patterns of GM and TA in pathologic gait has not been

addressed yet. The aim of the present study was to provide a methodological assessment of the variability of muscle activation during walking on solid ground in PDP, analysing: i) the symmetry in the activation modalities of muscles between right and left leg, ii) the different activation patterns (number and timing within each stride per muscle), and iii) the co-activation of antagonist muscles.

Materials and Methods

Participants:

Twenty PDPs (12 females ,8 males; 67.2±9.1 years old; 1.65±0.12 m; 67.3±13.1 Kg; Hoehn-Yahr stage III, 10 with diagnosis of freezing) participated in this study. All patients were in the ON state of Levodopa treatment during the experiment. The study was approved by the local scientific committee and institutional review board (Comitato Etico Interaziendale delle Provincie di Lecco, Como, Sondrio) and was in accordance with the Code of Ethics of the World Medical Association (Declaration of Helsinki, 1967). A complete explanation of the study protocol was provided to the patients and written informed consent was obtained before their participation in the study. This trial was registered on ClinicalTrials.gov NCT03015714.

Data acquisition:

Each participant performed a six-minutes walking test along a 15 m straight pathway at self-selected speed wearing own comfortable footwear. Angular velocities of the shanks were collected using two tri-axial sensors (OPAL, Apdm, sf=128 Hz) and EMG signals of TA and GM were acquired using wireless electromyograph, provided with embedded accelerometers (Cometa, Italy, sf=2000Hz), following SENIAM guidelines [161]. Three peaks were recognizable both in sensors and EMG accelerometers and used to synchronize the two systems.

Data Analysis:

Only strides walked along straight paths were considered, thus excluding turnings and freezing episodes. Gait events were identified from the angular velocity around the medio-lateral axis of the shank [20]. EMG data were band-pass filtered at 20–450 Hz [162,163] and then processed by a double threshold statistical detector to provide the onset and offset time instants of muscle activity in a completely user-independent way [164]. This technique [164] consists of selecting a first threshold ζ and observing m successive samples: if at least r0 out of successive m

samples are above the first threshold ζ, the presence of the signal is acknowledged. In this approach, the second threshold is represented by r0. Thus, the behaviour of the double-threshold detector is fixed by three parameters: the first threshold ζ, the second threshold r0, and the length of the observation window m. Their values are selected to jointly minimize the value of false-alarm probability and maximize probability of detection for each specific signal-to-noise ratio (SNR). A minimum value of 10 was considered for SNR [164]. The setting of the first threshold, ζ, is based on the assessment of the background noise level, as a necessary input parameter. Furthermore, the double-threshold detector requires to estimate the SNR in order to set the second threshold, r0. The values of the background noise level and the SNR, necessary to run double-threshold algorithm, is estimated using the statistical approach proposed by Agostini et al. [165]. The length duration of the observation window was set to 30 ms, as it is considered a suitable value for the study of muscle activation in gait analysis [164].

Muscle activation intervals were first normalized with respect to each gait cycle duration, and, successively, the number of times when muscle activates within a single gait cycle were calculated (n-activation modality).

Symmetry

Only patients showing a SNR greater than 10 for GM and TA in both limbs were considered for the symmetry investigation between right and left leg. Firstly, kinematic symmetry was analysed. For each subject, a paired-sampled t-test was performed on the stride times of right and left leg, showing that they were normally distributed. A one-way ANOVA with minimum level of significance of 5% was performed to compare the stride time values obtained from right and left leg. Then, the muscle activation modality of the single stride of one leg was compared with the corresponding previous and next one of the contralateral leg. In this manner, any symmetry in the number of muscle activations in the gait cycle between the two limbs was investigated.

Frequency and timing of different activation modalities

Including the gait cycles of all subjects, muscle activations were grouped according to the number of activations detected, i.e. relatively to the modalities of activations detected. Finally, timing of on/off instants were averaged for each specific modality of activation and relative standard errors (SE) were computed.

Co-activation

For each subject and activation modality, muscle activations were grouped according to the number

of myoelectric bursts, i.e. relative to their activation modality. On/off time instants were summed and normalized against the total number of walked strides. Then, resulting squared curves were summed across different subjects. Co-activation periods were computed as the overlapping epochs among activation intervals of the considered muscles [166].

Matlab R2018a (MathWorks BV, USA) was used for data analysis.

Results

Symmetry

Five subjects showed a SNR greater than 10 for GM and TA of both legs. None of them exhibited differences for stride time between right and left leg, with median values ranging from 0.96s to 1.17s (Figure 1).

Figure 1. Box plot (minimum, 25th percentile, median, 75th percentile, maximum values) for Stride time estimation as related to right and left leg of the five subjects showing a SNR greater than 10 for GM and TA of both limbs.

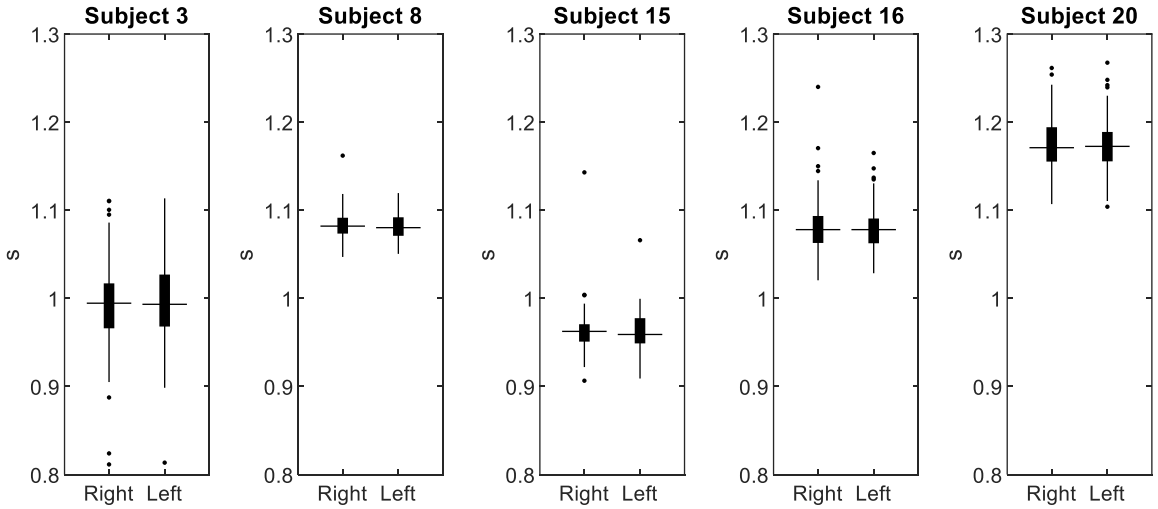

Considering the comparison between the activation modalities of one leg with the contralateral one, no recursive pattern was found in the number of muscle activations between the two limbs. An example of this behaviour was reported in Table 1, where no recursive modalities of activation were found in the previous and next stride of the left leg compared to the corresponding stride of right leg.

Table 1. A representative example of the occurrence of each modality of activation resulting from the comparison of the strides of the right leg, selected as reference, with the corresponding previous and next strides of the contralateral leg for GM (a) and TA (b).

a) GM			Right Leg			
			N=1	N=2	N=3	N=4
Left	Occurrence in % of activation modality previous stride	N=1	54%	41%	50%	-
		N=2	38%	46%	25%	
		N=3	8%	10%	25%	
		N=4	-	3%	-	
	Occurrence in % of activation modality next stride	N=1	42%	54%	25%	
		N=2	49%	31%	50%	
		N=3	8%	6%	25%	
		N=4	1%	-	-	

b) TA			Right Leg			
			N=1	N=2	N=3	N=4
Left	Occurrence in % of activation modality previous stride	N=1	-	-	-	-
		N=2	10%	20%	25%	-
		N=3	78%	59%	50%	85%
		N=4	22%	21%	25%	15%
	Occurrence in % of activation modality next stride	N=1	-	-	-	-
		N=2	22%	25%	12%	15%
		N=3	66%	57%	56%	77%
		N=4	22%	18%	29%	8%

Since all subjects showed symmetrical kinematic behaviour and in order to strengthen the statistical power of the analysis, muscle activation was considered together for right and left leg.

Frequency and timing of different activation modalities

Sixteen subjects for GM and thirteen for TA showed a SNR greater than 10 and were considered for the analysis. For each muscle, a mean (±standard deviation, SD) of 230 ± 96 strides was considered.

The most recurrent modality of activation for GM (Figure 1) consisted of two activations (2-activation modality), observed in 42.9 ± 0.8% of total strides. The first activation occurred for all patients in the transition between flat foot contact and push-off phase. Most of the subjects presented the second activation at the turn of pre- and initial swing. However, in some cases the second activation occurred during terminal stance (Subjects 17 and 18), at initial swing (Subject 4) or during mid-swing (Subjects 2, 10, 15, 20). The second most recurrent modality of activation showed a similar timing to the 2-activation modality for all patients, but with no activation during the swing

phase. This 1-activation modality was observed in 28.0 ± 1.0% of total strides. In a further 21.0 ± 0.9% of total strides, three activations were observed for GM (3-activation modality). The first two occurred by the end of terminal stance in all cases, with the exception of few subjects, showing the second activation from the terminal stance until the initial swing (Subject 2) and during the swing phase (Subject 10 and 15). The third activation occurred during initial and mid-swing phases for most of the subjects, with minor exceptions. The remaining 7.5 ± 0.6% and 2.5 ± 0.4% of total strides was characterized by four and five activations, respectively, with great variability in the on/off activation patterns (4-activation modality).

Figure 1. Gastrocnemius medialis: mean (+SE) percentage frequency of each of the different 5 modalities of activation patterns.

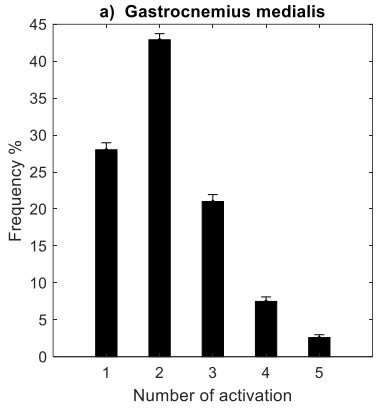

Figure 2. Mean (+SE) activation intervals in relation to the percentage of gait cycle for the modalities with 1 (a), 2 (b), 3 (c) and 4 (d) activations, detected in GM during walking. The toe off is used to determine the beginning of the swing phase and is represented by a red asterisk.

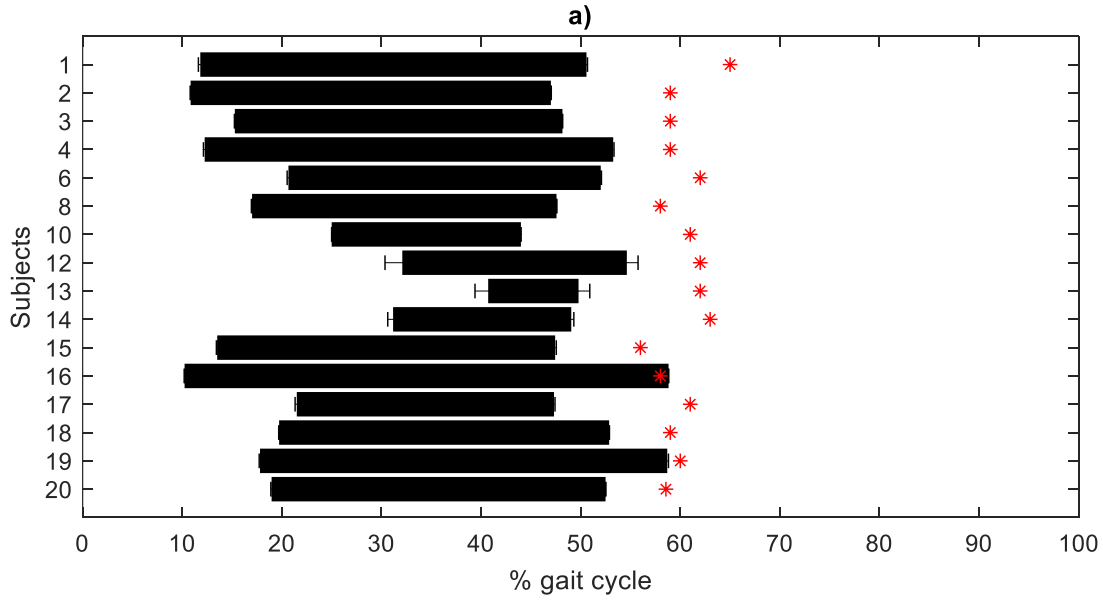

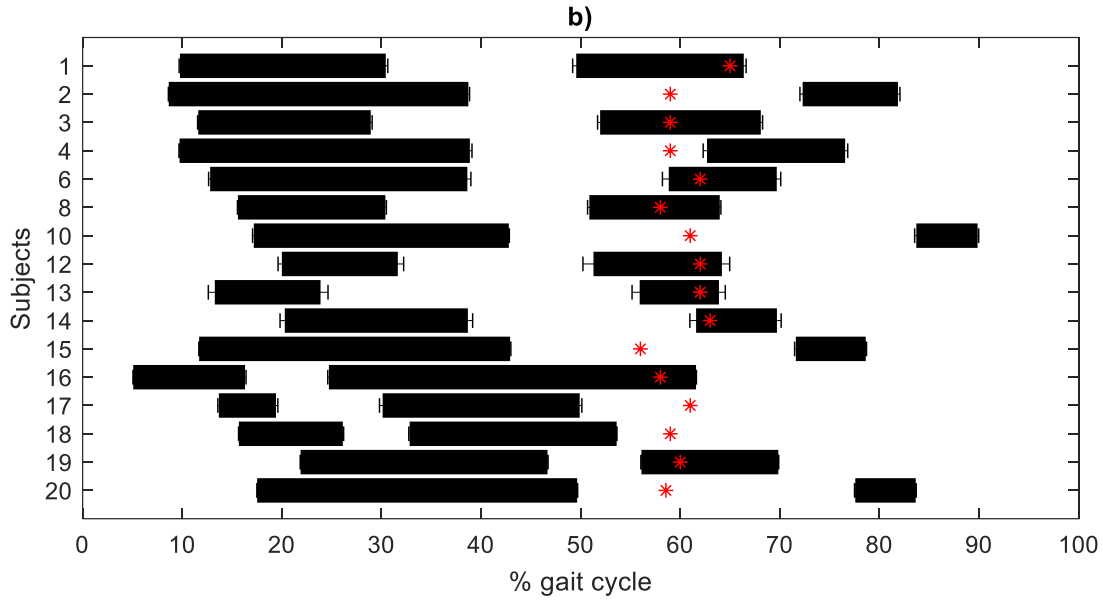
b)
Subjects
1
2
3
4
6
8
10
12
13
14
15
16
17
18
19
20
0
10
20
30
40
50
60
70
80
90
100
% gait cycle

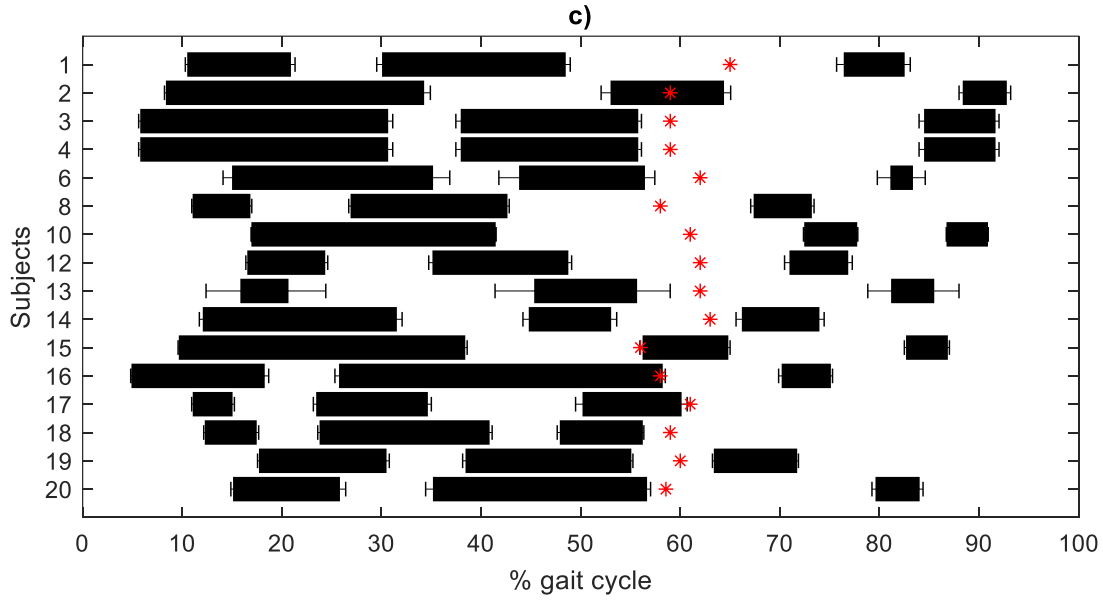
c)
Subjects
1
2
3
4
6
8
10
12
13
14
15
16
17
18
19
20
0
10
20
30
40
50
60
70
80
90
100
% gait cycle

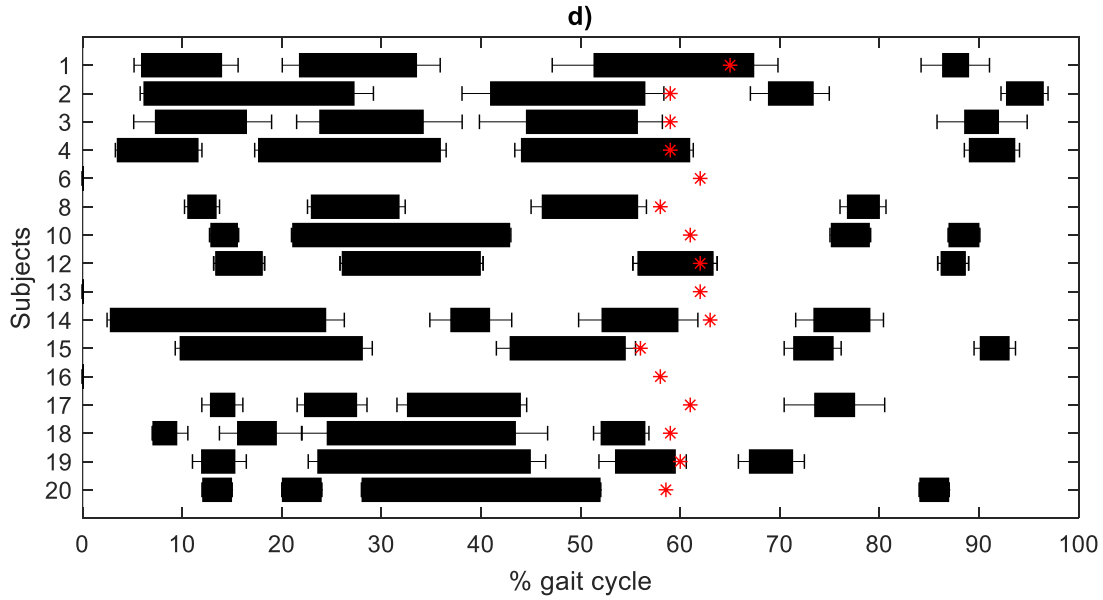
d)
Subjects
1
2
3
4
6
8
10
12
13
14
15
16
17
18
19
20
0
10
20
30
40
50
60
70
80
90
100
% gait cycle

For TA (Figure 4), the most recurrent modality of activation during gait cycle consists of three activations (3-activation modality), observed in 39.5 ± 0.7% of total strides (Figure 3): the first occurs at the beginning of the gait cycle (Subjects 1,3,6,11,15,16,17,18) or during the mid/final stance (Subjects 5,8,9,12,20), the second around stance-to swing-transition in the majority of the subjects, and the third in the terminal swing, with the only exception of one subject (Subject 16), showing an anticipation of this activation to the initial swing phase. The modality with 2 activations was reported in 17.9 ± 1.0% of the strides. The first activation occurred in the interval of the gait cycle from the final stance to the initial swing in the majority of the participants (Subjects 3,5,8,9,16,20) and, in few cases, during the initial stance (Subjects 6 and 16) and during the mid-stance (Subjects 1,15,18) phase, while the second activation generally occurred during the mid- or final swing, apart from a couple of participants (Subjects 6 and 16), showing this activation during the initial swing. In a 28.7 ± 0.9% and 9.8 ± 0.6% of total strides, 4- and 5-activation modalities were observed, respectively. Both modalities showed similar timing in muscles activation: the first activation occurred during the initial contact, the last activation during the final swing, the central activations showed great variability, occurring from mid-stance to final swing. Finally, the 3.0 % ± 0.4 % of total strides was characterized by 1 activation, comparing only in a small portion of patients (Subjects 1,3,5,9,12,18).

Figure 3. Tibialis anterior: mean (+SE) percentage frequency of each of the different 5 modalities of activation patterns.

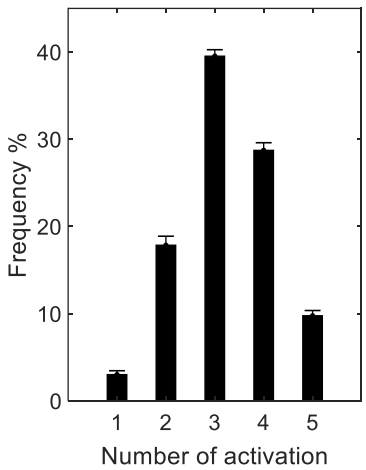

Figure 4. Mean (+SE) activation intervals in relation to the percentage of gait cycle for the modalities from 1 to 5 activations, detected in TA during walking. The toe off is used to determine the beginning of the swing phase and is represented by a red asterisk.

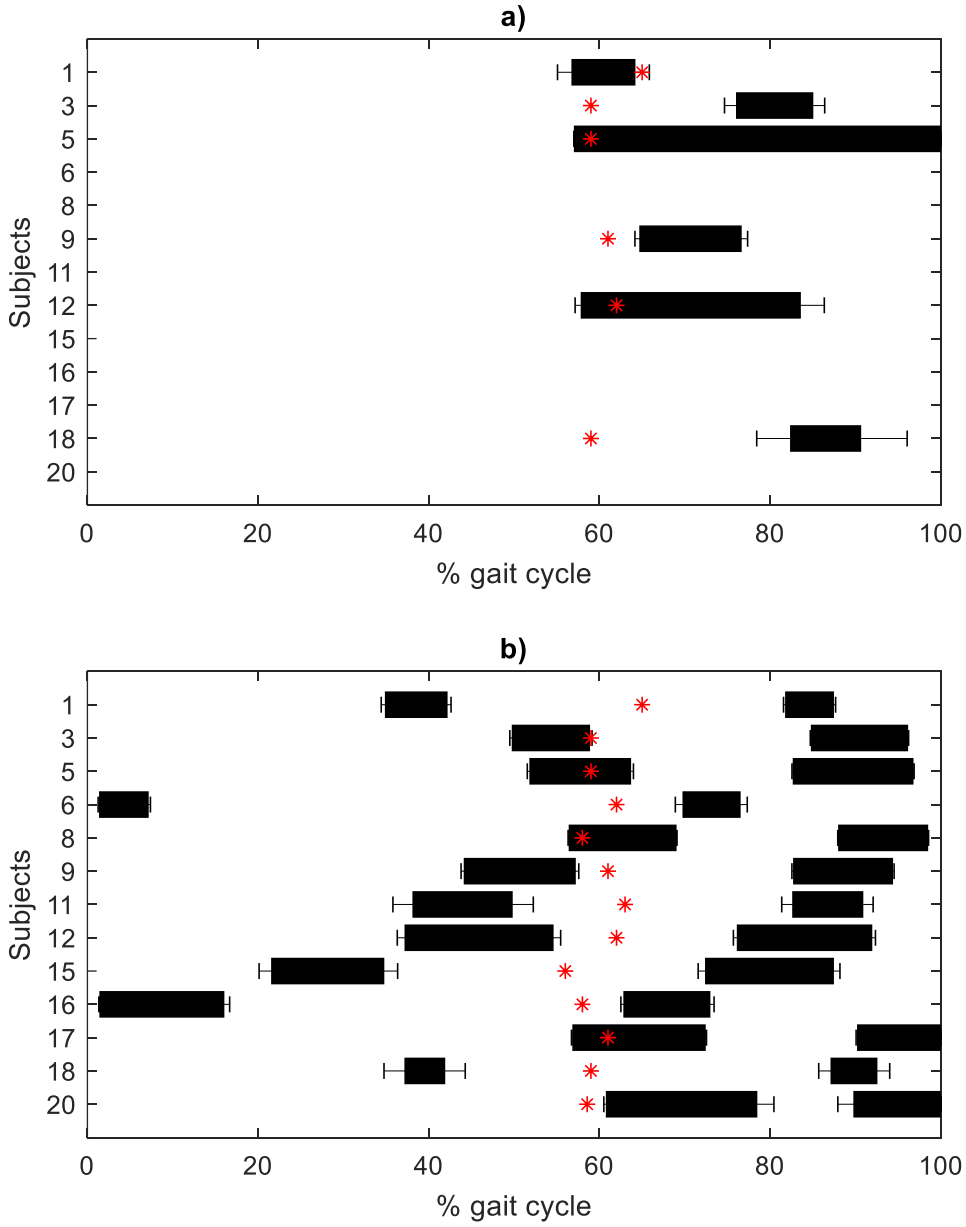

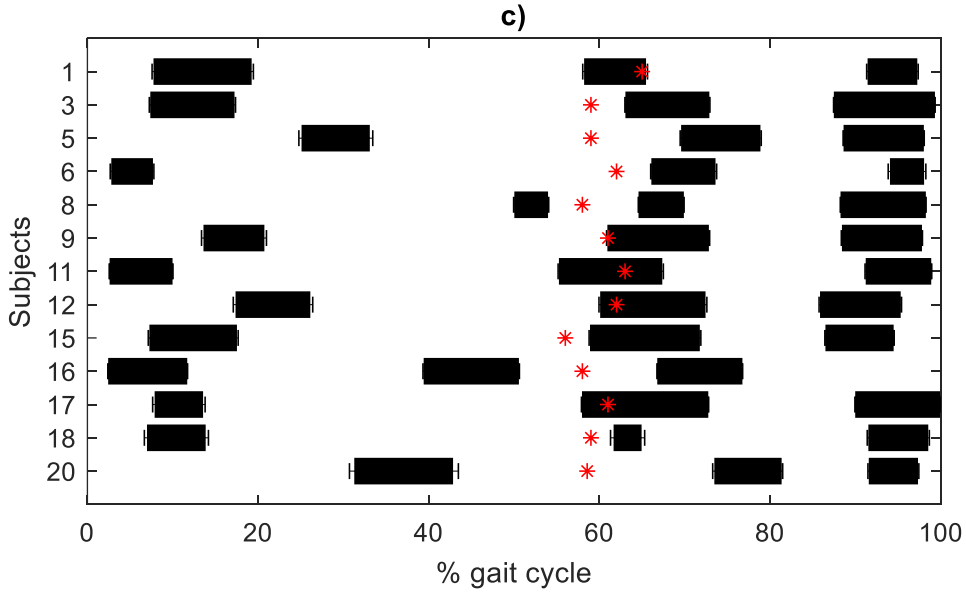
c)
Subjects
1
3
5
6
8
9
11
12
15
16
17
18
20
0
20
40
60
80
100
% gait cycle

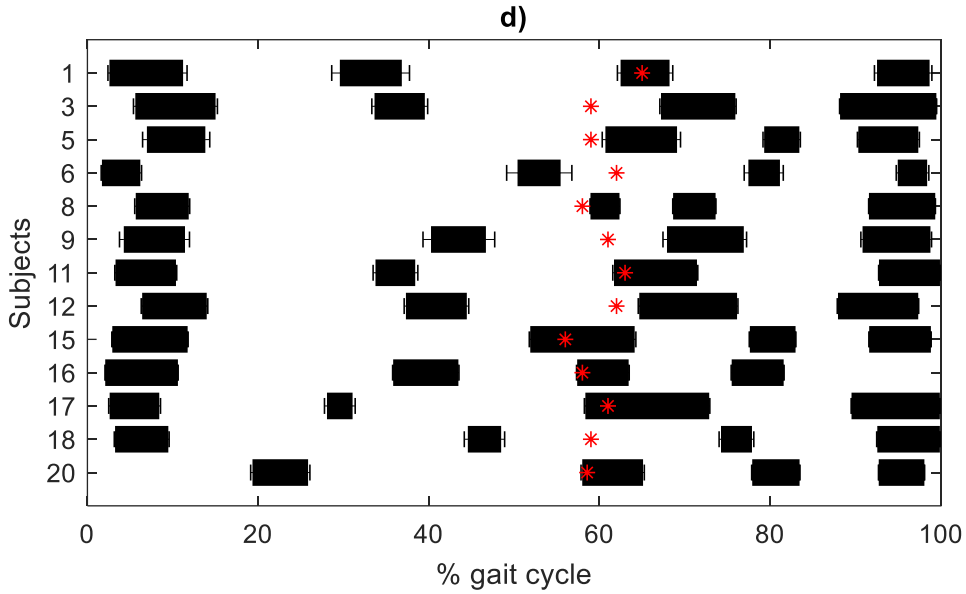
d)
Subjects
1
3
5
6
8
9
11
12
15
16
17
18
20
0
20
40
60
80
100
% gait cycle

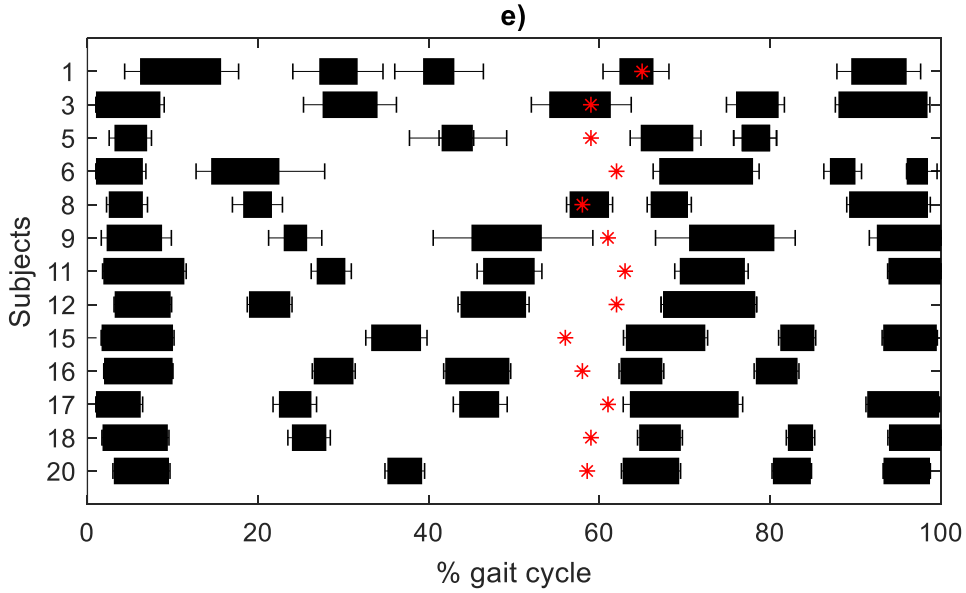
e)
Subjects
1
3
5
6
8
9
11
12
15
16
17
18
20
0
20
40
60
80
100
% gait cycle

Co-activation

All activation modalities of GM (from N=1 to N=4) showed an overlapping period with TA arising from the initial contact to the loading response, and another in the pre-swing phase (Figure 1). When GM presented 3- and 4- activation modalities, the overlapping period during pre-swing lasted until mid-swing (Figure 4 c and d). In the 2-, 3- and 4-activation modalities of GM (Figure 4b, c and d), another co-activation occurred during the terminal swing.

Figure 4. Normalised activation intervals of TA (continuous lines) detected in those strides where GM (dotted lines) showed 1- (a), 2- (b), 3- (c) and 4- (d) activation modality. Co-contractions intervals are highlighted in grey.

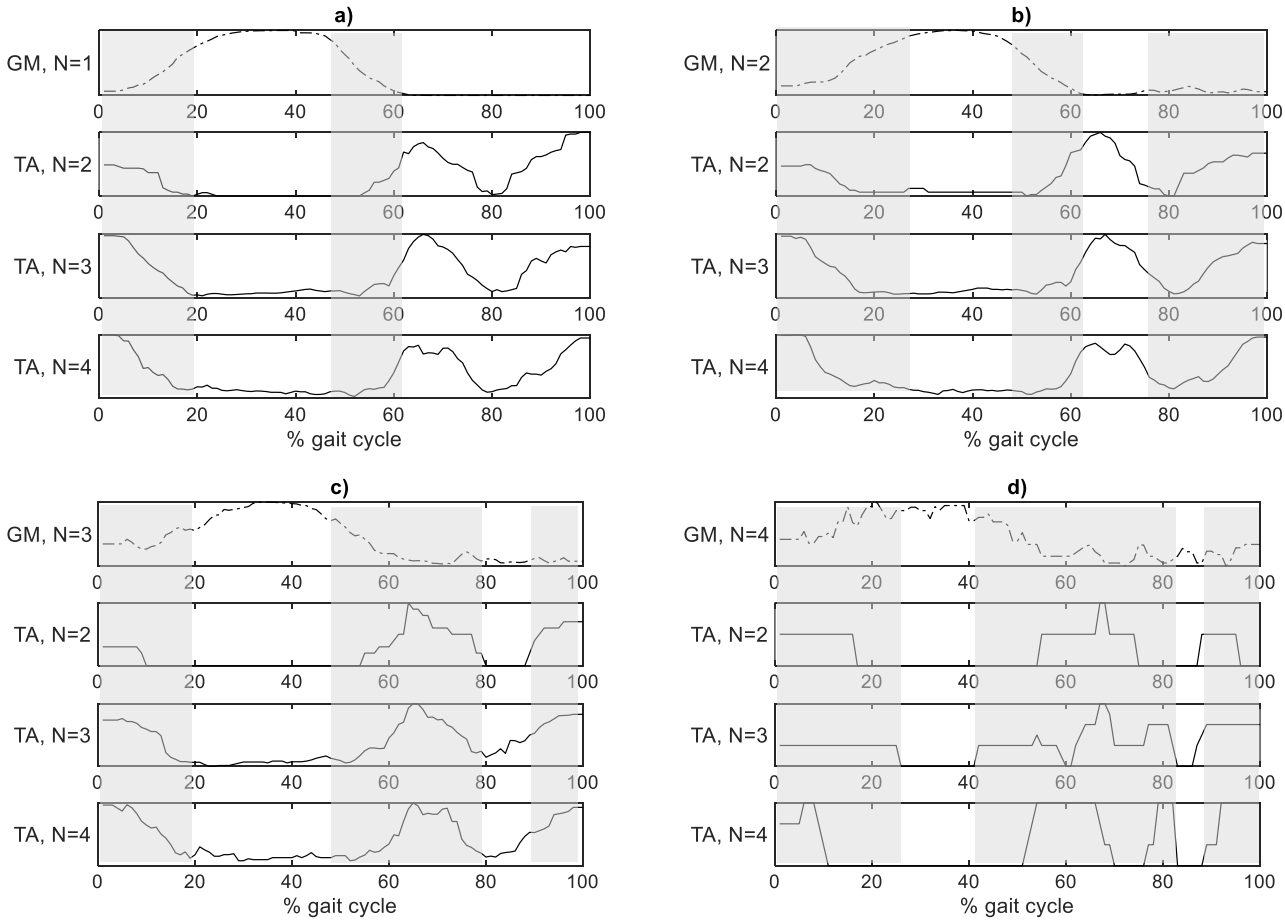

Discussion

In the present study, EMG signals of GM and TA were analysed during gait of 20 PDP, in order to assess different methodological aspects of muscle activation. The considered muscles showed different modalities in the number of activations and in the timing of signal onset and offset, as previously reported by other authors for healthy people [154]. This supports the need to consider not only the typical activation patterns reported in the literature for GM and TA during gait [18,167], but also the number and the timing of the muscle activation intervals in the single gait cycle.

The assessment of the stride time resulted in a kinematic symmetry between right and left leg. On the other hand, considering one leg at a time, the analysis of the number of activations in the previous and next stride of the contralateral limb did not show a recurrent pattern. Thus, no direct association between the modalities of activation of the right and left leg was found and the high degree of muscular variability reported also in previous studies [154,166,168], was confirmed. Both results support the successive analysis were no distinction was applied between the two limbs.

In general, comparable percentages in the frequency of different number of activation modalities were obtained for PDP both in GM and TA compared to healthy people. On the other hand, differences were found in the timing of activation for both muscles.

Previous authors [169] reported that the activity of GL is centred mainly in two regions of the gait cycle: between flat foot contact and push off and in the final swing. Accordingly, the activity occurring in the stance phase is observed in all patients across different activation modalities (N from 1 to 4) and is interpreted as the active participation in the dorsiflexion of the foot during the forward progression [18,167]. However, results from the current study showed slight differences in the timing of activations for N=3 compared to the healthy subjects. In particular, the first activation was generally shorter and delayed in PDP, comparing during foot flat and mid-stance phases instead than in early stance. This phenomenon might be associated to the reduced GM activity during the stance phase in PDP already shown when walking on treadmill and might be associated to the impaired proprioceptive feedback from extensor load receptors [170].

In PDP, the second region of activity mainly occurred during the push off (N=2), or early- and mid-swing (N=2,3,4) and almost never in the final swing (N=4), thus anticipating the traditional activation timing observed during the final swing in healthy people. In particular, for N=2 results showed that the second activation generally occurs just before or during the push-off phase, instead than on the mid-swing as in healthy people. These finding might be associated to the inadequate propulsion and reduced vertical ground reaction forces to propel the body forward in people with

Parkinson disease [171]. Similarly, a general anticipation of the activation for N=3, 4 was observed in PDP, occurring during pre- and mid-swing instead than in final swing as happened in healthy subjects.

Independently from the activation modality, results showed great variability across subjects in timing activation of GM during the swing phase. This augmented variability was reported also by di Nardo et al. [169], even if differed from the results obtained by Millet et al. [160], who showed reduced variability in GM activation of PDP. However, they considered the whole activation of the muscle, without distinguishing different modalities of activation.

For TA, the muscular activity of healthy people resulted to be centred mainly in two regions of the gait cycle. The first region occurred from the pre-swing to the following loading response, comparing in all the activation modalities (from N=2 to N=5), while the second occurred in the mid-stance. Conversely, in the N=2 and N=3 activation modalities of PDP, the activity at the beginning of the stride cycle was absent or delayed from initial contact to mid-stance and pre-swing phase, showing alterations of the normally contributes to foot positioning at the touch down [172]. These results were in agreement with Ferrarin et al., that reported absent or reduced activity of TA around ground contact, suggesting reduced foot clearance typical of the shuffling parkinsonian gait [172].

In healthy subjects, all the activation modalities showed muscle activity during the final swing phase. Comparable results were obtained for PD Patients, with the exception of one patient (Subject 16). In this case, both GM and TA activations were always confined before or in correspondence of mid-swing, and never lasted until the end of the swing phase. This behaviour confirmed the reported reciprocity of antagonist muscles and could be associated to the reduced foot lifting during the swing phase of gait in PDP, which produced smaller clearance between the toes and the ground [135].

Even if most of the subjects presented muscle activity during the late swing phase for all activation modalities as healthy people [169], these activations were generally shorter in time duration, especially for the N=2 and N=3 modalities. These observation might be confirmed by earlier studies of EMG profiles during normal walking and gait initiation in Parkinson's disease which reported a tendency of reduced TA activity compared with healthy controls [15,173], suggesting an altered dorsiflexion of the ankle during swing for foot clearance and placement. Moreover, this behaviour might also justify the anticipation observed in the activation of GM during the swing phase (N=2, 3, 4), thus compensating the shorter duration in TA activation in the same phase, according to the antagonist nature of GM and TA. In fact, other authors underlined that EMG changes in the posterior and anterior leg muscles of PD patients usually fail to affect reciprocity between antagonist groups [150,171,172,174].

The activation observed in healthy subjects for N=4 and N=5 modalities during mid-stance also occurred in PDP, but with greater variability, with difficulties in drawing conclusions about possible alteration of EMG pattern. However, these modalities represent about 35% of the total strides, thus influencing less the global assessment of muscle activation.

As deducible from the results described above, GM resulted mostly active during the stance phase of gait and TA at the beginning and at the end of the gait cycle. However, the high degree of muscular variability (Figure 1 and 3), reported also in previous studies [166,168,169], led to identify several co-activations throughout the gait cycle. Three co-activation periods between GM and TA were recognized in a single gait cycle (Figure 4). The first co-activation lasted from heel strike to the mid-stance phase. In the first half of this time period, the concomitant muscle activation could be attributable to the impulsive loading response of the ankle during the heel strike, where a greater risk of instability occurred and thus an optimal control was needed [175]. The second half of this first co-activation arose during the foot-contact phase (about at 20% of the gait cycle), when GM restrained the tibia rotation over the talus through the dorsiflexion control and decelerated the forward movement of the lower limb [18,156,166]. TA activation can be associate to the stabilization of the tibia after the weight acceptance, when the contralateral limb swing begins and thus almost the entire body weight is transferred to the ipsilateral lower limb. The second co-contraction occurred from the pre- to the initial swing phase. Previously [166], this concomitant activation of GM and TA was not considered as a proper co-contraction, since the two muscles acted on different joints. TA acted to stretch the tendinous tissue at the highest speeds, presumably to contribute to rapid dorsi-flexion of the foot during swing phase to enable foot clearance [176], while GM activity is commonly related to the plantar-flexion needed for the heel raising [2]. Conversely to healthy people, in PDP this co-contraction resulted longer and lasted until mid-swing in about 30% of the strides, when GM showed N=3 and N=4 activation modalities. The last overlapping period was identified in late swing, when GM adopted its 2-, 3- and 4-activation modality. This behaviour was in line with previous observations on healthy subjects [166]: the co-contraction in swing was due to a GM activity overlapping the simultaneous TA activation as ankle dorsi-flexor and was likely related to the GM foot-invertor function [154], to properly positioning the foot for the next heel strike. [18,166].

In this study, the comparison between muscle activation modalities were carried out between GL and GM, which may be considered a limitation. However, they represent different heads of the same muscle and concurred in the generation of plantarflexion moments during walking [177], without any reported difference in the biomechanical function. Moreover, some authors assessing

muscle activation during gait, did not specified the positioning of EMG channels in the lateral or medial head, and generally consider only ‘Gastrocnemius’ [150,173].

In conclusion, according to the results obtained in the present study: i) no recursive pattern was observe in the activation modalities of right and left leg, ii) the activation of GM during stance occurred with the same modalities as healthy people, suggesting active role of muscle in forward propulsion; iii) reduced/absent TA activity during initial contact due to the alterations of the normal contributes to foot positioning at the touch down; iv) anticipation of GM activation and reduced duration of TA activity during swing, highlighting reciprocity between the two muscles; v) co-contraction of GM and TA was observed during the early stance, push off and terminal swing phases.

In the future, differences in the activation modalities of GM and TA between freezers and non-freezers PDPs should be investigated, also considering the muscle activation in the strides leading up a freezing episode in an increased number of patients.

ACKNOWLEDGMENTS

Firstly, I would like to express my sincere gratitude to my supervisors Prof. Silvia Fantozzi and Prof. Rita Stagni for continuous support during my Ph.D. course, for their patience, motivation, and immense knowledge. Their guidance helped me in all the time of research activities and during the writing of this thesis.

My sincere thanks also go to Prof. Stelios Psycharakis, who provided me an opportunity to join his team during my Ph.D. visiting period abroad, and who gave me access to the wonderful pool at the University of Edinburgh, where lot of walking tasks were acquired during my stay there. Edinburgh represents to me an unforgettable city that will always remain in my heart.

I thank all my colleagues for the intellectually stimulating talks and for the time we spent together in the last years. A very special thanks go to Chiara and Valeria, the best friends I could hope to find during this journey, for the good time enjoying nature, the stimulating discussions, and the big laugh.

Also, I would like to thank my family and friends for uplifting me and sharing experiences with me during this trip. And finally, a heartfelt thank you to my Mum, for constantly guiding and supporting me my entire life, especially through these (sometimes difficult) last years.

REFERENCES

[1] A. Mirelman, S. Shema, I. Maidan, J.M. Hausdorff, Chapter 7 - Gait, in: B.L. Day, S.R. Lord (Eds.), Handb. Clin. Neurol., Elsevier, 2018: pp. 119–134. https://doi.org/10.1016/B978-0-444-63916-5.00007-0.

[2] D.A. Winter, The biomechanics and motor control of human gait, Univ. of Waterloo Press, Waterloo, Ontario, 1987.

[3] D. Hodgins, The importance of measuring human gait, Med Device Technol. 19 (2008) 44–7.

[4] S. Collado-Vázquez, J.M. Carrillo, Balzac y el análisis de la marcha humana, Neurología. 30 (2015) 240–246. https://doi.org/10.1016/j.nrl.2012.03.016.

[5] S. Fritz, M. Lusardi, White Paper: "Walking Speed: the Sixth Vital Sign":, J. Geriatr. Phys. Ther. 32 (2009) 2–5. https://doi.org/10.1519/00139143-200932020-00002.

[6] A. Middleton, S.L. Fritz, M. Lusardi, Walking Speed: The Functional Vital Sign, J. Aging Phys. Act. 23 (2015) 314–322. https://doi.org/10.1123/japa.2013-0236.

[7] S. Fahn, J. Jankovic, M. Hallett, Chapter 10 - Gait disorders: Pathophysiology and clinical syndromes, in: S. Fahn, J. Jankovic, M. Hallett (Eds.), Princ. Pract. Mov. Disord. Second Ed., W.B. Saunders, Edinburgh, 2011: pp. 241–249. https://doi.org/10.1016/B978-1-4377-2369-4.00010-X.

[8] A. Muro-de-la-Herran, B. Garcia-Zapirain, A. Mendez-Zorrilla, Gait Analysis Methods: An Overview of Wearable and Non-Wearable Systems, Highlighting Clinical Applications, Sensors. 14 (2014) 3362–3394. https://doi.org/10.3390/s140203362.

[9] G. Pacini Panebianco, M.C. Bisi, R. Stagni, S. Fantozzi, Analysis of the performance of 17 algorithms from a systematic review: Influence of sensor position, analysed variable and computational approach in gait timing estimation from IMU measurements, Gait Posture. 66 (2018) 76–82. https://doi.org/10.1016/j.gaitpost.2018.08.025.

[10] A. Vienne, R.P. Barrois, S. Buffat, D. Ricard, P.-P. Vidal, Inertial Sensors to Assess Gait Quality in Patients with Neurological Disorders: A Systematic Review of Technical and Analytical Challenges, Front. Psychol. 8 (2017). https://doi.org/10.3389/fpsyg.2017.00817.

[11] A. Parnandi, E. Wade, M. Matarić, Motor function assessment using wearable inertial sensors, in: 2010 Annu. Int. Conf. IEEE Eng. Med. Biol., 2010: pp. 86–89. https://doi.org/10.1109/IEMBS.2010.5626156.

[12] M.C. Bisi, F. Riva, R. Stagni, Measures of gait stability: performance on adults and toddlers at the beginning of independent walking, J. Neuroengineering Rehabil. 11 (2014) 131. https://doi.org/10.1186/1743-0003-11-131.

[13] A. Herrel, V. Schaerlaeken, C. Ross, J. Meyers, K. Nishikawa, V. Abdala, A. Manzano, P. Aerts, Electromyography and the evolution of motor control: limitations and insights, Integr. Comp. Biol. 48 (2008) 261–271. https://doi.org/10.1093/icb/icn025.

[14] M. Bertoli, A. Cereatti, D. Trojaniello, L. Avanzino, E. Pelosin, S. Del Din, L. Rochester, P. Ginis, E.M.J. Bekkers, A. Mirelman, J.M. Hausdorff, U. Della Croce, Estimation of spatio-temporal parameters of gait from magneto-inertial measurement units: multicenter validation among Parkinson, mildly cognitively impaired and healthy older adults, Biomed. Eng. Online. 17 (2018) 58. https://doi.org/10.1186/s12938-018-0488-2.

[15] V. Dietz, W. Zijlstra, T. Prokop, W. Berger, Leg muscle activation during gait in Parkinson's disease: adaptation and interlimb coordination, Electroencephalogr. Clin. Neurophysiol. Mot. Control. 97 (1995) 408–415. https://doi.org/10.1016/0924-980X(95)00109-X.

[16] J. Taborri, E. Palermo, S. Rossi, P. Cappa, Gait Partitioning Methods: A Systematic Review, Sensors. 16 (2016). https://doi.org/10.3390/s16010066.

[17] J.S. Kawalec, 12 - Mechanical testing of foot and ankle implants, in: E. Friis (Ed.), Mech. Test. Orthop. Implants, Woodhead Publishing, 2017: pp. 231–253. https://doi.org/10.1016/B978-0-08-100286-5.00012-3.

[18] J. Perry, J. Burnfield, Gait Analysis: Normal and Pathological Function, 2 edizione, Slack Inc, Thorofare, NJ, 2010.

[19] W.P.O. and J.W. Merton Root, Normal and Abnormal Function of the Foot: Clinical Biomechanics, Vol. II, Clinical Biomechanics Corp., 1977.

[20] A. Salarian, H. Russmann, F.J.G. Vingerhoets, C. Dehollain, Y. Blanc, P.R. Burkhard, K. Aminian, Gait assessment in Parkinson's disease: toward an ambulatory system for long-term monitoring, IEEE Trans. Biomed. Eng. 51 (2004) 1434–1443. https://doi.org/10.1109/TBME.2004.827933.

[21] R.C. González, A.M. López, J. Rodriguez-Uría, D. Álvarez, J.C. Alvarez, Real-time gait event detection for normal subjects from lower trunk accelerations, Gait Posture. 31 (2010) 322–325. https://doi.org/10.1016/j.gaitpost.2009.11.014.

[22] J. Kim, M.-N. Bae, K.B. Lee, S.G. Hong, Gait event detection algorithm based on smart insoles, ETRI J. 42 (2020) 46–53. https://doi.org/10.4218/etrij.2018-0639.

[23] E. Tileylioğlu, A. Yilmaz, Application of neural based estimation algorithm for gait phases of above knee prosthesis, Conf. Proc. Annu. Int. Conf. IEEE Eng. Med. Biol. Soc. IEEE Eng.

Med. Biol. Soc. Annu. Conf. 2015 (2015) 4820–4823. https://doi.org/10.1109/EMBC.2015.7319472.

[24] M. Goršič, R. Kamnik, L. Ambrožič, N. Vitiello, D. Lefeber, G. Pasquini, M. Munih, Online Phase Detection Using Wearable Sensors for Walking with a Robotic Prosthesis, Sensors. 14 (2014) 2776–2794. https://doi.org/10.3390/s140202776.

[25] A. Mannini, A.M. Sabatini, Machine learning methods for classifying human physical activity from on-body accelerometers, Sensors. 10 (2010) 1154–1175. https://doi.org/10.3390/s100201154.

[26] F. Bugané, M.G. Benedetti, G. Casadio, S. Attala, F. Biagi, M. Manca, A. Leardini, Estimation of Spatial-temporal Gait Parameters in Level Walking Based on a Single Accelerometer, Comput Methods Prog Biomed. 108 (2012) 129–137. https://doi.org/10.1016/j.cmpb.2012.02.003.

[27] D. Trojaniello, A. Cereatti, E. Pelosin, L. Avanzino, A. Mirelman, J. Hausdorff, U. Della Croce, Estimation of step-by-step spatio-temporal parameters of normal and impaired gait using shank-mounted magneto-inertial sensors: application to elderly, hemiparetic, parkinsonian and choreic gait, J. NEUROENGINEERING Rehabil. 11 (2014) 1–12.

[28] H.-K. Lee, S.-J. Hwang, S.-P. Cho, D.-R. Lee, S.-H. You, K.-J. Lee, Y.-H. Kim, H.-S. Choi, Novel algorithm for the hemiplegic gait evaluation using a single 3-axis accelerometer, Conf. Proc. Annu. Int. Conf. IEEE Eng. Med. Biol. Soc. IEEE Eng. Med. Biol. Soc. Annu. Conf. 2009 (2009) 3964–3966. https://doi.org/10.1109/IEMBS.2009.5333650.

[29] J. McCamley, M. Donati, E. Grimpampi, C. Mazzà, An enhanced estimate of initial contact and final contact instants of time using lower trunk inertial sensor data, Gait Posture. 36 (2012) 316–318. https://doi.org/10.1016/j.gaitpost.2012.02.019.

[30] S.H. Shin, C.G. Park, Adaptive step length estimation algorithm using optimal parameters and movement status awareness, Med. Eng. Phys. 33 (2011) 1064–1071. https://doi.org/10.1016/j.medengphy.2011.04.009.

[31] W. Zijlstra, A.L. Hof, Assessment of spatio-temporal gait parameters from trunk accelerations during human walking, Gait Posture. 18 (2003) 1–10.

[32] J.-A. Lee, S.-H. Cho, Y.-J. Lee, H.-K. Yang, J.-W. Lee, Portable activity monitoring system for temporal parameters of gait cycles, J. Med. Syst. 34 (2010) 959–966. https://doi.org/10.1007/s10916-009-9311-8.

[33] S. Khandelwal, N. Wickström, Identification of Gait Events using Expert Knowledge and Continuous Wavelet Transform Analysis, in: SciTePress, 2014: pp. 197–204. http://www.diva-portal.org/smash/record.jsf?pid=diva2:688909 (accessed October 11, 2017).

[34] P. Catalfamo, S. Ghoussayni, D. Ewins, Gait Event Detection on Level Ground and Incline Walking Using a Rate Gyroscope, Sensors. 10 (2010) 5683–5702. https://doi.org/10.3390/s100605683.

[35] B.R. Greene, D. McGrath, K.J. O'Donovan, R. O'Neill, A. Burns, B. Caulfield, Adaptive estimation of temporal gait parameters using body-worn gyroscopes, Conf. Proc. Annu. Int. Conf. IEEE Eng. Med. Biol. Soc. IEEE Eng. Med. Biol. Soc. Annu. Conf. 2010 (2010) 1296–1299. https://doi.org/10.1109/IEMBS.2010.5626400.

[36] K. Aminian, B. Najafi, C. Büla, P.-F. Leyvraz, P. Robert, Spatio-temporal parameters of gait measured by an ambulatory system using miniature gyroscopes, J. Biomech. 35 (2002) 689–699. https://doi.org/10.1016/S0021-9290(02)00008-8.

[37] J.M. Jasiewicz, J.H.J. Allum, J.W. Middleton, A. Barriskill, P. Condie, B. Purcell, R.C.T. Li, Gait event detection using linear accelerometers or angular velocity transducers in able-bodied and spinal-cord injured individuals, Gait Posture. 24 (2006) 502–509. https://doi.org/10.1016/j.gaitpost.2005.12.017.

[38] A.M. Sabatini, C. Martelloni, S. Scapellato, F. Cavallo, Assessment of walking features from foot inertial sensing, IEEE Trans. Biomed. Eng. 52 (2005) 486–494. https://doi.org/10.1109/TBME.2004.840727.

[39] A. Ferrari, P. Ginis, M. Hardegger, F. Casamassima, L. Rocchi, L. Chiari, A Mobile Kalman-Filter Based Solution for the Real-Time Estimation of Spatio-Temporal Gait Parameters, IEEE Trans. Neural Syst. Rehabil. Eng. 24 (2016) 764–773. https://doi.org/10.1109/TNSRE.2015.2457511.

[40] B. Mariani, M.C. Jiménez, F.J.G. Vingerhoets, K. Aminian, On-shoe wearable sensors for gait and turning assessment of patients with Parkinson's disease, IEEE Trans. Biomed. Eng. 60 (2013) 155–158. https://doi.org/10.1109/TBME.2012.2227317.

[41] D. Hamacher, N.B. Singh, J.H. Van Dieën, M.O. Heller, W.R. Taylor, Kinematic measures for assessing gait stability in elderly individuals: a systematic review, J. R. Soc. Interface. 8 (2011) 1682–1698. https://doi.org/10.1098/rsif.2011.0416.

[42] F. Riva, M.C. Bisi, R. Stagni, Orbital stability analysis in biomechanics: a systematic review of a nonlinear technique to detect instability of motor tasks, Gait Posture. 37 (2013) 1–11. https://doi.org/10.1016/j.gaitpost.2012.06.015.

[43] P. Tamburini, F. Storm, C. Buckley, M.C. Bisi, R. Stagni, C. Mazzà, Moving from laboratory to real life conditions: Influence on the assessment of variability and stability of gait, Gait Posture. 59 (2018) 248–252. https://doi.org/10.1016/j.gaitpost.2017.10.024.

[44] F. Riva, M.C. Bisi, R. Stagni, Gait variability and stability measures: minimum number of strides and within-session reliability, Comput. Biol. Med. 50 (2014) 9–13. https://doi.org/10.1016/j.compbiomed.2014.04.001.

[45] P. Tamburini, M.C. Bisi, R. Stagni, Frequency content of gait trunk acceleration: a longitudinal study, (2017) 2.

[46] P. Tamburini, D. Mazzoli, R. Stagni, Towards an objective assessment of motor function in sub-acute stroke patients: Relationship between clinical rating scales and instrumental gait stability indexes, Gait Posture. 59 (2018) 58–64. https://doi.org/10.1016/j.gaitpost.2017.09.033.

[47] F. Riva, M.J.P. Toebes, M. Pijnappels, R. Stagni, J.H. van Dieën, Estimating fall risk with inertial sensors using gait stability measures that do not require step detection, Gait Posture. 38 (2013) 170–174. https://doi.org/10.1016/j.gaitpost.2013.05.002.

[48] H.B. Menz, S.R. Lord, R.C. Fitzpatrick, Acceleration patterns of the head and pelvis when walking on level and irregular surfaces, Gait Posture. 18 (2003) 35–46.

[49] F.S. Labini, A. Meli, Y.P. Ivanenko, D. Tufarelli, Recurrence quantification analysis of gait in normal and hypovestibular subjects, Gait Posture. 35 (2012) 48–55. https://doi.org/10.1016/j.gaitpost.2011.08.004.

[50] M. Costa, C.-K. Peng, A. L. Goldberger, J.M. Hausdorff, Multiscale entropy analysis of human gait dynamics, Phys. Stat. Mech. Its Appl. 330 (2003) 53–60. https://doi.org/10.1016/j.physa.2003.08.022.

[51] M.C. Bisi, P. Tamburini, R. Stagni, A “Fingerprint” of locomotor maturation: Motor development descriptors, reference development bands and data-set., Gait Posture. 68 (2019) 232–237.

[52] C.J.C. Lamoth, P.J. Beek, O.G. Meijer, Pelvis-thorax coordination in the transverse plane during gait, Gait Posture. 16 (2002) 101–114.

[53] F. Takens, Detecting strange attractors in turbulence, in: D. Rand, L.-S. Young (Eds.), Dyn. Syst. Turbul. Warwick 1980, Springer Berlin Heidelberg, 1981: pp. 366–381.

[54] T.E. Lockhart, J. Liu, Differentiating fall-prone and healthy adults using local dynamic stability, Ergonomics. 51 (2008) 1860–1872. https://doi.org/10.1080/00140130802567079.

[55] M.A. Riley, R. Balasubramaniam, M.T. Turvey, Recurrence quantification analysis of postural fluctuations, Gait Posture. 9 (1999) 65–78. https://doi.org/10.1016/S0966-6362(98)00044-7.

[56] C.L. Webber, J.P. Zbilut, Dynamical assessment of physiological systems and states using recurrence plot strategies, J. Appl. Physiol. Bethesda Md 1985. 76 (1994) 965–973. https://doi.org/10.1152/jappl.1994.76.2.965.

[57] J.S. Richman, J.R. Moorman, Physiological time-series analysis using approximate entropy and sample entropy, Am. J. Physiol.-Heart Circ. Physiol. 278 (2000).

[58] S.M. Pincus, Approximate entropy as a measure of system complexity., Proc. Natl. Acad. Sci. 88 (1991) 2297–2301. https://doi.org/10.1073/pnas.88.6.2297.

[59] F. Riva, E. Grimpampi, C. Mazzà, R. Stagni, Are gait variability and stability measures influenced by directional changes?, Biomed. Eng. Online. 13 (2014) 56. https://doi.org/10.1186/1475-925X-13-56.

[60] A.H. Khandoker, S.B. Taylor, C.K. Karmakar, R.K. Begg, M. Palaniswami, Investigating Scale Invariant Dynamics in Minimum Toe Clearance Variability of the Young and Elderly During Treadmill Walking, IEEE Trans. Neural Syst. Rehabil. Eng. 16 (2008) 380–389. https://doi.org/10.1109/TNSRE.2008.925071.

[61] J.M. Hausdorff, D.A. Rios, H.K. Edelberg, Gait variability and fall risk in community-living older adults: A 1-year prospective study, Arch. Phys. Med. Rehabil. 82 (2001) 1050–1056. https://doi.org/10.1053/apmr.2001.24893.

[62] J.M. Baker, Gait Disorders, Am. J. Med. 131 (2018) 602–608. https://doi.org/10.1016/j.amjmed.2017.11.051.

[63] S. Sveinbjornsdottir, The clinical symptoms of Parkinson's disease, J. Neurochem. 139 Suppl 1 (2016) 318–324. https://doi.org/10.1111/jnc.13691.

[64] J.A. DeLisa, Gait Analysis in the Science of Rehabilitation, DIANE Publishing, 1998.

[65] J. Opara, A. Małecki, E. Małecka, T. Socha, Motor assessment in Parkinson`s disease, Ann. Agric. Environ. Med. 24 (2017) 411–415. https://doi.org/10.5604/12321966.1232774.

[66] M.E. Morris, Movement disorders in people with Parkinson disease: a model for physical therapy, Phys. Ther. 80 (2000) 578–597.

[67] C.A. Bailey, F. Corona, M. Murgia, R. Pili, M. Pau, J.N. Côté, Electromyographical Gait Characteristics in Parkinson's Disease: Effects of Combined Physical Therapy and Rhythmic Auditory Stimulation, Front. Neurol. 9 (2018). https://doi.org/10.3389/fneur.2018.00211.

[68] N. Giladi, A. Nieuwboer, Understanding and treating freezing of gait in parkinsonism, proposed working definition, and setting the stage, Mov. Disord. Off. J. Mov. Disord. Soc. 23 Suppl 2 (2008) S423-425. https://doi.org/10.1002/mds.21927.

[69] E. Heremans, A. Nieuwboer, S. Vercruysse, Freezing of gait in Parkinson's disease: where are we now?, Curr. Neurol. Neurosci. Rep. 13 (2013) 350. https://doi.org/10.1007/s11910-013-0350-7.

[70] M. Pau, F. Corona, R. Pili, C. Casula, M. Guicciardi, G. Cossu, M. Murgia, Quantitative assessment of gait parameters in people with Parkinson's disease in laboratory and clinical

setting: Are the measures interchangeable?, Neurol. Int. 10 (2018). https://doi.org/10.4081/ni.2018.7729.

[71] A. Santiago, J.W. Langston, R. Gandhy, R. Dhall, S. Brillman, L. Rees, C. Barlow, Qualitative Evaluation of the Personal KinetiGraphTM Movement Recording System in a Parkinson's Clinic, J. Park. Dis. 9 (2019) 207–219. https://doi.org/10.3233/JPD-181373.

[72] D. Rodríguez-Martín, A. Samà, C. Pérez-López, A. Català, J.M. Moreno Arostegui, J. Cabestany, À. Bayés, S. Alcaine, B. Mestre, A. Prats, M.C. Crespo, T.J. Counihan, P. Browne, L.R. Quinlan, G. ÓLaighin, D. Sweeney, H. Lewy, J. Azuri, G. Vainstein, R. Annicchiarico, A. Costa, A. Rodríguez-Molinero, Home detection of freezing of gait using support vector machines through a single waist-worn triaxial accelerometer, PLOS ONE. 12 (2017) e0171764. https://doi.org/10.1371/journal.pone.0171764.

[73] S.T. Moore, H.G. MacDougall, W.G. Ondo, Ambulatory monitoring of freezing of gait in Parkinson's disease, J. Neurosci. Methods. 167 (2008) 340–348. https://doi.org/10.1016/j.jneumeth.2007.08.023.

[74] M. Mancini, K. Smulders, R.G. Cohen, F.B. Horak, N. Giladi, J.G. Nutt, The clinical significance of freezing while turning in Parkinson's disease, Neuroscience. 343 (2017) 222–228. https://doi.org/10.1016/j.neuroscience.2016.11.045.

[75] S.T. Moore, D.A. Yungher, T.R. Morris, V. Dilda, H.G. MacDougall, J.M. Shine, S.L. Naismith, S.J. Lewis, Autonomous identification of freezing of gait in Parkinson's disease from lower-body segmental accelerometry, J. NeuroEngineering Rehabil. 10 (2013) 19. https://doi.org/10.1186/1743-0003-10-19.

[76] E. Jovanov, E. Wang, L. Verhagen, M. Fredrickson, R. Fratangelo, deFOG — A real time system for detection and unfreezing of gait of Parkinson’s patients, in: 2009 Annu. Int. Conf. IEEE Eng. Med. Biol. Soc., IEEE, Minneapolis, MN, 2009: pp. 5151–5154. https://doi.org/10.1109/IEMBS.2009.5334257.

[77] M. Mancini, K.C. Priest, J.G. Nutt, F.B. Horak, Quantifying freezing of gait in Parkinson's disease during the instrumented timed up and go test, in: 2012 Annu. Int. Conf. IEEE Eng. Med. Biol. Soc., IEEE, San Diego, CA, 2012: pp. 1198–1201. https://doi.org/10.1109/EMBC.2012.6346151.

[78] T.R. Morris, C. Cho, V. Dilda, J.M. Shine, S.L. Naismith, S.J.G. Lewis, S.T. Moore, A comparison of clinical and objective measures of freezing of gait in Parkinson's disease, Parkinsonism Relat. Disord. 18 (2012) 572–577. https://doi.org/10.1016/j.parkreldis.2012.03.001.

[79] M.D. Djuric-Jovicic, N.S. Jovicic, S.M. Radovanovic, I.D. Stankovic, M.B. Popovic, V.S. Kostic, Automatic Identification and Classification of Freezing of Gait Episodes in Parkinson's Disease Patients, IEEE Trans. Neural Syst. Rehabil. Eng. 22 (2014) 685–694. https://doi.org/10.1109/TNSRE.2013.2287241.

[80] S. Rezvanian, T. Lockhart, Towards Real-Time Detection of Freezing of Gait Using Wavelet Transform on Wireless Accelerometer Data, Sensors. 16 (2016) 475. https://doi.org/10.3390/s16040475.

[81] K. Ben Mansour, N. Rezzoug, P. Gorce, Analysis of several methods and inertial sensors locations to assess gait parameters in able-bodied subjects, Gait Posture. 42 (2015) 409–414. https://doi.org/10.1016/j.gaitpost.2015.05.020.

[82] F.A. Storm, C.J. Buckley, C. Mazzà, Gait event detection in laboratory and real life settings: Accuracy of ankle and waist sensor based methods, Gait Posture. 50 (2016) 42–46. https://doi.org/10.1016/j.gaitpost.2016.08.012.

[83] D. Trojaniello, A. Cereatti, U. Della Croce, Accuracy, sensitivity and robustness of five different methods for the estimation of gait temporal parameters using a single inertial sensor mounted on the lower trunk, Gait Posture. 40 (2014) 487–492. https://doi.org/10.1016/j.gaitpost.2014.07.007.

[84] J.A. Zeni, J.G. Richards, J.S. Higginson, Two simple methods for determining gait events during treadmill and overground walking using kinematic data, Gait Posture. 27 (2008) 710–714. https://doi.org/10.1016/j.gaitpost.2007.07.007.

[85] D. Bates, M. Mächler, B. Bolker, S. Walker, Fitting Linear Mixed-Effects Models using lme4, ArXiv14065823 Stat. (2014). http://arxiv.org/abs/1406.5823 (accessed July 2, 2018).

[86] N. Haji Ghassemi, J. Hannink, C.F. Martindale, H. Gaßner, M. Müller, J. Klucken, B.M. Eskofier, Segmentation of Gait Sequences in Sensor-Based Movement Analysis: A Comparison of Methods in Parkinson's Disease, Sensors. 18 (2018). https://doi.org/10.3390/s18010145.

[87] M.C. Bisi, R. Stagni, Evaluation of toddler different strategies during the first six-months of independent walking: A longitudinal study, Gait Posture. 41 (2015) 574–579. https://doi.org/10.1016/j.gaitpost.2014.11.017.

[88] A.M.F. Barela, S.F. Stolf, M. Duarte, Biomechanical characteristics of adults walking in shallow water and on land, J. Electromyogr. Kinesiol. 16 (2006) 250–256.

[89] D.A. Skelton, S.M. Dinan, Exercise for falls management: Rationale for an exercise programme aimed at reducing postural instability, Physiother. Theory Pract. 15 (1999) 105–120. https://doi.org/10.1080/095939899307801.

[90] E. Watanabe, N. Takeshima, A. Okada, K. Inomata, Comparison of water- and land-based exercise in the reduction of state anxiety among older adults, Percept. Mot. Skills. 91 (2000) 97–104. https://doi.org/10.2466/pms.2000.91.1.97.

[91] B.E. Becker, Aquatic therapy: scientific foundations and clinical rehabilitation applications, PM R. 1 (2009) 859–872. https://doi.org/10.1016/j.pmrj.2009.05.017.

[92] S. Fantozzi, A. Giovanardi, D. Borra, G. Gatta, Gait Kinematic Analysis in Water Using Wearable Inertial Magnetic Sensors, PloS One. 10 (2015) e0138105. https://doi.org/10.1371/journal.pone.0138105.

[93] K. Masumoto, T. Shono, S. Takasugi, N. Hotta, K. Fujishima, Y. Iwamoto, Age-related differences in muscle activity, stride frequency and heart rate response during walking in water, J. Electromyogr. Kinesiol. Off. J. Int. Soc. Electrophysiol. Kinesiol. 17 (2007) 596–604. https://doi.org/10.1016/j.jelekin.2006.06.006.

[94] K. Kaneda, H. Wakabayashi, D. Sato, T. Nomura, Lower extremity muscle activity during different types and speeds of underwater movement, J. Physiol. Anthropol. 26 (2007) 197–200.

[95] A.C. Severin, B.J. Burkett, M.R. McKean, M.G.L. Sayers, Biomechanical aspects of aquatic therapy: A literature review on application and methodological challenges - Kaenz, J. Fit. Res. 5 (2016) 49–62.

[96] S.P. Brown, L.F. Chitwood, K.R. Beason, D.R. McLemore, Deep Water Running Physiologic Responses: Gender Differences at Treadmill-Matched Walking/Running Cadences, J. Strength Cond. Res. 11 (1997) 107.

[97] D. Trojaniello, A. Cereatti, E. Pelosin, L. Avanzino, A. Mirelman, J.M. Hausdorff, U. Della Croce, Estimation of step-by-step spatio-temporal parameters of normal and impaired gait using shank-mounted magneto-inertial sensors: application to elderly, hemiparetic, parkinsonian and choreic gait, J. NeuroEngineering Rehabil. 11 (2014) 152. https://doi.org/10.1186/1743-0003-11-152.

[98] K. Masumoto, T. Shono, N. Hotta, K. Fujishima, Muscle activation, cardiorespiratory response, and rating of perceived exertion in older subjects while walking in water and on dry land, J. Electromyogr. Kinesiol. Off. J. Int. Soc. Electrophysiol. Kinesiol. 18 (2008) 581–590. https://doi.org/10.1016/j.jelekin.2006.12.009.

[99] M. Schwartz, A. Rozumalski, J. Trost, The effect of walking speed on the gait of typically developing children. - PubMed - NCBI, Eff. Walk. Speed Gait Typically Dev. Child. 41 (2008) 1639–50. https://doi.org/10.1016/j.jbiomech.2008.03.015.

[100] A.L. Hof, Scaling gait data to body size, Gait Posture. 4 (1996) 222–223. https://doi.org/10.1016/0966-6362(95)01057-2.

[101] S. Khandelwal, N. Wickström, Identification of Gait Events using Expert Knowledge and Continuous Wavelet Transform Analysis:, SciTePress. (2014) 197–204.

[102] J.-A. Lee, S.-H. Cho, Y.-J. Lee, H.-K. Yang, J.-W. Lee, Portable activity monitoring system for temporal parameters of gait cycles, J. Med. Syst. 34 (2010) 959–966. https://doi.org/10.1007/s10916-009-9311-8.

[103] W. Zijlstra, Assessment of spatio-temporal parameters during unconstrained walking, Eur. J. Appl. Physiol. 92 (2004) 39–44. https://doi.org/10.1007/s00421-004-1041-5.

[104] S.E.H. Davies, S.N. Mackinnon, The energetics of walking on sand and grass at various speeds, Ergonomics. 49 (2006) 651–660. https://doi.org/10.1080/00140130600558023.

[105] P. Zamparo, R. Perini, C. Orizio, M. Sacher, G. Ferretti, The energy cost of walking or running on sand, Eur. J. Appl. Physiol. 65 (1992) 183–187. https://doi.org/10.1007/BF00705078.

[106] K. Morrison, R.A. Braham, B. Dawson, K. Guelfi, Effect of a sand or firm surface walking program on health, strength and fitness in women aged between 60-75 years., J. Aging Phys. Act. 17 (2009) 196-209.

[107] H. Chen, B. Nigg, M. Hulliger, J. de Koning, Influence of sensory input on plantar pressure distribution, Clin. Biomech. 10 (1995) 271–274. https://doi.org/10.1016/0268-0033(95)99806-D.

[108] T.M. Lejeune, P.A. Willems, N.C. Heglund, MECHANICS AND ENERGETICS OF HUMAN LOCOMOTION ON SAND, (n.d.) 10.

[109] S. Oztoprak, M.D. Bolton, Stiffness of sands through a laboratory test database, Géotechnique. 63 (2013) 54–70. https://doi.org/10.1680/geot.10.P.078.

[110] S.N. Domenico, Elastic properties of unconsolidated porous sand, Geophysics. 42 (1977) 1339–1368.

[111] P. Kumar, Impact of Sand Training for Endurance Development among Athletes, Int. J. Appl. Res. 1 (2015) 503–506.

[112] M.E.L. van den Berg, C.J. Barr, J.V. McLoughlin, M. Crotty, Effect of walking on sand on gait kinematics in individuals with multiple sclerosis, Mult. Scler. Relat. Disord. 16 (2017) 15–21. https://doi.org/10.1016/j.msard.2017.05.008.

[113] T. Kim, B. Hwang, Effects of gait training on sand on improving the walking ability of patients with chronic stroke: a randomized controlled trial, J. Phys. Ther. Sci. 29 (2017) 2172–2175. https://doi.org/10.1589/jpts.29.2172.

[114] H.C. Pinnington, B. Dawson, The energy cost of running on grass compared to soft dry beach sand, J. Sci. Med. Sport. 4 (2001) 416–430. https://doi.org/10.1016/S1440-2440(01)80051-7.

[115] C. Wang, X. Wang, Z. Long, J. Yuan, Y. Qian, J. Li, Estimation of Temporal Gait Parameters Using a Wearable Microphone-Sensor-Based System, Sensors. 16 (2016) 2167. https://doi.org/10.3390/s16122167.

[116] J.R. Landis, G.G. Koch, The measurement of observer agreement for categorical data, Biometrics. 33 (1977) 159–174.

[117] R. Senden, I.C. Heyligers, K. Meijer, H. Savelberg, B. Grimm, Acceleration-based motion analysis as a tool for rehabilitation: exploration in simulated functional knee limited walking conditions, Am. J. Phys. Med. Rehabil. 90 (2011) 226–232. https://doi.org/10.1097/PHM.0b013e31820b151a.

[118] C. Morio, M.J. Lake, N. Gueguen, G. Rao, L. Baly, The influence of footwear on foot motion during walking and running, J. Biomech. 42 (2009) 2081–2088. https://doi.org/10.1016/j.jbiomech.2009.06.015.

[119] M. Buckthorpe, E. Pirotti, F.D. Villa, BENEFITS AND USE OF AQUATIC THERAPY DURING REHABILITATION AFTER ACL RECONSTRUCTION -A CLINICAL COMMENTARY, Int. J. Sports Phys. Ther. 14 (2019) 978–993.

[120] S. Heywood, J. McClelland, P. Geigle, A. Rahmann, R. Clark, Spatiotemporal, kinematic, force and muscle activation outcomes during gait and functional exercise in water compared to on land: A systematic review, Gait Posture. 48 (2016) 120–130. https://doi.org/10.1016/j.gaitpost.2016.04.033.

[121] C. Cadenas-Sanchez, R. Arellano, J. Vanrenterghem, G. López-Contreras, Kinematic Adaptations of Forward And Backward Walking on Land and in Water, J. Hum. Kinet. 49 (2015) 15–24. https://doi.org/10.1515/hukin-2015-0104.

[122] E.V. Passeri, M. Martinelli, V. Gatteri, S. Pivetti, C. Passeri, L. Cigolini, S. Chiari, A. Zenorini, P. Gaffurini, S. Bernardi, I. Poli, L. Bissolotti, Standard and water rehabilitation: An analysis of over 14 years' experience in patients with haemophilia or other clotting factor disorders after orthopaedic surgery, Haemoph. Off. J. World Fed. Hemoph. (2019). https://doi.org/10.1111/hae.13748.

[123] D. Volpe, D. Pavan, M. Morris, A. Guiotto, R. Iansek, S. Fortuna, G. Frazzitta, Z. Sawacha, Underwater gait analysis in Parkinson's disease, Gait Posture. 52 (2017) 87–94. https://doi.org/10.1016/j.gaitpost.2016.11.019.

[124] M. Getz, Y. Hutzler, A. Vermeer, Y. Yarom, V. Unnithan, The Effect of Aquatic and Land-Based Training on the Metabolic Cost of Walking and Motor Performance in Children with Cerebral Palsy: A Pilot Study, Int. Sch. Res. Not. (2012). https://doi.org/10.5402/2012/657979.

[125] A. Mooventhan, L. Nivethitha, Scientific Evidence-Based Effects of Hydrotherapy on Various Systems of the Body, North Am. J. Med. Sci. 6 (2014) 199–209. https://doi.org/10.4103/1947-2714.132935.

[126] M.C. Bisi, R. Stagni, Changes of human movement complexity during maturation: quantitative assessment using multiscale entropy. - PubMed - NCBI, Comput. Methods Biomech. Biomed. Engin. 21 (2018) 325–331.

[127] K.E. Adolph, W.G. Cole, M. Komati, J.S. Garciaguirre, D. Badaly, J.M. Lingeman, G. Chan, R.B. Sotsky, How Do You Learn to Walk? Thousands of Steps and Dozens of Falls Per Day, Psychol. Sci. 23 (2012) 1387–1394. https://doi.org/10.1177/0956797612446346.

[128] D.J. Clark, Automaticity of walking: functional significance, mechanisms, measurement and rehabilitation strategies, Front. Hum. Neurosci. 9 (2015). https://doi.org/10.3389/fnhum.2015.00246.

[129] B. Najafi, J.L. Helbostad, R. Moe-Nilssen, W. Zijlstra, K. Aminian, Does walking strategy in older people change as a function of walking distance?, Gait Posture. 29 (2009) 261–266. https://doi.org/10.1016/j.gaitpost.2008.09.002.

[130] M.C. Bisi, R. Stagni, Complexity of human gait pattern at different ages assessed using multiscale entropy: From development to decline, Gait Posture. 47 (2016) 37–42. https://doi.org/10.1016/j.gaitpost.2016.04.001.

[131] E.A.F. Ihlen, A. Weiss, A. Bourke, J.L. Helbostad, J.M. Hausdorff, The complexity of daily life walking in older adult community-dwelling fallers and non-fallers, J. Biomech. 49 (2016) 1420–1428. https://doi.org/10.1016/j.jbiomech.2016.02.055.

[132] L. Brognara, P. Palumbo, B. Grimm, L. Palmerini, Assessing Gait in Parkinson's Disease Using Wearable Motion Sensors: A Systematic Review, Diseases. 7 (2019) 18. https://doi.org/10.3390/diseases7010018.

[133] M. Morris, R. Iansek, T. Matyas, J. Summers, Abnormalities in the stride length-cadence relation in parkinsonian gait, Mov. Disord. Off. J. Mov. Disord. Soc. 13 (1998) 61–69. https://doi.org/10.1002/mds.870130115.

[134] J.R. Hughes, S.G. Bowes, A.L. Leeman, C.J. O'Neill, A.A. Deshmukh, P.W. Nicholson, S.M. Dobbs, R.J. Dobbs, Parkinsonian abnormality of foot strike: a phenomenon of ageing and/or one responsive to levodopa therapy?, Br. J. Clin. Pharmacol. 29 (1990) 179–186. https://doi.org/10.1111/j.1365-2125.1990.tb03617.x.

[135] M.P. Murray, S.B. Sepic, G.M. Gardner, W.J. Downs, Walking patterns of men with parkinsonism, Am. J. Phys. Med. 57 (1978) 278–294.

[136] S. Kimmeskamp, E.M. Hennig, Heel to toe motion characteristics in Parkinson patients during free walking, Clin. Biomech. Bristol Avon. 16 (2001) 806–812.

[137] A. Salarian, H. Russmann, F.J.G. Vingerhoets, C. Dehollain, Y. Blanc, P.R. Burkhard, K. Aminian, Gait assessment in Parkinson's disease: toward an ambulatory system for long-term monitoring, IEEE Trans. Biomed. Eng. 51 (2004) 1434–1443. https://doi.org/10.1109/TBME.2004.827933.

[138] W. Kong, J. Lin, L. Waaning, S. Sessa, S. Cosentino, D. Magistro, M. Zecca, R. Kawashima, A. Takanishi, Comparison of gait event detection from shanks and feet in single-task and multi-task walking of healthy older adults, in: 2016 IEEE Int. Conf. Robot. Biomim. ROBIO, 2016: pp. 2063–2068. https://doi.org/10.1109/ROBIO.2016.7866633.

[139] B. Mariani, M.C. Jiménez, F.J.G. Vingerhoets, K. Aminian, On-shoe wearable sensors for gait and turning assessment of patients with Parkinson's disease, IEEE Trans. Biomed. Eng. 60 (2013) 155–158. https://doi.org/10.1109/TBME.2012.2227317.

[140] M.D. Latt, H.B. Menz, V.S. Fung, S.R. Lord, Acceleration Patterns of the Head and Pelvis During Gait in Older People With Parkinson's Disease: A Comparison of Fallers and Nonfallers, J. Gerontol. Ser. A. 64A (2009) 700–706. https://doi.org/10.1093/gerona/glp009.

[141] M. El-Gohary, S. Pearson, J. McNames, M. Mancini, F. Horak, S. Mellone, L. Chiari, Continuous monitoring of turning in patients with movement disability, Sensors. 14 (2013) 356–369. https://doi.org/10.3390/s140100356.

[142] J.C. Alvarez, D. Alvarez, A. López, R.C. González, Pedestrian navigation based on a waist-worn inertial sensor, Sensors. 12 (2012) 10536–10549. https://doi.org/10.3390/s120810536.

[143] A. Paraschiv-Ionescu, C.J. Newman, L. Carcreff, C.N. Gerber, S. Armand, K. Aminian, Locomotion and cadence detection using a single trunk-fixed accelerometer: validity for children with cerebral palsy in daily life-like conditions, J. NeuroEngineering Rehabil. 16 (2019). https://doi.org/10.1186/s12984-019-0494-z.

[144] C.C. Walton, J.M. Shine, J.M. Hall, C. O'Callaghan, L. Mowszowski, M. Gilat, J.Y.Y. Szeto, S.L. Naismith, S.J.G. Lewis, The major impact of freezing of gait on quality of life in Parkinson's disease, J. Neurol. 262 (2015) 108–115. https://doi.org/10.1007/s00415-014-7524-3.

[145] J.G. Nutt, B.R. Bloem, N. Giladi, M. Hallett, F.B. Horak, A. Nieuwboer, Freezing of gait: moving forward on a mysterious clinical phenomenon, Lancet Neurol. 10 (2011) 734–744. https://doi.org/10.1016/S1474-4422(11)70143-0.

[146] E.E. Tripoliti, A.T. Tzallas, M.G. Tsipouras, G. Rigas, P. Bougia, M. Leontiou, S. Konitsiotis, M. Chondrogiorgi, S. Tsouli, D.I. Fotiadis, Automatic detection of freezing of gait

events in patients with Parkinson's disease, Comput. Methods Programs Biomed. 110 (2013) 12–26. https://doi.org/10.1016/j.cmpb.2012.10.016.

[147] M. Sawada, K. Wada-Isoe, R. Hanajima, K. Nakashima, Clinical features of freezing of gait in Parkinson's disease patients, Brain Behav. 9 (2019). https://doi.org/10.1002/brb3.1244.

[148] A. Delval, A.H. Snijders, V. Weerdesteyn, J.E. Duysens, L. Defebvre, N. Giladi, B.R. Bloem, Objective detection of subtle freezing of gait episodes in Parkinson's disease, Mov. Disord. Off. J. Mov. Disord. Soc. 25 (2010) 1684–1693. https://doi.org/10.1002/mds.23159.

[149] G.V. Prateek, I. Skog, M.E. McNeely, R.P. Duncan, G.M. Earhart, A. Nehorai, Modeling, Detecting, and Tracking Freezing of Gait in Parkinson Disease Using Inertial Sensors, IEEE Trans. Biomed. Eng. 65 (2018) 2152–2161. https://doi.org/10.1109/TBME.2017.2785625.

[150] A. Nieuwboer, R. Dom, W. De Weerdt, K. Desloovere, L. Janssens, V. Stijn, Electromyographic profiles of gait prior to onset of freezing episodes in patients with Parkinson's disease, Brain. 127 (2004) 1650–1660. https://doi.org/10.1093/brain/awh189.

[151] A.L. Silva de Lima, L.J.W. Evers, T. Hahn, L. Bataille, J.L. Hamilton, M.A. Little, Y. Okuma, B.R. Bloem, M.J. Faber, Freezing of gait and fall detection in Parkinson's disease using wearable sensors: a systematic review, J. Neurol. 264 (2017) 1642–1654. https://doi.org/10.1007/s00415-017-8424-0.

[152] M.W. Cornwall, T.G. Mcpoil, The Influence of Tibialis Anterior Muscle Activity on Rearfoot Motion during Walking, Foot Ankle Int. 15 (1994) 75–79. https://doi.org/10.1177/107110079401500205.

[153] B. Bordoni, A. Waheed, M. Varacallo, Anatomy, Bony Pelvis and Lower Limb, Gastrocnemius Muscle, in: StatPearls, StatPearls Publishing, Treasure Island (FL), 2019. http://www.ncbi.nlm.nih.gov/books/NBK532946/ (accessed October 14, 2019).

[154] F. Di Nardo, G. Ghetti, S. Fioretti, Assessment of the activation modalities of gastrocnemius lateralis and tibialis anterior during gait: a statistical analysis, J. Electromyogr. Kinesiol. Off. J. Int. Soc. Electrophysiol. Kinesiol. 23 (2013) 1428–1433. https://doi.org/10.1016/j.jelekin.2013.05.011.

[155] F. Di Nardo, A. Strazza, A. Mengarelli, S. Cardarelli, A. Tigrini, F. Verdini, A. Nascimbeni, V. Agostini, M. Knaflitz, S. Fioretti, EMG-Based Characterization of Walking Asymmetry in Children with Mild Hemiplegic Cerebral Palsy, Biosensors. 9 (2019) 82. https://doi.org/10.3390/bios9030082.

[156] A. Mengarelli, A. Gentili, A. Strazza, L. Burattini, S. Fioretti, F. Di Nardo, Co-activation patterns of gastrocnemius and quadriceps femoris in controlling the knee joint during walking, J. Electromyogr. Kinesiol. 42 (2018) 117–122. https://doi.org/10.1016/j.jelekin.2018.07.003.

[157] E. Stlberg, B. Falck, The role of electromyography in neurology, Electroencephalogr. Clin. Neurophysiol. 103 (1997) 579–598. https://doi.org/10.1016/S0013-4694(97)00138-7.

[158] A. Oliveira de Carvalho, A.S.S. Filho, E. Murillo-Rodriguez, N.B. Rocha, M.G. Carta, S. Machado, Physical Exercise For Parkinson's Disease: Clinical And Experimental Evidence, Clin. Pract. Epidemiol. Ment. Health CP EMH. 14 (2018) 89–98. https://doi.org/10.2174/1745017901814010089.

[159] T. Adam Thrasher Ph.D, S. Fisher M.D, Muscle Activation Signals During Parkinson's Disease Gait Are More Rhythmic Than Normal, J. Neurol. Res. Ther. 1 (2015) 1–9. https://doi.org/10.14302/issn.2470-5020.jnrt-15-750.

[160] R.A. Miller, M.H. Thaut, G.C. McIntosh, R.R. Rice, Components of EMG symmetry and variability in parkinsonian and healthy elderly gait, Electroencephalogr. Clin. Neurophysiol. Mot. Control. 101 (1996) 1–7. https://doi.org/10.1016/0013-4694(95)00209-X.

[161] H. Hermens, B. Freriks, The state of the art on sensors and sensor placement procedures for surface electromyography: a proposal for sensor placement procedures, Roessingh Research and Development, Enschede, 1997.

[162] J. Liu, D. Ying, W.Z. Rymer, EMG burst presence probability: a joint time-frequency representation of muscle activity and its application to onset detection, J. Biomech. 48 (2015) 1193–1197. https://doi.org/10.1016/j.jbiomech.2015.02.017.

[163] U. Rashid, I.K. Niazi, N. Signal, D. Farina, D. Taylor, Optimal automatic detection of muscle activation intervals, J. Electromyogr. Kinesiol. 48 (2019) 103–111. https://doi.org/10.1016/j.jelekin.2019.06.010.

[164] P. Bonato, T. D'Alessio, M. Knaflitz, A statistical method for the measurement of muscle activation intervals from surface myoelectric signal during gait, IEEE Trans. Biomed. Eng. 45 (1998) 287–299. https://doi.org/10.1109/10.661154.

[165] V. Agostini, M. Knaflitz, An Algorithm for the Estimation of the Signal-To-Noise Ratio in Surface Myoelectric Signals Generated During Cyclic Movements, IEEE Trans. Biomed. Eng. 59 (2012) 219–225. https://doi.org/10.1109/TBME.2011.2170687.

[166] A. Mengarelli, E. Maranesi, L. Burattini, S. Fioretti, F. Di Nardo, Co-contraction activity of ankle muscles during walking: A gender comparison, Biomed. Signal Process. Control. 33 (2017) 1–9. https://doi.org/10.1016/j.bspc.2016.11.010.

[167] D.H. Sutherland, The evolution of clinical gait analysis part l: kinesiological EMG, Gait Posture. 14 (2001) 61–70. https://doi.org/10.1016/S0966-6362(01)00100-X.

[168] S. Rosati, V. Agostini, M. Knaflitz, G. Balestra, Muscle activation patterns during gait: A hierarchical clustering analysis, Biomed. Signal Process. Control. 31 (2017) 463–469. https://doi.org/10.1016/j.bspc.2016.09.017.

[169] F. Di Nardo, A. Mengarelli, E. Maranesi, L. Burattini, S. Fioretti, Assessment of the ankle muscle co-contraction during normal gait: A surface electromyography study, J. Electromyogr. Kinesiol. 25 (2015) 347–354. https://doi.org/10.1016/j.jelekin.2014.10.016.

[170] G. Albani, G. Sandrini, G. Künig, C. Martin-Soelch, A. Mauro, R. Pignatti, C. Pacchetti, V. Dietz, K.L. Leenders, Differences in the EMG pattern of leg muscle activation during locomotion in Parkinson's disease, Funct. Neurol. (n.d.) 7.

[171] E. Ueno, N. Yanagisawa, M. Takami, Gait disorders in parkinsonism. A study with floor reaction forces and EMG., Adv Neurol. 60 (1993) 414–8.

[172] M. Ferrarin, I. Carpinella, M. Rabuffetti, M. Rizzone, L. Lopiano, P. Crenna, Unilateral and Bilateral Subthalamic Nucleus Stimulation in Parkinson's Disease: Effects on EMG Signals of Lower Limb Muscles During Walking, IEEE Trans. Neural Syst. Rehabil. Eng. 15 (2007) 182–189. https://doi.org/10.1109/TNSRE.2007.897000.

[173] H. Mitoma, R. Hayashi, N. Yanagisawa, H. Tsukagoshi, Characteristics of parkinsonian and ataxic gaits: a study using surface electromyograms, angular displacements and floor reaction forces, J. Neurol. Sci. 174 (2000) 22–39. https://doi.org/10.1016/S0022-510X(99)00329-9.

[174] C.J. Andrews, Influence of dystonia on the response to long-term L-dopa therapy in Parkinson's disease, J. Neurol. Neurosurg. Psychiatry. 36 (1973) 630–636. https://doi.org/10.1136/jnnp.36.4.630.

[175] S. Cardarelli, A. Gentili, A. Mengarelli, F. Verdini, S. Fioretti, L. Burattini, F. Di Nardo, Ankle Muscles Co-Activation Patterns During Normal Gait: An Amplitude Evaluation, in: H. Eskola, O. Väisänen, J. Viik, J. Hyttinen (Eds.), EMBEC NBC 2017, Springer, Singapore, 2018: pp. 426–429. https://doi.org/10.1007/978-981-10-5122-7_107.

[176] G. Lichtwark, The role of the tibialis anterior muscle and tendon in absorbing energy during walking, J. Sci. Med. Sport. 18 (2014) e129. https://doi.org/10.1016/j.jsams.2014.11.109.

[177] C.A. Francis, A.L. Lenz, R.L. Lenhart, D.G. Thelen, The Modulation of Forward Propulsion, Vertical Support, and Center of Pressure by the Plantarflexors during Human Walking, Gait Posture. 38 (2013) 993–997. https://doi.org/10.1016/j.gaitpost.2013.05.009.